# ABNORMAL COMBUSTION

# METHANOL VERSUS GASOLINE

A. D. B. YATES, B.Sc.(Eng), M.Sc.(Eng) Cape Town

August 1988

Submitted to the University of Cape Town in
fulfilment of the requirements for the degree of
Doctor of Philosophy

ABSTRACT

The maximum efficiency of conventional gasoline engines is largely determined by the compression ratio, and this is limited by the onset of knock. The maximum cylinder size is similarly constrained. The relatively higher knock resistance of methanol opens up possibilities for increased efficiency or engine size.

The auto-ignition of methanol and gasoline was characterised in terms of fundamental parameters and the results were compared. The research findings were used in the analysis of a particular combustion chamber design to assess the potential of using squish as a means of avoiding knock in a large, spark-ignition methanol engine.

A simple knock model was proposed wherein the auto-ignition behaviour of a fuel was expressed in a global chemical-kinetic form involving pressure, temperature and time. A single-cylinder, Ricardo E6 research engine was used to obtain data for methanol and gasoline, which represented border-line knocking for a wide variety of operating conditions. The analytical solution was sought using regression techniques, which also served to quantify the accuracy of the analysis system.

Two fundamental differences between the knock mechanisms of gasoline and methanol were identified:

i) the auto-ignition reactions of methanol were an order of magnitude faster than those of gasoline, and

ii) whilst an increase in pressure has the effect of promoting knock with gasoline, it has the reverse effect with methanol.

The implications of these differences are very significant. Traditional methods of knock suppression involving the design of the combustion chamber to promote turbulence would have no effect with methanol. Similarly, the methanol engine size would not be constrained by knock.

These aspects were subsequently investigated using a Daimler Benz OM 407 engine, of which one cylinder was modified to spark ignition. Low-compression pistons were fitted having a combustion-chamber bowl and a squish-zone periphery. A special cylinder head was provided by Daimler Benz AG, Stuttgart, West Germany which featured 179 thin-film surface thermocouples arrayed across the combustion chamber face. Data from these thermocouples was used to determine the local heat flux and to follow the flame propagation. The knock characterisation data was utilised to predict the bulk end-gas temperature which, together with the heat-flux data, permitted an unsteady-state heat-transfer analysis to be carried out to determine the thermal boundary layer development.

The results of this analysis revealed that the principal knock-supressing mechanism of the squish design relied on increased combustion rate rather than end-gas cooling for its effect. Although the thermal boundary layer approached full development in the case of gasoline, with methanol, the increased combustion rate, attendant with the increased compression ratio, resulted in a less-developed boundary layer. Thus the end-gas core temperature was equal to the adiabatic temperature and it was deduced that the squish design had very little potential for suppressing knock in a methanol engine. It was concluded that, whilst the maximum efficiency of the gasoline engine could be increased by combustion chamber design modifications that would increase the rate of flame propagation and hence prevent knock at high compression ratios, there was less scope for improving the maximum efficiency of a methanol engine.

Although end-gas cooling was not seen to be a viable option for controlling methanol knock, it was observed that the evaporative cooling of the fuel itself was very effective as a means of lowering the overall cycle temperature and it was noted that this was the reason underlying the sensitivity exhibited by methanol to the Research and Motor Octane tests. This, and the possibilities with regard to engine size, low-speed operation and anti-knock additives were recommended for follow-on research.

## ACKNOWLEDGEMENTS

I would like to thank Daimler Benz AG who provided the low-compression pistons and the special cylinder head which was fitted with 178 surface thermocouples. The assistance of Mr M. Bargende of Daimler Benz with the commissioning of the cylinder head is gratefully acknowledged.

A real debt of gratitude is owed to Associate-Professor K. F. Bennett, whose supervision and guidance kept this thesis on track, and whose encouragement kept me going when enthusiasm flagged.

Finally I would like to thank my wife, Karin Yates, who endured months of my anti-social behaviour and supplied me with countless cups of tea.

TABLE OF CONTENTS

## NOMENCLATURE

| | |
|---|---|
| A,A´ | Constants of proportionality |
| $A_n$,$B_n$ | Fourier coefficients |
| a,b | Annand heat transfer coefficients |
| B | Temperature coefficient |
| BTDC | Before top dead centre |
| C | Constant |
| $C_m$ | Mean piston speed |
| Cp | Specific heat at constant pressure for gas |
| c | Specific heat of the wall material |
| D | Bore diameter |
| h | Convective heat transfer coefficient |
| IVC | Inlet valve closure |
| k | Polytropic exponent or thermal conductivity. |
| m | Mass of air |
| Nu | Nusselt number |
| n | Pressure coefficient or mass fraction burned |
| Q,q | Heat energy |
| q | Heat flux |
| P | Absolute pressure |
| SQ | Least squares standard deviation |
| R,r | Radius |
| Re | Reynolds number |
| RON | Research Octane number |
| T | Absolute temperature |
| TDC | Top dead centre |
| t | Time |
| U | Internal energy |
| V | Volume |
| W | Work energy or Woschni reference velocity |
| x | Distance from a position origin |
| | |
| $\alpha$ | Chemical species concentration or thermal diffusivity |
| $\Phi$,$\phi$ | Equivalence ratio or angular velocity |
| $\Phi_n$ | Variable abbreviation |
| $\rho$ | Density of the wall material |
| $\tau$ | Ignition delay |

### Subscripts

| | |
|---|---|
| 0 | Origin |
| 1 | Initial stage of a process |
| 2 | Final stage of a process |
| b | Burned |
| c | Critical condition |
| f | Final |
| fp | Flame position |
| i | Inlet condition or incremental counter |
| l | Latent heat of evaporation |
| n | Incremental counter |
| r | Residual cylinder gas condition |
| t | Time |
| u | Unburned |
| w | Combustion chamber Wall |

# CHAPTER 1

# INTRODUCTION

## 1.1 BACKGROUND AND OBJECTIVES

Along with the continued progress of automotive engine development, engineers and economists have constantly monitored the viability of alternative fuels, that is, fuels other than those in current usage, knowing that someday a replacement will undoubtedly be introduced. And already, in some parts of the world such as Brazil, the United States of America and parts of Europe, alternative fuels such as the alcohols - methanol and ethanol, are being used as replacements and supplements to both gasoline and diesel.

With regard to alternative fuels, South Africa is, in many respects, a world leader. SASOL synthetic gasoline and diesel, made from coal, provides about a third of the country's transport fuel needs. For several years, the alcohol which forms a by-product of the SASOL process and comprises chiefly ethanol plus some higher alcohols, has been blended into premium gasoline, although distribution has been regional, limited to those parts of the country served by the Natref Refinery.

In a recent techno-economic study, conducted by the CSIR [1], it was concluded that:

> "The methanol option of synfuel production to meet the national self-sufficiency objectives for fuel supply, has economic advantages over other synfuels from the point of view of both operating and capital costs."

Thus, there are clear indications that the alcohols are likely to play an increasing role in the future fuel supply, not only of this country, but also of many parts of the world, and there is a

corresponding need to conduct more research into the whole spectrum of alcohol fuel utilisation. This need has been recognised by the world research community and seven international conferences have been held on the subject of "Alcohol Fuel Technology" in the past ten years. In South Africa too, aspects of operating vehicles on methanol such as emissions, lubrication and material compatibility have been studied by the Energy Research Institute at the University of Cape Town [2,3,4].

Table 1, shown below, lists some of the more important properties of methanol. For comparison, the typical values for gasoline and diesel are also listed.

Table 1. Properties of methanol and typical gasoline and diesel [5]

| Property | units | Methanol | Gasoline | Diesel |
|---|---|---|---|---|
| Chemical formula | | $CH_3OH$ | $C_{8.8}H_{14.8}$ | $C_{14.5}H_{30}$ |
| Atomic Hydrogen/Carbon | ratio | 4 | 2.14 | 2.07 |
| Molecular weight | | 32 | 98 | 204 |
| Liquid density at 20°C | kg/l | 0.795 | 0.74 | 0.84 |
| Boiling point | °C | 65 | 32-186 | 177-356 |
| Heat of evaporation | kJ/kg | 1109 | 293-377 | 251 |
| Calorific heat $H_u$ | MJ/kg | 19.66 | 43.95 | 42.53 |
| Stoichiometric ratio | kg/kg | 6.4 | 14.9 | 14.55 |
| Research Octane number | | 110 | 93 | - |
| Motor Octane number | | 92 | 87 | - |
| Cetane number | | 3 | 14 | 45-55 |

Whilst methanol appears to be a very attractive alternative fuel to replace gasoline in spark ignition engines, its combustion characteristics make it unsuitable for use in a compression ignition engine (diesel engine). From the South African point of view, this is a serious disadvantage because the introduction of methanol as a gasoline replacement only would require a significant adjustment to the country's refinery processes to accommodate the new required gasoline/diesel product ratio. Several novel concepts for utilising methanol as a diesel

replacement have been considered [6,7,8]. However, perhaps the most obvious concept is to simply replace the diesel engine by a methanol-powered, spark-ignition engine.

This approach has been considered [9] and appears to be an attractively simple possibility, although suffering some disadvantages in terms of higher fuel consumption. Moreover, such a concept would be restricted in terms of engine size. The maximum cylinder size of a spark-ignition engine is limited by the capabilities of the fuel for which it is designed. In this regard, the most important requirement of a spark-ignition fuel pertains to its "knock" resistance, this being indicated by the fuel's Octane number. This plays a major role in determining the compression ratio of the engine and also the size of the individual cylinders of the engine. In general, the higher the compression ratio or the larger the cylinder size of an engine, the higher must be the Octane number of the fuel used. From thermodynamic and heat-loss considerations, a higher compression ratio or a larger cylinder size would result in more efficient fuel consumption and a compromise is necessary to optimise between Octane number and engine efficiency. (It is not just a coincidence that all the current generation of automotive spark-ignition engines which are designed for gasoline, have nearly the same cylinder size and similar compression ratios.)

If methanol were to be introduced as an alternative fuel, the current trends in optimum engine cylinder size and compression ratio would not necessarily be applicable because methanol has a significantly greater knock resistance than that of conventional gasoline, see table 1. Also, the phenomenon of knock in spark-ignition engines with conventional gasoline is by no means fully understood, and research into the knock behaviour of alternative fuels has been limited in most cases to parametric studies only.

Thus, it was the aim of this thesis to examine and compare the knocking combustion of methanol and gasoline and to look at the influence of combustion chamber shape and size. In order to achieve this objective, it was necessary to first study the

knocking behaviour of methanol from a fundamental mechanism point of view. The knocking behaviour of methanol has not been investigated in any depth before and this therefore represents original research. The second phase of the thesis, where the data that describes the knocking mechanism was used to derive information about the combustion and heat transfer in an engine is, similarly, an original technique.

## 1.2 THESIS OUTLINE

The research described by this thesis was conveniently divided into two distinct phases.

Firstly, basic research work was conducted using a single-cylinder Ricardo E6 research engine to study the auto-ignition characteristics of methanol relative to gasoline in some depth. This research was based on the pioneering work conducted at the Massachusetts Institute for Technology, where the spontaneous-ignition (auto-ignition) of fuels under conditions of elevated pressure and temperature was characterised in the form of global chemical-rate equations for each fuel [10]. For the present research, a similar approach was adopted. With the Ricardo engine operating under knocking conditions, and using temperatures that were calculated from the measured pressure, it was possible to deduce the values of the constants that characterised the global rate equations for gasoline and methanol and to deduce some preliminary conclusions about the relative knock mechanisms of these two fuels.

In the second phase, a detailed combustion analysis was carried out using a large spark-ignition engine. The choice of engine was influenced by the general interest in the use of methanol as a diesel replacement and consisted of a Daimler Benz type OM 407 engine, of which one cylinder was modified for spark-ignition operation. This 11.4 litre, six-cylinder diesel engine had a bore of 125mm and is typical of the type of engine that is used in heavy-duty long-haul trucks. A special cylinder head was provided

by Daimler Benz AG which featured 178 thin-film thermocouples arrayed across the combustion-chamber surface. The ø1mm sheathed, "K" type thermocouple pairs were routed through holes in the cylinder head and the temperature-measuring junction was formed by a 4µm layer of gold plating. The resulting fast-response temperature measurements were used to generate two-dimensional maps showing the flame propagation and the wall temperature at each crank angle, from which the local heat flux was determined. Additionally, with the engine operating at the point of knocking, the characteristic rate constants for each fuel which had been determined from the Ricardo engine tests in the first phase the project, were applied in order to evaluate the bulk end-gas temperature in the squish region. All this information, coupled with a one-dimensional, unsteady heat transfer calculation was used to analyse the local thermal boundary layer conditions for both methanol and petrol operation, and thereby to assess the effectiveness of the combustion chamber design as a means of cooling the end-gas region and thereby suppressing the spontaneous ignition of the two fuels.

# CHAPTER 2

# RICARDO ENGINE TESTS

Basic research work was conducted using a single-cylinder Ricardo E6 research engine to compare the auto-ignition characteristics of methanol and gasoline. The primary aim of this research was to characterise the knocking mechanism of the two fuels for subsequent analysis in the OM 407 engine. However, the investigation also revealed significant differences in the fundamental knock mechanisms of the two fuels which have interesting implications.

## 2.1 LITERATURE OVERVIEW

There are essentially two main theories that have been proposed as possible explanations of the knock phenomenon:

a) That knock is a detonation phenomenon. This implies that a shock-wave front develops during the propagation of the regular, spark-ignited flame and initiates a reaction of the end-gas at detonation speed whilst travelling through the yet unburned mixture. The energy released by the chemical reaction serves to maintain the shock front immediately ahead of it. Detonation waves of this description are commonly observed when studying the combustion of flammable gases in long tubes

b) Alternatively, that knock is a spontaneous auto-ignition phenomenon, where a body of end-gas is brought to a near homogeneous reaction under the influence of the high temperature and pressure established under the combined action of the piston movement and the regular flame propagation.

In either event, knocking is characterised by a localised high pressure region within the combustion chamber which, on relaxing, disturbs the thermal boundary layer of stagnant gas that insulates the combustion chamber walls and causes excessive heat loss and engine damage.

### 2.1.1 The Detonation Theory

The phenomenon of knocking taxed the ingenuity of the early researchers because the speed with which the events occurred made it an extremely awkward subject to study. It was suspected from the earliest that knocking might be a detonation phenomenon and in 1947, Miller [11] reported that he had obtained conclusive photographic evidence of a detonation wave originating in the end-gas after it had apparently auto-ignited. Schlieren photographs of the combustion chamber of a knocking engine were captured at 40 000 frames/sec. The bulk of the evidence boiled down to an interpretation of one single frame, which provoked much lively discussion at the time. Miller's attempts to obtain photographic records at higher film speeds were confounded by equipment problems and produced questionable results.

A crucial aspect of a detonation mechanism is the velocity of the associated gas movement as the detonation front develops. Lewis and Von Elbe [12] laid the early groundwork for an analysis of gas movement by considering the position of the molecules in the flame front in relation to their original and final positions. The unburned gas is compressed by the expansion of the hot products of combustion. However, as the flame front passes over each molecule, their outward movement is arrested and the now burned gas is compressed by the rising pressure until, by the time that the flame reaches the chamber walls, each molecule has returned to its original pre-ignition location since the gas is again of uniform density. They used a typical flame propagation profile, as indicated by a series of flame photographs, and computed the burned and unburned gas speeds. The highest gas speeds occurred behind the flame front as it approached the

combustion chamber wall, with the gas achieving speeds 40% higher than the observed flame propagation speed.

Under conditions of knocking combustion, flame propagation speeds of 250 to 500 m/s were estimated by Jost [13] as determined from photographic records. These speeds were confirmed by Curry [14] who used a number of ionization probes to follow the flame travel. This would imply that gas velocities could approach sonic conditions in the burned gas region whilst the flame propagation was still subsonic, although it should be emphasized that the simplistic analysis above was based on the assumption of uniform pressure throughout the combustion chamber which would tend to become invalid as sonic conditions were approached. The effect of localised higher pressure regions in the vicinity of the flame front would however promote more rapid flame propagation and hence greater gas velocities than estimated.

The gas motion discussed above could only be achieved by the establishment of a pressure gradient within the combustion chamber. That slight pressure fluctuations or pulses exist with normal combustion is well known [12,15]. Obviously, the faster the flame speed, the more vigorous would be the required gas motion and the greater the pressure fluctuations would be. These pressure fluctuations are particularly noticeable with engines operating on hydrogen which has a high natural flame speed [16] and also methanol [5]. It could be argued that significant pressure pulses associated with normal combustion is evidence of combustion bordering on the threshold of a detonation wave. Lewis and Von Elbe reported pressure pulses with hydrogen combustion in a constant volume bomb that were so severe that the pressure recording transducer was destroyed.

In recent years, the evidence supporting the auto-ignition theory of knock has accumulated convincingly and somewhat over-shadowed the detonation wave concept. However, a recent publication by Maly et al [17] has renewed interest in the auto-ignition versus detonation issue. A comprehensive analytical representation of combustion in a closed vessel was developed and used to describe

the nature of events that were thought to occur with combustion. An important facet of their discussion concerned the equations governing the velocity of the gas flow across the flame front. They were able to show that this velocity could easily reach sonic magnitudes with very modest flame propagation speeds as the flame approached the cylinder walls. Whilst this information is closely aligned to the foregoing discussion, it was noted that their combustion analysis contained an error. Referring to the sketch below, the burned gas velocity was determined by considering the combustion to occur in two imaginary steps; an incremental combustion at constant pressure which would cause the cylinder contents to expand ($R \rightarrow R+\Delta R$), followed by an incremental shrinking of the combustion chamber back to its original volume which would cause the cylinder pressure to increase. The unburned gas motion associated with the shrinkage, "$\delta r_1$" was taken to signify an actual gas velocity towards the approaching flame front which, when the temperature rise across the flame front and the associated gas expansion was accounted for, equated to the burned gas velocity behind, and away from, the flame. This unburned mass flux, "$\delta r_1$", directed towards the flame front, was a consequence of the hypothetical contraction of the combustion chamber. In their equation pertaining to gas motion, the compression movement of the unburned gas caused by the incremental combustion, "$\Delta r_{1b}$", which was directed away from the flame front, was overlooked. Thus the real-world gas movement would be determined from the difference between these opposing gas movements, "$\Delta r_{1b}-\delta r_1$", and not only "$\delta r_1$" as was assumed.

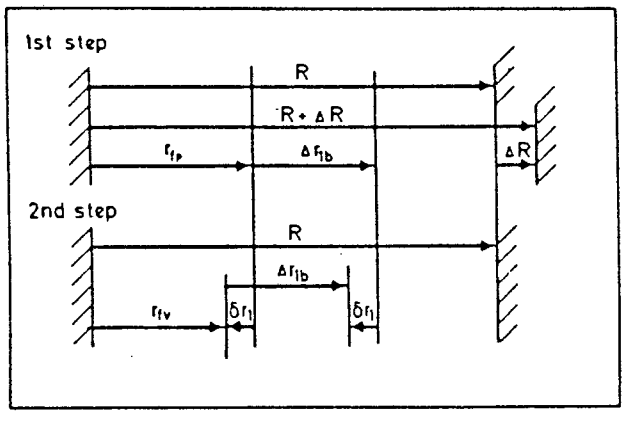


A schematic representation of the two-step combustion process as the flame advances from "$r_{fp}$" to "$r_{fp}+\Delta r_{1b}$" [17].

## 2.1.2 The Auto-Ignition Theory

Assuming knock to be a spontaneous auto-ignition phenomenon, it would be reasonable to suppose that the character of the engine knock depends on the mass fraction involved in the auto-ignition and the rate at which the auto-ignition proceeds.

Considering the idealised Otto cycle, the pressure (P) within the cylinder during the constant-volume combustion phase can be related to the mass fraction (n) burned by the approximate expression:

$$n = \frac{(P - P_1)}{(P_2 - P_1)} \qquad [12]$$

where the subscripts 1 and 2 refer to the initial and end conditions of the constant-volume process. The position of the flame front, as a function of pressure may be determined by assuming that the end-gas is compressed polytropically according to the expression:

$$P\ V^k = \text{Const}$$

Thus, at any point during the combustion, the pressure, volume and mass fraction of the end-gas may be computed. If the end-gas mixture were to auto-ignite instantaneously, the combustion would be constrained to take place within the volume of the end-gas at that instant since there could be no instantaneous expansion. There would consequently be a localised pressure rise in the end-gas region. The magnitude of this pressure discontinuity would be dependent on the mass fraction involved and could be calculated. Assuming typical engine values of pressures and volumes, an instantaneous combustion involving an end-gas mass fraction of 10% would cause a local pressure rise of about 200 bar.

In engines operating with moderate to heavy knock, the pressure rise has been reported in the vicinity of 15 bar [18]. Clearly then, the auto-ignition process is nowhere near instantaneous and

there is time for considerable expansion of the end-gas volume. Male [19] demonstrated that the auto-ignition process was not an homogeneous reaction of the end-gas by means of photographs taken at 500 000 frames/sec. He concluded that the auto-ignition reaction was initiated at many discrete nuclei from which combustion proceeded as a host of radially propagating flame fronts.

Probably the nearest example of instantaneous combustion was described by Curry [20]:

> "This was accomplished by placing within the engine, a lead-azide blasting squid which had a heating value of approximately 10% of the normal heating value of the fuel-air charge. With the engine operating at 900 rpm and iso-octane as the fuel, the squib was detonated by an electrical circuit approximately 5°BTDC and the pressure history of the combustion initiated by the squib was followed. The rate of pressure rise was unmeasurable and far exceeded any observed with knocking combustion."

Evidence of both gradual and rapid auto-ignition was reported by Taylor et al [21]. Using a rapid compression machine to study the auto-ignition of the whole charge, they observed that the auto-ignition of benzene was very much more gradual compared to that of iso-octane and n-heptane. Thus the combustion of benzene might be regarded as representing the transition from normal combustion to knocking combustion according to the auto-ignition theory.

The bulk of the experimental evidence appears to support the auto-ignition theory, at least as far as conventional hydrocarbon fuels are concerned. However the auto-ignition mechanism appears to be very complex and attempts to model the chemical kinetics are usually restricted to a simplified approach.

The situation is further confused by the fact that the combustion of most hydrocarbon fuels takes place in two distinct stages. This is particularly relevant to the present research which involves methanol and is discussed more fully below.

2.1.3 Two Stage Combustion

Two stage combustion was observed by Taylor et al [21] in their early research work with rapid compression machines and was studied in detail by Downs et al [22], Minkoff et al [23] and Fish [24], to name a few. The general conclusions were that the combustion of most hydrocarbons proceeds in two stages. The first stage involves a weakly exothermic reaction which produces intermediate products that are sufficiently stable to temporarily halt the reaction process. The second stage is strongly exothermic and is associated with a very significant temperature rise.

Within the framework of the auto-ignition theory, the first stage of combustion was seen as presensitising the end-gas which enables it to auto-ignite sufficiently rapidly to cause knocking. This conclusion was drawn by Downs et al [22] in the light of fuels such as benzene and methane which do not exhibit a two stage character in their combustion. Benzene had already been identified as a fuel that tends to auto-ignite more gradually and it was argued that since there was no first stage combustion to presensitise the mixture, the auto-ignition reactions in a single complex oxidation mechanism would inevitably be slower.

The list of fuels that exhibit only one, high-temperature combustion stage includes benzene and methane [22], methanol [25], ethanol [15], and hydrogen [13]. The majority of hydrocarbon fuels, however, appear to exhibit a two phase combustion character.

Fish [24] elaborated on the concept of two stage combustion and was able to demonstrate that the magnitude of the delay period between cool flame and hot ignition was related to the pressure rise during the cool flame. He concluded that, since it was the cool-flame reactions that control the subsequent hot-ignition process, if the cool-flame pressure rise could be reduced sufficiently, the delay before the start of hot-ignition would be increased to the point where knock was avoided.

The most recent findings by Pitz and Westbrook [26] seriously undermine some of these earlier conclusions. By simultaneously solving 13 reaction equations that were considered to be the most important to occur in the first, low-temperature stage of combustion of n-butane, and some 238 chemical reactions occurring in the second, high-temperature stage, they were able to accurately predict the onset of knock under given conditions of pressure and temperature. The surprising observation was that the low-temperature oxidation mechanism played an insignificant role in determining the onset of knock. This contradiction was noted by Miller [27], who summarised the problem in the following questions:

"- Are the cool flames observed by Downs, Walsh and Wheeler present in engines but of no consequence as far as knock is concerned?

- Is the kinetic modeling analysis of knock chemistry by Westbrook and Pitz essentially correct, or is their treatment of cool-flame kinetics inadequate?

- Is n-butane a special case?

- Is the effect of cool flames simply a thermal one? This possibility would be masked in the Westbrook-Pitz calculations which were performed with assumed pressures and temperatures."

The implications of these recent findings could be far reaching but further research seems indicated as a first priority.

The fact that methanol does not exhibit a two-stage combustion character, unlike the hydrocarbon fuels that include gasoline, indicates that an attempt to model the knock behaviour of methanol and gasoline should be treated with caution since their combustion chemistry is obviously very different.

## 2.2 THEORETICAL BASIS

Theoretical research which attempts to describe detailed chemical kinetics generally assumes that the kinetics of a reaction are known. The analysis then assumes reaction paths consisting of several successive and parallel stages with the participation of unstable intermediate products. Although the development of numerical methods of analysis have rendered such specifically formulated problems completely soluble, the modelling techniques are not yet entirely reliable, as discussed above. This is not surprising when one appreciates the extremely complex phenomena involved and their explosive nature.

Traditional methods of research into combustion problems usually entailed the study of the inverse problem, that is, to deduce from the observed phenomenological characteristics of the combustion process, the kinetics and mechanism of the chemical reactions which led to inflammation. A number of expressions have been proposed of varying complexity and, considering the uncertainty surrounding the knock mechanism of gasoline and the even greater uncertainty with regard to the knock mechanism of methanol, the simplest approach was selected.

The theoretical approach assumed that the production of the chemical species or chain-carriers necessary for auto-ignition to take place, could be expressed by a generalised gross reaction which was expected to be valid for the limited pressure and temperature range encountered in spark-ignition engine operation. (Full details of the derivation are given in appendix A). The proposed reaction was assumed to have the form:

$$\frac{d\alpha}{dt} = \alpha A' P^n e^{-\frac{B}{T}} \qquad (2.1)$$

Where:
- $\alpha$ = concentration of the pertinent reaction component
- $A'$ = constant
- $P$ = pressure
- $n$ = pressure coefficient
- $T$ = gas temperature
- $B$ = temperature coefficient

The solution of the differential equation involved the assumption that auto-ignition occurs at some critical time, $t_c$, corresponding to the attainment of a critical concentration of the chain carriers, $\alpha_c$, given as,

$$1 = \int_{t_o}^{t_c} \frac{dt}{A\, P^{-n}{}_{(t)}\, e^{\frac{B}{T(t)}}} \qquad (2.2)$$

If the pressure and temperature were constant, this critical time could be computed by a straightforward integration of the equation (2.2),

$$\tau = (t_c - t_o) = A\, P^{-n}\, e^{\frac{B}{T}} \qquad (2.3)$$

where $\tau = (t_c - t_o)$ is usually referred to as the auto-ignition delay and applies to the situation encountered with the use of rapid compression machines [10].

The engine data was used to solve for the constants in equation 2.2 which characterised a particular fuel. From a mathematical view point, since there are three unknowns, "A", "n" and "B", at least three different sets of conditions are required in order to determine a solution. In practice, ten or more engine set-up conditions were used and the solution, which was therefore over-determined, was found by means of a regression technique. The details of this are also included in appendix A.

This theoretical approach was adopted for the present investigation of gasoline and methanol because it featured the following important attributes:

a) The knock mechanism included terms that expressed the primary dependence on time, pressure and temperature.

b) The analysis could be conducted using an actual engine.

c) By definition, the knock mechanism was applicable to a range of engine operating conditions, and was not based on the analysis of a single cycle.

d) Unlike the Octane tests, the knock model characterised only the fuel and was independent of the engine used.

### 2.2.1 Temperature Determination

As indicated by equation 2.2, an accurate knowledge of the reactant gas temperature and pressure history was fundamental to the present study of auto-ignition and knock. Whilst the measurement of pressure represents a lesser problem, the direct measurement of the instantaneous gas temperature within the engine combustion chamber is technically more difficult.

The possibility of measuring the gas temperature directly was given careful consideration. A review of the literature indicated that temperature measurement in engines generally necessitates a severe modification to the combustion chamber shape and is subject to considerable uncertainty.

Glukstein researched the potential for the measurement of end-gas temperature by means of the speed of sound [28]. A range of fuels were investigated at different inlet temperatures and ignition timings and compression ratios. The knock point was found to vary with pressure, but it was apparently independent of temperature, with knock always occurring at about 727°C. The authors interpreted this finding as factual although it may be that the temperature measurement technique was not sufficiently precise to discern the exact end-gas temperature, since the acoustic apparatus inevitably measured the average temperature of a finite volume which was arranged to be in the vicinity of the end-gas region. Interestingly, the ignition timing was shown to increase the end-gas temperature linearly by 5°C per degree of advance, whilst the effect of engine speed was shown to be insignificant.

Agnew conducted a similar investigation using the two-wavelength infra-red radiation method [29]. The combustion chamber was distorted by fitting a spacer between the cylinder head and the block, with the end-gas volume arranged to coincide with the optical access region.

The measured gas temperature was checked against the calculated temperature for motoring engine tests. This method of verification was obviously limited to the accuracy of the pressure and air flow measurement and the assumptions involved in the calculation. Whilst the accuracy was somewhat uncertain, the precision was nevertheless determined at about 28°C.

When the engine was fired, some problems were experienced with the reflected light from the advancing flame which reduced the accuracy of the end-gas temperature determination. Nevertheless, data from the tests with a firing engine indicated an increase in the end-gas temperature with ignition timing of 2.8°C per degree advance, but contrary to Glukstein's findings, Agnew found that an increase in engine speed from 1000 to 2000 rev/min resulted in a 44°C increase in gas temperature at TDC.

Another technique that has been tried, involving sodium line reversal and absorption spectroscopy, was not very successful [30].

Comparatively recently, the use of laser techniques have been applied to engine research. Coherent anti-Stokes Ramen spectroscopy (CARS) has been demonstated to be capable of measuring instantaneous, localised temperatures within an engine with an accuracy of about ±50°C [27]. A CARS facility was recently purchased by the Council for Scientific and Industrial Research (CSIR) and it is currently based at the University of Cape Town. However, it will be some time yet before the system could be used for engine research and as such, CARS did not represent a viable option for the present research programme.

As an alternative to direct temperature measurement, the determination of the temperature by calculation has to be based on several assumptions which involve a degree of estimation and conjecture. However it was noted that, for the most part, calculation methods tend to result in systematic errors rather than random errors. Moreover, in all the temperature-measurement techniques described above, the accuracy and precision of the technique was verified in comparison with the calculated temperatures and therefore the simplest option was chosen, ie, to evaluate the temperature by calculation.

## 2.3 EXPERIMENTAL TESTS

The single cylinder engine used for these studies was the Ricardo E6 research engine. Principal details of the engine are:

| | |
|---|---|
| Bore | 75 mm |
| Stroke | 111 mm |
| Connecting Rod | 242 mm |
| Compression Ratio | Variable |

The tests were conducted at borderline knock with wide open throttle and under a variety of speeds, compression ratios, ignition timings and inlet temperatures. The two fuels tested were commercial grade 98 RON pump gasoline and standard commercial grade methanol. A stoichiometric air/fuel ratio was maintained throughout the tests. The full details of the experimental tests and the analytical equipment are given in Appendix B.

Two main software routines were written to analyse the test data. The first program processed the raw pressure signal and determined the temperature of the unburned portion of the cylinder contents up to the point of knock. The second program's function was to characterise the fuel in terms of its knock

behaviour from the pressure and temperature data originating from all the engine operating conditions.

An overview of the software routines are included in Appendix B. However, since the temperature was the most critical parameter upon which the subsequent analysis was based, the method of its calculation warrants particular attention.

The measured parameters were the ambient temperature and pressure, the mass of the intake air, the fuel flow rate, the exhaust temperature, the pressure in the cylinder and the engine speed. The parameters are depicted diagrammatically below, as well as the additional information that had to be deduced in order to solve for the temperature at the point of inlet valve closure (IVC).

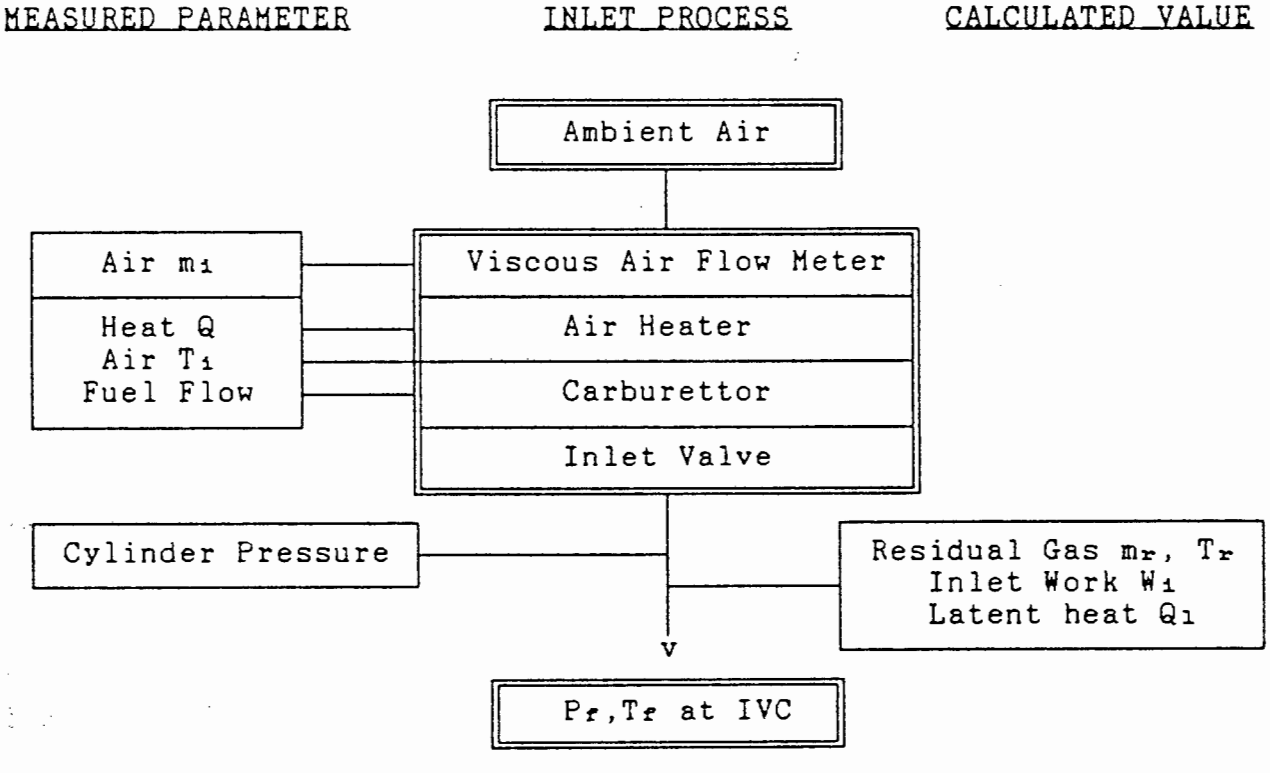


An unfortunate disadvantage of the piezo-electric transducer used for the pressure measurement was its inability to hold a DC signal. Thus the absolute pressure zero reference was not known and had to be computed together with the temperature.

An energy balance was performed on the inlet mixture at the point of inlet valve closure (IVC), as indicated by equation 2.4 below. This equation was based on the energy content of the residual exhaust gas remaining in the cylinder, the incoming air-fuel mixture, the work done by the piston on the gas during the inlet stroke and the latent heat of evaporation of the fuel.
Since a knowledge of the pressure was required for some of these energy terms, and the absolute pressure zero reference was not known at this point, an iterative solution was adopted, using an estimated value for the pressure reference for the first calculation.

$$m_i\, Cp_i\, (T_f - T_i) + m_r\, Cp_r\, (T_f - T_r) + W_i + Q_i = 0 \qquad (2.4)$$

The heat loss or gain from the inlet tract and cylinder walls was not included in this calculation since data essential to the calculation was not known. The presence of liquid fuel in the system prevented a realistic estimate of the heat transfer being made. However, it was assumed that, because of the relatively small temperature difference between the inlet mixture and the manifold walls, the resultant heat transfer would be insignificant. This assumption was supported by Borman [31]. Similarly, the heat transfer from the cylinder walls was estimated to be relatively small during the intake process.

Another source of inaccuracy concerned the mass of the residual mixture trapped in the cylinder at the end of the exhaust stroke, $m_r$. This was calculated from the residual gas volume, the residual temperature and the residual pressure. However, these values had to be estimated. The residual temperature, $T_r$, was assumed to be the same as that measured for the exhaust gas in the exhaust port. The residual gas volume was assumed to be represented by the clearance volume and the pressure was assumed to be represented by the pressure transducer signal at the top dead centre (TDC) point between the intake and exhaust strokes. In view of the valve overlap period of some 18° crank angle (CA), these parameters were a representative estimate, and the calculated residual gas mass was therefore an approximation.

The primary residual gas constituents were determined assuming complete combustion. The work done by the piston on the incoming mixture, $W_1$, was computed from the pressure-volume diagram. Finally the latent heat component, $Q_1$, was included. At the point of inlet valve closure, the fuel was not necessarily fully evaporated and therefore the degree of fuel evaporation was calculated from an expression for the equilibrium partial pressure of the fuel. This assumption would be reasonable on account of the finely divided fuel droplets and the good mixing introduced by the induction process.

The temperature during compression, up to the point of ignition, was calculated from the ideal gas law, using the measured pressure and the computed values for the mass of the trapped gas mixture and the cylinder volume.

Once ignition had occurred, the volume of the unburned gas was unknown and the calculation of the temperature was continued in small time increments. For each time increment, the calculation involved two steps. First, a theoretical pressure and temperature was determined for the whole mixture as if no further combustion had taken place. This calculation involved a first law energy balance between the work done by the piston, the heat loss and the change in internal energy of the unburned gas.

$$dQ + dW = dU \qquad (2.5)$$

The calculation of heat loss was based on the empirical formula proposed by Woschni [31].

$$h = 0.820\, D^{-0.2}\, P^{0.8}\, (2.28\, C)^{0.8}\, T^{-0.53} \qquad (2.6)$$

where
- $h$ = Heat transfer coefficient ($kW/m^2K$)
- $D$ = Bore (m)
- $P$ = Pressure (bar)
- $C$ = Piston speed (m/s)
- $T$ = temperature (K)

The heat loss has very little effect on the end-gas temperature. Typically, the total heat loss amounts to 4 to 6% of the total

fuel energy [32], and most of this heat loss occurs during the expansion stroke. The subject of heat transfer is discussed in greater depth in Section 3 of this thesis.

The determination of the mixture properties was based on the final temperature from the previous step. Secondly, the mixture was imagined to undergo an adiabatic compression process to raise the pressure up to the measured value, from which the final temperature was determined.

$$\frac{P_1}{P_2} = \left[ \frac{T_1}{T_2} \right]^{\frac{k}{k-1}} \qquad (2.7)$$

The calculation was performed in steps of one crankshaft degree and halted at the point that knock occurred.

## 2.4 DISCUSSION OF RESULTS

The results of the calculations for the characteristic constants for the two fuels are tabulated below.

TABLE 2.1 The characteristic fuel constants deduced from the Ricardo test data.

| Fuel | Constant (msec) | Pressure Coefficient | Temperature Coefficient | Correlation Coefficient |
|---|---|---|---|---|
| Gasoline | $1.68\ 10^{-3}$ | -0.66 | 8950 | 0.87 |
| Methanol | $3.28\ 10^{-4}$ | 0.64 | 7749 | 0.38 |

It was immediately apparent from the relative magnitudes of the constants that the character of methanol and gasoline knocking was fundamentally different. In addition, correlation coefficients indicated that the gasoline data fit to the theoretical expression was significantly better than that for methanol.

2.4.1 Discussion of the gasoline results

Before consideration was given to the behaviour of methanol, the gasoline results were examined in relation to the findings of other researchers. By et al [33] compared the results of a number of such research programmes and their findings for gasoline are summarised below:

$$\tau = 0.017095\ P^{-1.48}\ e^{\frac{7457}{T}} \qquad \text{(Rifkin \& Walcutt)}$$

$$\tau = 0.816 \times 10^{-12}\ \Phi^{-1.04}\ P^{-2.57}\ e^{\frac{32400}{T}} \qquad \text{(Burwell \& Olson)}$$

$$\tau = 10^{-3} \left[ \frac{P}{R\ T} \right]^{-.72} e^{\left[ -8.387 + \frac{18310}{T} \right]} \qquad \text{(Vermeer, Meyer \& Oppenheim)}$$

$$\tau = 19.75 \left[ \frac{RON}{100} \right]^{3.4107} P^{-1.7}\ e^{\frac{3800}{T}} \qquad \text{(Douaud \& Eyzat)}$$

Where, $\tau$ = the auto-ignition delay. (msec)
P = Pressure (Bar)
T = Temperature (K)
$\Phi$ = the equivalence ratio
RON = the Research octane number

It was noted that the magnitude of the constants in the above equations varied enormously, for example, the temperature constant varied from 3800 to 32400, and the constant of proportionality varied by several orders of magnitude. However, it should be noted that the above formulae express the sensitivity of the ignition delay to a *change* in pressure and/or temperature. To understand the reason for such variation, it is helpful to consider the partial derivatives of the ignition delay equation 2.3 with respect to pressure and temperature:

$$\frac{\delta\tau}{\delta P} = -\ n\ A\ P^{(-n-1)}\ e^{\frac{B}{T}}$$

$$\frac{\delta\tau}{\delta T} = -\ \frac{B}{T^2}\ A\ P^{-n}\ e^{\frac{B}{T}}$$

These equations may be conveniently rearranged to express the percentage change in delay in terms of a percentage change in pressure or temperature:

$$\frac{\delta\tau}{\tau} = - n \frac{\delta P}{P} \qquad (2.8)$$

$$\frac{\delta\tau}{\tau} = - \frac{B}{T} \frac{\delta T}{T} \qquad (2.9)$$

Thus, the constants "n" and "B" may be regarded as characterising the rate-controlling knock reaction mechanism with respect to pressure and temperature. The value of the constant "A" in equation 2.3 serves only to peg the fuel's ignition delay in absolute terms. This is clearly indicated by the RON correction term in Douaud and Eyzat's formula. Equation 2.8 indicates that the ignition delay is sensitive to a small percentage change in pressure according to the magnitude of the constant "n", and similarly, equation 2.9 shows that the delay would respond to a small percentage change in temperature according to the magnitude of the ratio "B/T". Given experimental data which ranges over a very narrow band of the pressure and temperature spectrum, the multi-variant analysis, which separates and calculates these pressure and temperature gradients, is clearly very sensitive to any experimental inaccuracy. This is an important problem that is inherent to this particular research approach.

The above formulae are compared together with the experimental gasoline results in figure 1, where the temperature corresponding to a fixed delay of 2ms has been computed for each of the above formulae over a range of pressures typical to engine operation. Since the above formulae were derived under widely differing test conditions (shock tubes, continuously stirred tank reactors, motored and fired engines), the absolute value of the temperature in figure 1 varied considerably.

It may be appreciated from figure 1, that the percentage change in temperature, corresponding to the 15 bar pressure variation,

was small and, with the possible exception of the work of Douaud and Eyzat, the value of the temperature constant, "B", might have been made the same throughout. In other words, the slight variation in the slopes of the different sets of data could easily be attributed to uncertainty in the determination of the gas temperature, rather than a factual difference in the fuels that were studied. Temperature was deliberately chosen as the dependent variable in this discussion because it was the source of the greatest uncertainty in the analysis techniques of the above-mentioned researchers.

Thus it was concluded that values for the constants that characterise the knocking mechanism of gasoline that were determined in this present study were similar in general trend to the findings of other researchers within the tolerance band afforded by the simplified theoretical model and the accuracy of the temperature calculation. Since the accuracy of the temperature calculation appeared to be such a crucial issue, this aspect was investigated in greater depth.

### 2.4.2 The accuracy of the temperature calculation

The overview of the end-gas temperature analysis, which was described in section 2.3, highlighted the assumptions that were implicit in the calculation. However, besides the assumptions, the precision of the measured parameters represented a source of possible inaccuracy. A sensitivity analysis was therefore conducted to assess how the final end-gas temperature was affected by a small change in the value of each measured parameter. The magnitude of the small change was chosen to represent the estimated precision of each parameter at its extreme limit. The results are shown in figure 2, from which it may be seen that inaccuracies of 20°C in the calculation of the gas temperature could occur from a single parameter, although to some extent, such errors could be partly systematic rather than errors of precision.

Using the characteristic constants given in table 2.1, the temperature was calculated and compared to the measured value for each test, from which a standard error of the estimate was determined. The results are illustrated in figure 3, and yielded a standard error of the estimate of 12.2°C. This did not confirm that the form of equation 2.2 was correct, but rather confirmed the magnitude of the scatter due to measurement and calculation inaccuracies.

There was no corresponding method of cross-referencing to check the accuracy of the absolute value of the calculated temperature.

### 2.4.3 Discussion of methanol results

The attempt to condense the chemical kinetic behaviour of a fuel to a single, global expression, as discussed in section 2.2, involves a number of assumptions and simplifications. Also, the analysis technique, to solve for the characteristic fuel constants, requires the calculation of the gas temperature which has been shown to be subject to inaccuracies. Despite these problems, the gasoline data was found to correlate well with the theoretical model, as shown by the correlation coefficient of 0.87 in Table 2.1, and a standard error of the estimate of 12.2°C in figure 3. When the methanol data was analysed in a similar manner, the correlation coefficient was found to be 0.38. Moreover, when the characteristic constants, given in table 2.1 for methanol were used to calculate the temperature at the measured pressure and engine speed and the result was compared to the experimental temperature value for each test, the comparison yielded an standard error of the estimate of 36.5°C, as shown in figure 4.

A number of possible explanations were considered to account for the very poor correlation given by the analysis of the methanol data:

a) The difficulty of temperature determination, particularly with regard to the effects of the high latent heat of methanol, could explain the low correlation.

b) As was discussed in section 2.1.1, despite the accumulation of evidence to suggest that gasoline knocks by way of an auto-ignition mechanism, much of the evidence was not applicable in the case of methanol. Obviously the auto-ignition knock model would not correlate with a detonation mechanism if this was the basis for methanol knock.

c) The assumptions, which were implicit in the theoretical knock mechanism and which concerned the reaction process, may not hold true for methanol. It was noted in section 2.1.3 that the chemistry of combustion of methanol was different from that of gasoline in as much that it did not proceed in two stages. This difference may have been reflected in the knock model which assumed the presence of some rate-limiting chemical species which, on attaining a critical concentration, initiated a very rapid chemical chain reaction.

d) It was possible that the experimental procedure and the analysis technique could contain an inherent flaw.

The first possibility was discounted on the grounds that, despite the known uncertainty of the temperature calculation, the gasoline results had shown a good statistical correlation.

The possible existence of a detonation mechanism was shelved until the latter two possibilities had first been considered and rejected.

It was noted in section 2.1.3 that the combustion chemistry of gasoline was exceedingly complex, and that the physical meaning of the two-stage combustion was simply the formation of intermediate products that were sufficiently stable to temporarily halt the reaction process. The fact that the

combustion of methanol occurred in one stage was therefore not considered significant. However combustion chemistry of the relatively simple methanol molecule involves far fewer possible reaction steps, compared to gasoline. Thus, it could be expected that the auto-ignition reaction kinetics of methanol, from fuel to product, could be extremely fast.

If this were the case, the time step "dt" used in the solution of equation 2.2 would have to be at least an order of magnitude smaller than the total reaction time if the pressure and temperature dependencies were to be resolved. In the analysis, a time step corresponding to one degree of crank-shaft revolution was used which may have been too long.

On the basis of the foregoing discussion, and assuming that the auto-ignition reactions of methanol were indeed orders of magnitude faster than the engine speed, the rate of the pressure and temperature rise, prior to auto-ignition, would be irrelevant. The only significant parameters in the analysis of the auto-ignition would be the final value of the pressure and the temperature prior to knock. This hypothesis was tested as shown in figure 5, by comparing the temperature immediately prior to knock with the corresponding pressure. As indicated, a measure of correlation was apparent which, assumed to be linear to a first approximation, indicated a correlation coefficient of 0.71 and the standard error of the estimate of 15.6°C. This was a significant improvement on the results shown in table 2.1.

As yet unpublished research that has been in progress at the University of Cape Town, involving a chemical kinetic approach to modelling the combustion of methanol has arrived at similar findings with regard to the very rapid reaction rate that occurs when methanol auto-ignites. The chemical kinetic model also indicated an extremely abrupt transition from negligible chemical activity to spontaneous ignition within a very narrow temperature band.

The correlation shown in figure 5, revealed a positive slope in the pressure - temperature relationship which was interesting. The overall reaction of methanol:

$$2\ CH_3OH + 3\ O_2 \ ==>\ 2\ CO_2 + 4\ H_2O$$

reveals that 5 moles of methanol and oxygen produce 6 moles of carbon-dioxide and water. Thus there is a net increase in volume in the reaction and the effect of pressure would be to retard the process, as reflected in the experimental data.

Whilst the argument thus far was based on conjecture, the hypothesis was reinforced by comparing the temperature prior to knock with the engine speed, shown in figure 6. A low correlation coefficient of 0.30 signified that the reaction rate (temperature) was not of the same order of magnitude as the engine speed. Considering figures 5 and 6 together, it appeared that the knock mechanism of methanol was a chemical rather than a physical phenomenon, and that the auto-ignition theory was therefore not rejected by the findings.

The primary objective of this research was to ultimately characterise the knock behaviour of the fuel in terms of the fundamental properties such as temperature and pressure. In this regard, the relationship between pressure and temperature indicated in figure 5 for methanol was considered adequate. The linear regression equation was thus of the form:

$$T = 1000 + 1.86.P$$

where $T$ = the absolute temperature prior to knock (K)
$P$ = the absolute pressure prior to knock (bar)

It was possible to make a parametric comparison between the knock behaviour of methanol and gasoline, as shown in figure 7. The knock-limited temperature for both fuels was plotted as a function of pressure and, as was done in figure 1, a typical ignition delay of 2ms was chosen for the gasoline data. It may be

seen that methanol can withstand a higher end-gas temperature before knock occurs which is in accord with the known fact that methanol is relatively resistant to knocking as indicated by its high Octane rating (see table 1).

However, the really interesting characteristic of figure 7 was revealed in the relative slopes of the knock-limited temperature. The trend for gasoline indicated that if the pressure is increased, the maximum temperature that may be tolerated at the knock-limit decreases, whilst for methanol the trend was reversed: If the pressure was increased, the maximum temperature that could be tolerated at the knock-limit also increased.

In an engine, the pressure and temperature are linked to some extent as a result of the polytropic compression law.

$$P\ V^{k} = \text{Const}$$

Neglecting heat loss for the moment, an increase in pressure will result in an increase in temperature, and both these conditions promote knock in the case of gasoline. However, in the case of methanol, the increase in pressure will tend to suppress knocking, although in the adiabatic example, the effect of the rising temperature will dominate. This is illustrated in figure 7 by the polytropic compression curve corresponding to k = 1.40.

If the effect of heat loss in the end-gas region is also considered, it is possible to conceive of the situation where the increase in temperature resulting from an increase in compression ratio was lessened to such an extent by the heat loss, that the increase in knock-supressing pressure was dominant over the knock-inducing increase in temperature. Under such circumstances, the compression ratio could be increased indefinitely, or at least within the range of applicability of the observed trends. This situation is illustrated in figure 7 by the polytropic compression curve corresponding to k = 1.25, where the slope of the compression curve is tending towards a slope which runs

parallel to the knock-limited temperature profile for methanol. Thus, if the end-gas could be cooled, by designing the combustion chamber to create high gas velocities that would improve heat transfer for example, then a significant increase in compression ratio, with an attendant increase in thermodynamic efficiency might be possible.

The effect of engine speed represents an important factor in the above argument. As the engine speed increases, there is less time for heat loss and the polytropic compression exponent tends towards the adiabatic compression exponent. Thus it would appear that methanol has attractive potential as a fuel for highly-efficient, slow-running engines, and one obvious application is the use of methanol as an alternative fuel for diesel engines. This particular application is the subject of the second half of this thesis.

It is interesting to consider the results of this research study against the background of other methods of characterising the knock behaviour of fuels such as the Octane tests. The limitation of such tests is that the knock behaviour is characterised relative to a reference fuel at a single engine operating point, and the relative trends for the test fuel in terms of changes in pressure, temperature and time is not revealed. Even taking the Research and the Motor Octane tests together, which represent two different operating conditions and indirectly yield two of the three variables, this still represent an inadequate matrix from which to characterise the knock behaviour of a fuel uniquely. This problem is evident when one considers the wealth of literature generated by researchers attempting to specify some sort of "knock index" based on the Octane test methods.

## 2.5 CONCLUSIONS WITH REGARD TO RICARDO ENGINE TESTS

The principal conclusions of the Ricardo tests are summarised below:

1. The determination of the end-gas temperature was the most important aspect of this investigation. Random scatter due to experimental accuracy was quantified but the possibility of systematic errors originating from inaccurate assumptions could not be checked. As far as possible, the instrumentation was calibrated or verified.

2. The theoretical model which was used to characterise the basic knock behaviour of gasoline, was too simplified to reveal the details of the underlying chemical kinetic mechanisms of combustion. However the model correlation with the gasoline data was good and was in line with the general findings of other researchers who have used this approach

3. The initial analysis of the methanol data failed to correlate with the gasoline knock model and evidence was found to suggest that the knock behaviour of methanol was distinctly different from that of gasoline. It was suspected that the rate of the methanol auto-ignition reaction was not compatible with the rate of data capture and this hypothesis was reinforced when allowance was made for a relatively rapid combustion rate, and a simplified empirical regression analysis yielded an acceptable correlation. A null-hypothesis test for correlation with engine speed confirmed that the methanol knock mechanism was indeed very rapid.

4. The possibility of the knock mechanism of methanol being a detonation phenomenon was considered. However, although the experimental results indicated an obvious difference between the knocking mechanism of gasoline and methanol, the auto-ignition theory proved adequate to describe the behaviour of both fuels

5. An important and significant difference was observed in the relative response of the knock-limited temperature of gasoline and methanol to a change in pressure. The trend for gasoline indicated that the maximum temperature that may be tolerated at the knock-limit decreases with an increase in pressure, whilst for methanol the trend was reversed. Given a maximum temperature, an increase in pressure had the effect of suppressing the auto-ignition of methanol. This, coupled with the possibility of utilising the combustion-chamber design to increase the end-gas cooling, appeared to indicate an attractive possibility for extending the knock-limited compression ratio of methanol.

6. The method of characterising fuels directly in terms of pressure, temperature and time has distinct advantages over indirect methods such as the Research Octane test and the Motor Octane test. The fact that three constants were required to characterise each fuel could explain much of the confusion that surrounds the applicability of the Research and Motor methods since the solution for three unknowns with two equations is indeterminate.

# CHAPTER 3

## DAIMLER BENZ OM 407g ENGINE TESTS

The findings of the Ricardo engine research, discussed in chapter 2, indicated several interesting avenues for further investigation, perhaps the most significant being the potential role of the combustion-chamber design as a means of suppressing the end-gas temperature and hence the spontaneous auto-ignition of methanol at high compression ratios. To this end, a detailed heat transfer analysis was performed on a spark-ignition engine which featured a bowl-in-piston combustion chamber and incorporated substantial squish areas in the end-gas zone. As with the Ricardo tests, the knock-limited performance of methanol was compared with that of gasoline.

The engine which was used for this research was a six-cylinder diesel engine, of which one cylinder was modified for spark-ignition operation. The engine, a Daimler Benz OM 407 had a total displacement of 11.4 litre and a bore of 125mm. A range of pistons was available having different sized combustion chambers and hence different compression ratios. A special cylinder head was provided from Daimler Benz AG, Stuttgart, which featured 179 thin-film thermocouples arrayed across the combustion-chamber surface. The ø1mm sheathed, "K" type thermocouple pairs were routed through holes in the cylinder head and the temperature-measuring junction was formed by a 4µm layer of gold plating. The resulting fast-response temperature measurements were used to generate two-dimensional maps showing the flame propagation and the wall temperature at each crank angle, from which the local heat flux was determined.

The choice of engine was influenced by the general interest in the use of methanol as a diesel replacement. The possibility of utilising methanol in a large spark-ignition engine was another observation emanating from the Ricardo test results. It was noted in chapter 2 that, since the spontaneous-combustion reactions of methanol were an order of magnitude faster than the engine cycle events, auto-ignition could not be averted by rapid flame propagation as was the case with modern gasoline engines or, conversely, that the knock-limited performance of a methanol engine was relatively insensitive to engine size or speed.

The unsteady-state heat-transfer situation in the squish zone was not an easy topic to study. However, the analysis was facilitated by operating the engine at borderline-knock conditions and using the characteristic knock constants for the fuel, obtained from the Ricardo-engine tests, to predict the bulk end-gas temperature in the knock region. In other words, the onset of knock itself was used to signal a known gas-temperature situation.

## 3.1 LITERATURE OVERVIEW

The research was initiated by looking at the inter-related subjects of combustion-chamber design, the mechanism of squish and heat-transfer analysis in engines. This was the basis against which the subsequent experimental data and results for gasoline and methanol were compared.

### 3.1.1 Combustion-chamber design considerations

Knock may be regarded as a race taking place between the naturally occurring reactions in the compressed end-gas and the chemical reactions induced by the passage of the spark-ignited flame. If the flame reactions consume the entire charge before the naturally occurring reactions reach a critical point, there is no auto-ignition and hence no knock. However, if the naturally occurring reactions win the race, auto ignition occurs and the

engine knocks. With gasoline, factors such as reduced engine speed and increased flame transit distance increase the tendency of an engine to knock by allowing more time for the chemical reactions to take place in the end-gas.

The design of a combustion chamber for a spark-ignition engine involves a compromise between several conflicting requirements. From the thermodynamic viewpoint, the compression ratio, and hence the pressure and temperature should be maximised. However, the occurrence of knock represents a barrier to the increased compression ratio. Since the auto-ignition originates in the end-gas region, an obvious concept is to cool this region whilst increasing the compression ratio. This may be achieved by designing the combustion chamber with the end-gas region having a high surface area-to-volume ratio, or having high gas velocities to increase the heat transfer. However, the energy loss stemming from end-gas cooling represents an overall reduction in efficiency which may, to some extent, negate the benefit of the increased compression ratio. In the case of the gasoline engine, reducing the time that the end-gas is exposed to elevated temperatures is the other obvious concept for the suppression of knock. Typically, this is achieved by having a smaller cylinder size or by means of increased turbulence to promote rapid combustion. If used in conjunction with end-gas cooling, reduced combustion duration also reduces the time that heat loss can take place, and it is not always clear which concept is dominant.

The application of these combustion chamber design concepts was illustrated in a recent overview publication by Ricardo Engineering, which revealed that by suitable design, it is possible to operate engines with 1 to 2 compression ratios higher than conventional combustion chamber designs, whilst using the same quality fuel [34]. Three designs were compared: The Nissan NAPS-Z open chamber, the high-ratio, compact chamber in head design (HRCC), and the four-valve pent-roof chamber. A sketch of the three designs is shown below. With the NAPS-Z chamber, fast burn was achieved by using twin spark plugs and high swirl level. The HRCC design had a high level of squish to provide end-gas

cooling and a short flame path to promote fast burning. The pent-roof design had a central spark plug coupled with complex interaction from the two inlet flows which gave very rapid combustion.

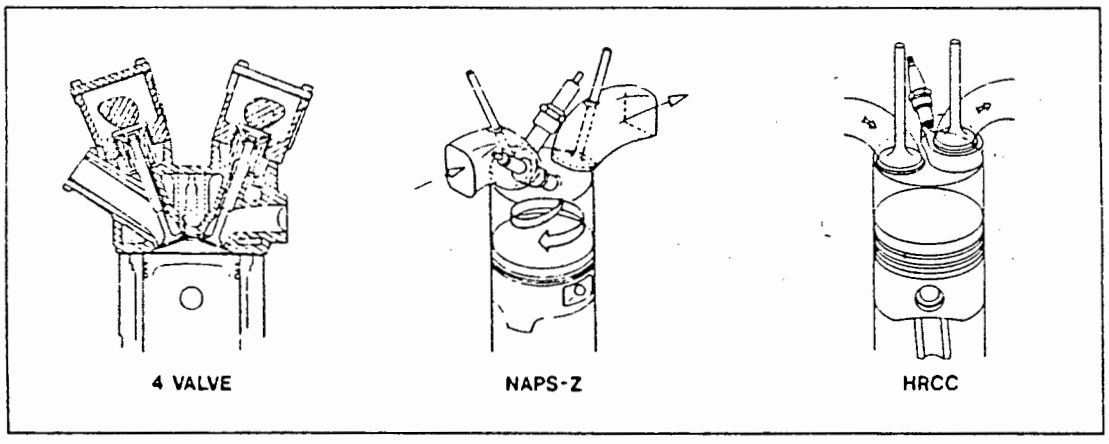


Three combustion chambers studied by Ricardo Engineering (34)

On the subject of combustion chamber designs, both Dye [35] and Caris [36] emphasizes that rapid combustion is necessary for high efficiency and maximum lean burning. The general principle was to concentrate the clearance volume around the point of ignition as compactly as possible. Data for a disc chamber was compared to a bowl-in-piston design. The compact chamber showed a combustion duration equal to half that of the disk chamber, although the shorter combustion duration resulted in higher peak pressures occurring earlier in the cycle and consequently slightly higher end-gas temperatures. Besides maximising efficiency, some associated relationships were also considered. The length of flame travel was shown to be related to the knock limit and turbulence was shown to increase the knock limit. This conclusion was based on results obtained using shrouded inlet valves, which despite having a unacceptable influence on engine breathing at high speed, served to demonstrate that the turbulence generated during the intake process persists until the combustion phase. It was presumed that the turbulence generated by squish was the mechanism responsible for the observed increase in the knock limit for the bowl in the piston design and squish was identified as the most important single design change that could be used to further increase the knock limit.

The mechanism whereby turbulence increases the combustion rate was studied by Gatowski [37] with the aid of a transparent, flow-visualisation engine. Several combustion chamber features were investigated, the aim being to maximise the rate of combustion. Turbulence was found to be the general mechanism for increased combustion rate but it was shown to have some negative impacts too; it increased heat loss and decreased the maximum power.

Shrouded inlet valve test results indicated that the general shape of the developing flame front is un-affected but that the valve-induced turbulence makes the flame more wrinkled. Although the swirl does not alter the flame shape, it does substantially increase the burning rate. Since the combustion rate is proportional to the burning velocity and the flame area it was presumed that the increased rate of burning resulted from the flame wrinkles which increased the flame-front area.

Another means of reducing combustion time involves the use of multiple ignition. Diggs [38] experimented with a side-valve CFR research engine which was equipped with 17 spark plugs and was used to investigate the relationship between burn speed and knock, without changing other engine parameters.

It was postulated that, if an increased combustion rate acts to increase the end-gas pressure and temperature, the benefit that might be expected from the reduced end-gas residence time would be offset to some extent. The end-gas temperature was estimated from the pressure measurement and, when all plugs were fired simultaneously, the final pressure and temperature was found to be 3.5 bar and 22°C higher than with one plug only. This increase in pressure and temperature was considered to be negligible in terms of its likely effect on knock and it was noted that shorter combustion duration that resulted when all the plugs were fired together resulted in a significantly reduced Octane requirement. It was also observed that if the spark plug was sited far away from the exhaust valve, the octane requirement of the engine increased. It was inferred from this result that heat loss in the end-gas region was an important consideration and that the end-

gas region should be arranged as far from the hot exhaust valve as possible. Whilst this conclusion is not necessarily disputed, it should be noted that in this case, the selection of different spark-plug positions also resulted in different flame propagation geometries and consequently different overall combustion rates, which may have independently influenced the octane requirement.

Test results with combustion chamber deposits shortened the combustion durations when firing a single plug, but this did not apply when all 17 plugs were fired. The effect of thermal insulation on heat loss could not be separated from the changed burn duration and the results pertaining to the effects of deposits were inconclusive.

The relationship between combustion rate and turbulence, whether initiated by the inlet process or by the piston motion, was demonstrated by means of a sophisticated theoretical model by Maly [39]. During the initial stages, flame propagation was shown to be sensitive to external conditions such as initial temperature and heat loss. However, once the flame front had established itself as a stable, self-propagating flame front, the rate of combustion was almost exclusively dependent on the time function of the micro-turbulence.

Reviewing the Ricardo test results in the light of the above discussion, it may be appreciated that the traditional techniques of knock control applicable to gasoline do not necessarily apply in the case of methanol. Since the auto-ignition reactions of methanol are an order of magnitude more rapid than those of gasoline, methods of knock control involving more rapid combustion are not applicable. Moreover, it follows that methanol is not subject to the same knock-limited engine-size constraints that apply to gasoline since the flame transit time is not a relevant factor. The chief parameters that determine whether methanol will auto-ignite are the temperature and, to a lesser extent, the pressure of the end-gas. This leaves end-gas cooling as the only viable option for extending the knock limit of the methanol engine.

### 3.1.2 The mechanism of squish as a means to control knock

Since the Daimler Benz experimental engine featured squish prominently in its combustion-chamber design, this aspect was considered in some depth.

The reference to the Ricardo HRCC combustion chamber design cited end-gas cooling in the squish zone as the reason for its beneficial effect. Whilst there is no doubt that squish is an effective means of controlling gasoline knock, not all researchers are in agreement as to the reason for its effectiveness.

For example, Caris [36] concluded that increased turbulence, generated by the squish action, was responsible for the improved knock resistance. The importance of the piston crown to head clearance was discussed in relation to actual test data. A reduction in bump clearance from 4.7mm to 1mm, reduced the octane requirement by 12 numbers. Although it was difficult to separate the effects of squish and quench, it was noted that the end of combustion generally occurred when the piston was already on the down stroke. As the piston began to descend, it was argued that the flame front was sucked into the squish zone which would result in a reduced combustion time and it was therefore unlikely that quenching was the dominant mechanism. It was concluded that the reduction in bump clearance must result in a substantial increase in turbulence. When the bump clearance was reduced by the accumulation of deposits, however, the knocking tendency increased which was ascribed to the attendant increase in compression ratio.

Gatowski [37] also studied squish as an alternative method of increasing the combustion rate and found that the turbulence generated by the squish action was very localised and limited to that part of the combustion chamber close to the inner edge of the squish region. It was presumed that the high squish velocities resulted in localised heat loss to the chamber walls and therefore the squish zone should be sited on the opposite

side of the combustion chamber from the spark plug in order to function as a means of knock suppression. In their discussion, however, the authors considered yet another possibility. An indirect consequence of the squish design is that making part of the combustion chamber smaller results in the other part of the chamber becoming more open, with the result that the flame can initially grow unobstructed, with maximum surface area and thus maximum speed.

This last observation was observed experimentally by Lucas [40]. In tests using ionization probes with different combustion chamber shapes, it was found that the squish design exhibited a slightly higher initial flame speed when compared to the disk combustion chamber designs, and a slightly lower flame speed during the latter flame travel period. A simulation model was developed which confirmed the experimental findings and indicated that 50% squish area yields the maximum combustion rate.

Unlike the Maly combustion model, Lucas' simulation showed that the burning velocity may be affected by increased charge temperature as well as by enhanced charge turbulence. The simulation was used to explain the increased flame dispersion in the latter part of the combustion which was noted with squish chambers and was attributed to flame quenching effects in the squish zone. The bump clearance was 0.8mm in this particular experiment.

Thus there are four distinctly different explanations for the mechanism whereby squish suppresses knock:

a) The quenching effect of the large surface area to volume ratio in the squish region reduces the temperature of the end-gas.

b) The high squish velocity results in increased heat transfer in the squish zone which, in turn, results in a lower end-gas temperature.

c) The turbulence generated by the squish action results in a rapid combustion rate that suppresses knock by reducing the time available for auto-ignition reactions to occur.

d) The compact combustion chamber shape that indirectly results from the squish design promotes rapid combustion by virtue of the large initial flame-front area. This suppresses knock by reducing the time available for auto-ignition reactions to occur.

It was recognised that the confusion surrounding the mechanism of squish was, in part, reflected in the lack of understanding of heat transfer in engines as a whole. However, whilst gasoline would respond favourably to any one of the above mechanisms, methanol could be expected to respond favourably to only the first two which involve end-gas cooling. Thus it was appropriate that the present research effort should concentrate on the problem of heat transfer in the squish zone, and its potential for the suppression of methanol knock.

### 3.1.3 Heat-transfer in engines

Two heat-transfer problems were contained within the Daimler-Benz investigation. Firstly, the thermocouple signals were used to determine the heat-flux into the cylinder head. Secondly, the heat transfer through the gas thermal boundary layer was studied. Whilst these were very specific analysis problems, it was helpful to consider the more general subject first.

The difficulties associated with the study of heat transfer in engines were summarised very concisely by Borman [31]

"The heat flux to the surface of a reciprocating-engine combustion chamber varies from zero to as high as 10MW/m² and back to zero again in less than 10msec. The flux also varies dramatically with position; portions of a surface only 1cm apart can receive peak fluxes differing by as much as 5MW/m². To add to the complexity, the flux pattern varies considerably from cycle to cycle."

There have been many different approaches to analyse heat transfer in engines; they may be categorised five main groups:

- Global (one zone) thermodynamic models
- Zonal (more than one zone) thermodynamic models
- One-dimensional fluid-dynamic models
- Multi-dimensional fluid-dynamic models
- Radiant heat-transfer models

3.1.3.1 Global models: These models deal with the overall empirical heat transfer coefficients which are generally assumed to be the same for all heat transfer surfaces within the cylinder. A quasi-steady state assumption is used, as indicated by the expression,

$$q'' = h\ A\ (T - T_w) \qquad kW/m^2$$

where $q''$ is the heat flux, "h" the heat transfer coefficient, "T" is the bulk gas temperature and "$T_w$" is the wall surface temperature. To incorporate different wall temperatures in different parts of the combustion chamber, the expression may be modified,

$$q'' = h \sum_{n=1}^{N} A_n\ (T - T_{wn}) \qquad kW/m^2$$

A number of researchers have proposed models based on empirical correlations with engine data. Eichelberg [31] made the first measurement of instantaneous heat flux and proposed the following formula,

$$h = 7.67 \times 10^{-3}\ C_m^{0.33}\ (P\ T)^{0.5} \qquad kW/(m^2K)$$

where "$C_m$" is the mean piston speed and "P" and "T" the pressure and temperature. This formula was widely used and was modified slightly by various subsequent researchers to correlate with specific test results.

Dimensional analysis was considered as a means to a more fundamental expression for heat flux. The energy equation, which consists of the storage, conduction, convection, pressure work and heat generation terms, contains too many unknowns to be solved in its entirety and simpler models have been proposed of the form,

$$Nu = C\ Re^{n}$$

Taylor [18] showed that the time-averaged heat flux exponent, "n", ranged from 0.5 to 0.9, depending on the engine type and when the Reynolds number was based on the cylinder bore with a mass flow rate that was equivalent to the mean mass flow rate through the engine.

Annand [41] proposed the following formula which is based on the similarity law of steady turbulent heat transfer.

$$q'' = a \frac{k}{D} Re^{0.7}(T - T_w) + b\ (T^4 - T_w^4) \qquad kW/m^2$$

where "a" is a constant ranging from 0.35 to 0.8 depending on the intensity of the charge motion. The second term represents the radiant heat flux and was based on gray-body radiation. The constant, "b", was suggested to be $4.3 \times 10^{-12}$ $kW/m^2K^4$ for spark ignition engines.

Woschni's equation [42] is yet another widely used correlation based on the similarity law, but derived from an engine heat balance.

$$h = 0.0136\ W^{0.8}\ P^{0.8}\ D^{-0.2}\ T^{-0.547} \qquad kW/(m^2K)$$

where the reference velocity, "W", represents the mean gas velocity affecting the heat transfer and is given for each stroke of the engine cycle.

Hohenberg [31] made a slight modification to Woschni's formula to give a better correlation of the time-averaged heat flux calculated from experimental data obtained using one-dimensional heat-flux probes.

It should be stressed that the local models were not intended to describe the details of the local and unsteady heat transfer effects because they deal with the overall effects on the engine cylinder and they employ quasi-steady state assumptions. Such global models should not be expected to reveal details of local and instantaneous heat transfer conditions, even though the data from which they were obtained were typically instantaneous local values.

3.1.3.2 Zonal modeling: Zonal modelling divides the chamber gas volume into a relatively small number of control volumes, each of which has its own temperature history and heat-transfer coefficient. Additionally, the fraction of the heat-transfer surface area which is exposed to each gas volume must be estimated. Predictions of heat rejection from each control volume are usually made using global models applied to each zone. Zonal modeling is suited to the study of spark-ignition engine operation under knocking conditions, in as much as the local conditions are treated separately. However, the unsteady nature of the heat transfer should be also taken into account if the situation is to be analysed correctly, and this requires a more sophisticated analysis technique.

3.1.3.3 One-dimensional fluid-dynamic models: Blumberg [43] stressed the importance of considering the temperature gradient normal to the wall. The global models, which are empirical Nusselt-Reynolds number relationships derived from the equations for steady turbulent flow in pipes and over plates, have severe limitations in that the boundary layer effects are ignored, the time variation of the Nusselt number is ignored and there is no provision for predicting the effects of engine and combustion

chamber design changes, such as increased swirl or squish. Results were presented for an engine simulation that was carried out where the thermal boundary layer was modelled. It was postulated that heat was removed from a growing boundary layer adjacent to the cylinder surfaces rather than from the bulk gases. The steady growth of the boundary layer during the combustion and expansion phase was illustrated and, coupled with an adiabatic core calculation, gave accurate NOx predictions.

The assumption of a one-dimensional temperature distribution normal to the wall surface is valid only where the temperature gradient normal to the wall is much steeper than the parallel components. This is the case for a disk-shaped combustion chamber during the compression cycle, for example. Calculations of this type generally correlate better with measured heat flux profiles as was illustrated by Borman, referring to the work of Oguri [31], where the convective term from the energy equation was eliminated by assuming an effective conductivity for the gas boundary layer. The calculation was less precise when the gas flow was not lamina. A reasonable analysis of the squish zone should be possible using this technique.

3.1.3.4 Multi-dimensional models: Whilst models of this type have the possibility of predicting very detailed information about the conditions within the engine combustion chamber, they are still in a stage of early development and progress is dependent on the development of accurate turbulence models and boundary layer models.

3.1.3.5 Radiation models: The radiation heat transfer in spark ignition engines has been estimated at about 10% of the total heat transfer [31]. For the purposes of this research, where the heat transfer prior to the flame arrival was of interest, and bearing in mind that the radiation heat-transfer law relates to the difference of the temperature to the fourth power, the radiation effects were considered to be insignificant and consequently ignored.

## 3.2 THEORETICAL BASIS

### 3.2.1 Heat flux calculation from wall temperature measurement

The total heat flux on the wall surface was calculated by solving the unsteady heat conduction equation for the heat transfer within the cylinder wall, with the boundary condition given by the surface temperature measurements.

The assumption was made that the heat flow was one-dimensional and that the hot junction temperature measured by the thermocouple is the true surface temperature. Since the unsteady component of the interior wall temperature field exists only within a relatively shallow depth from the surface, the unsteady component of the temperature gradient which is perpendicular to the wall is usually much larger than that parallel to the surface. Thus, the assumption of one-dimensional heat flow is reasonable for the transient component but may not hold true for the time-averaged component.

Details of the solution of the one-dimensional, unsteady heat conduction equation and the derivation of the expression for the heat flux is given in appendix C. The final form of the heat flux contains two terms, the average heat flux plus the time-variable component:

$$\frac{dq}{dt} = \dot{q}_m + k \sum_{n=1}^{N} \left[ \frac{n\omega}{2a} \right]^{0.5} \cdot \left[ (A_n+B_n) \cos(n\omega t) + (B_n-A_n) \sin(n\omega t) \right] \qquad (3\text{-}1)$$

In practice, the value of average heat flux, "$\dot{q}_m$", is not known. However, at some point during the compression stroke, the wall surface temperature must equal the gas temperature and at that point, the heat flux is zero. Since the gas temperature may be calculated with reasonable accuracy during the compression stroke, and the wall temperature was measured, the value of "$\dot{q}_m$" may be determined for that condition.

3.2.2 Thermal boundary layer calculation.

With the engine operating at border-line knock conditions, the Ricardo knock-characterisation data was used to determine the bulk end-gas temperature. With this data, and with the measured surface temperature at the location of the auto-ignition origin, it was possible to determine the boundary layer temperature profile.

A similar approach to that of Oguri was adopted (see section 3.1.3), in that the convective term from the energy equation was eliminated by assuming an effective conductivity for the gas boundary layer. This simplification was reasonable since the area of interest was in the squish zone, where the gas flow was predominantly parallel to the cylinder-head surface. The distance between the piston-crown and the cylinder head was divided into 50 equal elements. The calculation was initiated at the point where the gas temperature and the wall temperature were equal. At each successive crank angle, the temperature of each element was incremented as a result of the pressure work. The gas temperature profile was calculated using Schmidtt's method described by Holman [44] and Schlichting [45], to match the total heat loss from the end-gas zone with the heat flux into the cylinder head that was determined by the method described in section 3.2.1 above.

The heat flux to the piston was assumed to be equal to that flowing into the cylinder head. This assumption was justified on the basis of typical data given by Borman [31]. The reported figures indicated that about 50% of the heat lost went into the piston and about 30% into the cylinder head. However, when allowance was made for the surface area of the piston bowl, the heat-flux per unit area was approximately the same for both the piston and the cylinder head. The remaining 20% heat flux was assumed to be lost to the valves and the cylinder walls.

## 3.3 EXPERIMENTAL TESTS

The engine used for these studies was a Daimler Benz OM 407 diesel engine, of which one cylinder was fitted with special low compression ratio pistons and instrumented with the special thermocouple cylinder head. Details of the thermocouple construction are given in Appendix D. Figure 8 shows a plan view of the cylinder head and the arrangement and numbering of the thermocouples. On commissioning, it was found that thermocouple number 10, (Tc 10), was defective.

The principal details of the test cylinder were:

| | |
|---|---|
| Bore | 125 mm |
| Stroke | 155 mm |
| Connecting rod | 256 mm |
| Compression Ratio | 9.5 (Gasoline tests) |
| | 12.5 (Methanol tests) |

The tests were conducted using one of the six cylinders converted to spark ignition and inlet manifold fuel injection. Details of the experimental arrangement and the analytical equipment are given in Appendix D.

The tests were conducted at borderline knock with wide-open throttle and at 1300 rev/min. As with the Ricardo tests, the fuels used were commercial grade 98 RON gasoline, and standard grade methanol.

Details of the software routines that were developed to analyse the data are included in Appendix D.

### 3.3.1 Experimental test details

The gasoline tests were conducted first owing to the possibility of damage occurring to the thermocouple cylinder head during the methanol knocking tests. Initially, the standard cylinder head

with a pressure transducer access hole was fitted. The trigger and ignition point were calibrated against the motoring pressure signal and tests were conducted to establish the boundaries of air flow, fuel flow and ignition timing that would permit knock-free and knocking operation.

It was found that the 8.5:1 compression ratio was too high to permit knock-free operation at wide open throttle with the timing set in the normal range that would result in the peak pressure occurring about 15° after TDC.

On removal of the cylinder head slight signs of piston crown damage were evident, having the classical rough erosion appearance attributed to knocking. A photographic reproduction of the piston damage is shown in figure 9. The damage was not sufficiently severe to warrant changing the piston and was considered a bonus in that the exact locations of the knock origin were clearly evident.

The standard cylinder head was replaced by the thermocouple head. A series of tests was performed with the engine operating without knocking and all the thermocouple signals were scanned. The pressure trace before and after the scan was also recorded. A single test sequence of knocking operation was undertaken whilst monitoring a thermocouple array which projected radially into the area of known knock origin. During this test two thermocouples, numbers 3 and 70, were damaged and it was decided to limit the knocking test to avoid further damage to the cylinder head.

The piston was changed to raise the compression ratio to 11.5:1 and the standard cylinder head was fitted. The fuel system was drained and flushed with commercial grade methanol and firing tests resumed. This compression ratio was found to be too low and knocking could not be induced at any speed. It was apparent that the combustion was close to knocking by the level of high frequency combustion noise generated toward the end of combustion.

The piston was changed again to raise the compression ratio to 12.5:1. Tests with the standard cylinder head indicated that knocking was easily induced at this compression ratio. Knocking was deliberately induced with the intention of producing a witness mark on the piston crown as was done in the petrol tests. On two occasions the knocking pressure trace began advancing, signifying that the increased combustion-chamber temperatures associated with the knocking had induced preignition and this was confirmed by switching off the ignition which had no effect. A solenoid valve had been incorporated in the fuel injection system to cope with just this situation and control was easily re-established. Despite the moderately severe knocking, on removal of the cylinder head, no sign of knock damage was found on either the piston or the cylinder head, which was unexpected. However, the subject of knock damage is considered in the light of the experimental observations in section 3.4.

The thermocouple head was fitted. The intention was to monitor all the thermocouples firstly with the engine slightly throttled and non-knocking, followed by a scan under knocking conditions. However, whilst the engine was being warmed up preparatory to the non-knocking scan, a preignition situation developed, possibly originating from the combustion deposits that had accumulated on the cylinder head during the petrol tests which had not been removed for fear of damaging the gold plating. The fuel supply was switched off but not before a few severe knocking cycles had occurred (estimated about 5 cycles). It was subsequently established that 38 thermocouples were damaged as a result of this mishap. Figure 10 depicts the thermocouple locations where damage occurred.

The non-knocking tests were conducted followed by a limited scan at wide open throttle with knocking combustion. After these tests it was found that altogether 65 thermocouples were defective, most being situated on the outer circumference and in the area situated furthermost from the spark plug. On removing the cylinder head, it was apparent that the cause of the thermocouple failure was due to stripping of the gold film. In addition,

cracks were found between the spark plug aperture and both the inlet and exhaust valve apertures. Figures 11 and 12 show photographs of the damage to the cylinder head. The piston showed no sign of knock damage, as is apparent from the photograph shown in figure 13. However, burnt oil stains were evident on the top-land area which appeared streaked beneath the exhaust valve and indicated the swirl pattern.

## 3.4 DISCUSSION OF RESULTS

### 3.4.1 OM 407 Test Results With Gasoline

As this was the basis for comparison, attention was first given to the analysis of the gasoline combustion characteristics and the gasoline flame propagation.

A typical example of two thermocouple traces is shown in figure 14 and 15. These traces represent the average of 50 engine cycles. The point of flame arrival was clearly evident, shown arrowed in each figure. In figure 14, the thermocouple was sited near the spark plug. After the flame had passed over the thermocouple at -6°CA, the product gas temperature was progressively heated by the subsequent pressure rise until a peak temperature was registered at about +30°CA. Figure 15 shows the trace of a thermocouple sited in the squish zone at the outer extremity of the flame travel. Here flame arrival was much later, at +7°CA. Prior to the flame arrival, there was a significant temperature rise corresponding to the compression of the unburned gas by the rising pressure.

With the engine operating close to the knock point at steady state conditions, all the thermocouples were sampled over 50 cycles and averaged. The point of flame arrival was determined for each thermocouple and the results were processed by a contouring program. The inlet and exhaust valve areas were filled using linear interpolation and a simple smoothing algorithm was used. The result is shown in figure 16.

What was immediately apparent from the flame propagation contours was the excellent correlation between the end-gas zones indicated by the thermocouples and the sites where the piston was damaged as a result of severe knocking, shown in figure 9. The contours under the inlet and exhaust valve should be regarded with caution, particularly where the valve is tangent to the bore since in that region there were no thermocouple readings to permit interpolation and the readings had to be extrapolated.

Besides the outer extremities of the piston crown, there was evidence of an end-gas zone within the piston bowl. This was confirmed by the evidence of high temperature burning of the surface carbon deposits within the piston bowl, shown in figure 9. That knock does not always occur at the outer extremities of the combustion chamber was noted by Baker [46], who presented results based on a Ford 2.01 OHC engine fitted with different cylinder heads to give different amounts of swirl. His analysis of the detonation cycles with the low-swirl head revealed occasional bulk detonation instead of the more usual end-gas detonation.

The two surface temperature traces shown, in figure 14 and 15 for positions near the spark plug and in the squish zone respectively, indicated a significant difference in temperature across the surface of the cylinder head. This was studied more closely using the contouring program to plot isotherms of the average temperature. Shown in figure 17, a maximum average temperature of 458°C was recorded in the vicinity of the spark plug and the exhaust valve whilst temperatures of about 200°C were measured in the end-gas zone. The comparing figures 16 and 17, the similarity between the temperature gradient across the cylinder head and the flame propagation profile was clearly evident. This was to be expected in the light of the findings of Lewis and Von Elbe [12], who showed that, for combustion in a closed vessel, the burned-gas temperature is not uniform and that the flame origin is the highest temperature zone, extending radially outward to the lowest temperature zone at the point where the flame terminated. These contour plots served to confirm

the importance of using a large number of surface temperature measurements. For example, Lee [47], who used only two surface thermocouples in his study of the mechanism of knock damage, tacitly assumed that his measured temperature values were representative of the whole combustion chamber, which is quite clearly incorrect.

As stated earlier, a full scan of all the thermocouples was not undertaken under knocking conditions to minimise the chance of damage to the cylinder head. Instead, a single test sequence of knocking operation was undertaken whilst monitoring a thermocouple array which projected radially into the area of known knock origin. It was apparent that the thermocouple recording was made before the engine had reached thermal equilibrium, since the local surface temperature levels were generally lower than those indicated in figure 17.

From the 50 cycles captured, a typical example of knocking combustion and non-knocking combustion was selected for discussion. Figure 18 shows the two pressure traces superimposed. Although the knocking trace showed a vibration following the knock itself, the actual knocking frequency of about 6.7 kHz was too high to be digitised at a sample frequency of 1° per reading and was therefore attenuated by the low-pass filter. The corresponding thermocouple traces for two locations are shown in figure 19. The signal noise levels were reduced by taking a five-point average. As might be expected, the knock cycle resulted in a greater surface-temperature rise at both thermocouple locations. Although the surface temperature appeared to indicate the flame arrival before knock was registered by the pressure transducer, this was attributed to the data smoothing algorithm although it is also possible that the knock originated at some other point away from the presumed knock source near the recorded thermocouples.

The heat flux was calculated from the surface temperature data, as described in Appendix C, and the results corresponding to the two thermocouples depicted in figure 19, are shown in figures 20

and 21. As indicated by the temperature rise, the peak heat flux under knocking conditions rises two to threefold above the peak value for normal operation. This was greater than the 70% heat-flux increase reported by Enomoto [32] for knocking operation, although the increase would undoubtedly depend on the level of knock intensity. The difference in the magnitude of the heat flux shown in figures 20 and 21 was interesting. The peak heat flux of the 5 adjacent thermocouples, corresponding to the knocking and non-knocking cycles used in the above discussion, are depicted in the form of a bar-chart in figure 22. Whilst the peak heat flux under normal combustion was relatively constant at about 4MW/m², the knocking combustion revealed a distinct trend, with the minimum peak heat flux occurring at the supposed knock origin, and increasing on either side. Before discussing this observation further, it is necessary to look at the heat flux data in conjunction with the knock-characterisation information which was obtained with the aid of the Ricardo engine and to solve for the boundary-layer temperature profile.

### 3.4.2 Heat-flux analysis and gasoline end-gas temperature

Borman [31] noted that the measured surface temperature varies considerably and almost randomly from cycle-to-cycle under steady engine operation. The reason for these variations was attributed to local randomness in the flow field and averaging over many engine cycles was advocated to cancel out the random variation. Thus, the result of a heat flux analysis of 50 consecutive engine cycles of the thermocouple number 11 is shown in figure 23. The estimated flame arrival time, indicated in figure 16, corresponded with the heat flux having already risen to 50% of its maximum value. It was assumed that this followed as a consequence of the smoothing algorithm although it is interesting to note that a similar situation was reflected in the data which was presented by Borman.

Figure 23, which was typical of the heat flux in the end-gas zone, revealed two characteristic peaks, a small peak at -17°CA and a major peak at 14°CA. The main peak clearly corresponded with the flame arrival. The much smaller peak was thought to relate to the heat transfer associated with the squish-gas motion. As the piston nears TDC, the high gas velocities associated with the squish action result in increasing heat transfer. However, with the expansion of the burning gas following ignition, this inward flow is arrested, and the heat flux drops again.

A similar effect was noted by Alkidas [48] who used heat flux probes (fast response surface thermocouples) in a divided-chamber diesel engine (Comet head). For two probes situated in the engine main chamber, the heat flux showed two distinct peaks similar to the ones shown in figure 23, one just before TDC and the second at about 30° ATDC. The first peak was ascribed to the effects of the compression gas motion and the second to the effects of combustion in the main chamber. The effect of increasing the engine speed from 1000 rev/min to 2500rev/min resulted in a compression heat flux peak increase of 0.7 to 1.0 MW/m², and a combustion heat flux peak increase of 27 to 36 MW/m².

The characteristic fuel constants obtained from the Ricardo tests were used to determine the gas temperature in the end-gas region under knocking conditions. The pressure diagram and engine speed provided the necessary basis for the calculation and the gas temperature was calculated in the manner described in section 2.3, the only difference being that, in this case, the starting temperature was unknown and had to be determined by trial and error, until the point at which knock occurred corresponded with the theoretical characteristic expression for gasoline.

$$1 = \int_{t_o}^{t_c} \frac{dt}{1.68\times10^{-3}\, P(t)^{-0.66}\, e^{\frac{8850}{T(t)}}} \qquad (3\text{-}2)$$

Figure 24 shows the resulting temperature development diagram and the corresponding measured surface temperature.

The one-dimensional heat transfer analysis, described in section 3.2.2, was conducted using the known bulk gas temperature and the measured heat flux. Figure 25 shows the gas temperature profile at the point of knock, corresponding to thermocouple position 11. The adiabatic temperature (computed from the pressure diagram) is also shown and it may be seen that core temperature was cooled to 24°C below the adiabatic temperature.

This result indicates clearly that squish design in this particular engine did not appreciably lower the end-gas temperature, although it should be noted that the bump clearance for an engine of this size was larger than is generally possible with smaller engines (1.5mm as opposed to less than 1mm).

The same analysis was performed on the adjacent thermocouple positions with interesting results. Figure 26 shows the temperature profile at position 3, the absolute outer extremity. Here there was a significant cooling effect on the end-gas resulting in a final temperature which was about 150°C below the adiabatic temperature, although the final temperature was lower than the peak temperature, as is shown in figure 27, where the gas temperature and the adiabatic temperature are shown on a time base. The gas temperature rose to 700°C before the heat loss took effect.

This result may relate to an observation made by Maly [39], who noted that increasing the squish clearance is beneficial in reducing or eliminating knock damage to the head gasket. If one accepts the conclusions of Lee [47], that knock damage is primarily caused by the mechanical action of the shock wave, then it is to be expected that the primary damage will occur at the combustion chamber periphery where the first shock wave reflection occurs. Moreover, the act of increasing the squish clearance will allow the adiabatic core to extend deeper into the squish zone which gives less opportunity for the initial shock wave to develop before it reflects off the nearest wall.

Moving inwards, the thermal boundary layer profile corresponding to position 23 is shown in figure 28. Here too, the final temperature was more than 100°C below the adiabatic temperature. This was ascribed to the higher heat flux prior to the flame arrival that was measured at the rim of the piston bowl and confirmed the discussion in section 3.1.2 referring to the very localised turbulence and heat transfer associated with the squish design.

Finally, the temperature profile at position 37, at the edge of the piston bowl, is shown in figure 29. The analysis predicts that adiabatic temperatures will be achieved here because the thermal boundary layer is only 1mm to 2mm in thickness. Although this is probably true, the assumptions implicit in the one-dimensional analysis are not strictly valid outside of the swish zone. The possibility of adiabatic temperatures occurring in the piston bowl corresponds with the evidence of some auto-ignition having originated there, despite that fact that the flame would arrive at the edge of the piston bowl first.

It should be emphasised that the end-gas temperature profile calculation was based on the measured heat flux up to the point of flame arrival. It is interesting to note that the areas of greatest end-gas cooling, at the piston-bowl edge and at the outermost extremity of the squish zone, corresponded with the areas of peak heat flux that occurred following knocking combustion, as was indicated in figure 22. This would seem to confirm that these areas represent the zones of greatest turbulence.

### 3.4.3 OM 407 Test Results With Methanol

As was done with the petrol tests, the engine was operated using methanol close to the knock point and at steady state conditions, and all the thermocouples were sampled over 50 cycles and averaged. The point of flame arrival for each thermocouple was processed by the contouring program to yield figure 30. It should

be reiterated that a significant number of thermocouples in the end-gas region had been damaged at this point and some of the detail of the flame profile in that area was inferred from the data interpolation.

Despite the lack of data beneath the inlet and exhaust valves, the extrapolation of the data at the periphery of the valves indicated a complete fragmentation of the flame front. The end-gas zone appeared to be situated in the squish area farthest from the spark plug which corresponded to the area where most of the thermocouple damage occurred.

It was clear from figure 30 that the flame shape and propagation was very much more distorted by turbulence in the case of methanol than was the case for petrol. Despite the spark plug being situated in the centre of the combustion chamber, by the time that a flame front was detectable, the flame kernel had apparently moved 15mm from its origin, indicating the presence of significant gas motion. The shape of the flame front as it developed indicated the presence of considerable swirl, as might be expected from the smaller piston bowl diameter.

The surface temperature was mapped as shown in figure 31. The hottest surface coincided closely with that for the petrol tests. There was also a remarkable correlation between the inferred flame activity in the valve areas and the inferred surface temperature, bearing in mind that these two parameters were obtained independently from the thermocouple data.

Figure 32 shows 20 consecutive recordings for thermocouple number 27, sited close to the end-gas zone. Of the 20 cycles, 19 were normal combustion cycles whilst one was a violent knocking cycle, causing a surface temperature rise of about 70°C. This compares to a rise of about 50°C for petrol, shown in figure 18. This illustrates a subjective observation that was noted whilst conducting the tests, that for each engine cycle, methanol tends to either knock very severely or not at all.

It was noted that for petrol there was a slight discrepancy between the thermocouple signal of an abrupt rise in the surface temperature and the indication of knocking from the pressure transducer signal. With methanol the pressure response was simultaneous as shown by figure 33 which represents the pressure transducer signal corresponding to the knocking trace. The surface temperature measured by thermocouple number 153, situated on the opposite side of the inlet valve from thermocouple number 27 also indicated an instantaneous response to the knock, as shown in figure 34. The simultaneous rise in the surface temperature at 0° in both traces, corresponding with the pressure signal spike, was clearly indicative of a shock wave.

### 3.4.4 Heat-flux analysis and methanol end-gas temperature

The heat flux calculation for methanol combustion at border-line knocking conditions was analysed in the same manner as that of the gasoline data. An example of the heat flux for thermocouple number 17 is shown in figure 35. As was the case with gasoline, there was evidence of squish-induced turbulence at about -18°CA which resulted in a small peak in the heat flux, which diminished as the squish was counter-acted by the gas motion associated with the flame propagation.

The bulk end-gas temperature was determined by trial error to correlate with the simplified methanol knock model that was proposed and discussed in Chapter 2, ie.

$$T(max) = 1000 + 1.86\ P(max) \qquad (3\text{-}3)$$

The resulting temperature diagram revealed an interesting feature. Figure 36 shows the gas temperature development with time and it may be noted that for half the compression stroke, the gas temperature was sub-zero. This was attributed to fuel evaporation. The fuel was injected into the inlet port in liquid form and, allowing for the difference in air-fuel ratios between methanol and gasoline, it was known to have a latent heat capacity of about 900% of that of gasoline.

The heat flux calculations were treated in a similar manner to those of gasoline. The resulting thermal boundary layer for two thermocouple locations is shown in figures 37 and 38. In both cases, the end-gas core temperature was the same as the adiabatic temperature, as shown, with relatively little development of the thermal boundary layer having taken place. The explanation for this difference between the analysis for methanol compared to gasoline was traced to the relative combustion rates. Comparing figures 16 for gasoline and 30 for methanol, the combustion duration for methanol was about 20% shorter than that of gasoline. This meant that there was 20% less time for heat loss to occur in the case of methanol.

The reason for the difference in combustion rate was ascribed to the increased compression ratio which, as was already noted, resulted in increased turbulence. As was discussed in section 3.1.1, the concepts of end-gas cooling and the promotion of rapid combustion are mutually exclusive, since end-gas cooling requires a gradual temperature rise to be effective whilst rapid combustion results in a fast temperature rise. Hence it was clear from figures 37 and 38 that, for effective end-gas cooling in the case of methanol in the OM 407 engine, a piston-crown to head clearance of much less that 1mm would be required, since the thermal boundary layer at the time of flame arrival was only about 0.5mm.

The relatively thin thermal boundary layer in the case of methanol, raises an interesting point of comparison between the knock behaviour of methanol and gasoline. Borman made an observation concerning the boundary layer thickness and knock [31]. He noted that, in practice, a substantial amount of the cylinder mass (10-20%) is cooled in the boundary layer to a temperature well below the core temperature, and consequently does not attain knock conditions at the same instant as the end-gas core itself. The manifestation of this situation would relate to the intensity of the auto-ignition, the thicker the thermal boundary layer, the more gradual would be the transition from knock-free operation to knocking operation. It is possible that

the effect of the relatively less developed thermal boundary layer in the case of methanol correlates with the subjective observation already noted, that methanol either knocks severely or not at all.

## 3.4 CONCLUSIONS WITH REGARD TO THE OM 407 TESTS.

The principal conclusions of the Daimler Benz 407 engine tests are summarised below:

1. The mapping of the flame profile, indicated by the sudden rise in surface temperature, correlated with the mapping of the combustion chamber average surface temperature for both the gasoline tests and the methanol tests. Confirmation of the flame profile was obtained in the form of slight knock damage that left witness marks on the piston after the gasoline tests and resulted in damage to selected thermocouples after the methanol tests.

2. The flame-mapping data indicated that the turbulence and swirl was increased significantly by the increased compression ratio in the methanol tests. This finding was confirmed by the combustion duration, which was 26°CA from ignition to peak pressure in the case of gasoline and 23°CA in the case of methanol. On the basis of the tests reported by Maly, this difference was assumed to be solely due to the different levels of turbulence and swirl in the two tests.

3. The application of the knock model, derived from the Ricardo tests, was used to determine the gas temperature in the end-gas region. This data, in conjunction with the surface temperature data, revealed that the end-gas region was not effectively cooled by the squish design, and that the core temperature of the end-gas was essentially the adiabatic temperature that was calculated by assuming isentropic compression. It was however found that the thermal boundary layer was virtually fully developed in the case of the

gasoline tests whilst in the methanol tests, the more rapid combustion resulted in a less developed boundary layer, despite the greater turbulent gas velocities. Thus, for this particular engine, the squish design was found to be effective as a means for suppressing knock with gasoline by virtue of the rapid combustion which reduced the time available for the relatively slow auto-ignition pre-reactions. Since the methanol auto-ignition reactions were very fast and, since squish was not effective in cooling the end-gas temperature, it was concluded that the squish design in this particular engine had no beneficial effect with regard to the suppression of methanol knock.

4. The possibility of using squish to cool the end-gas region in an engine was not excluded *per se* by the findings of this research. The thermal boundary layer was calculated to be about 0.5mm at the point of flame arrival for methanol, from which it may be inferred that a bump clearance between the cylinder head and the piston crown of 1mm or less, could potentially have a cooling effect. However, it was clear that the squish design inherently generates turbulence and results in a compact combustion chamber, both of which cause an increase in combustion rate which reduces the time available for heat loss to occur.

5. Although engine speed was not examined in this study, all the literature pertaining to heat loss from engines indicated that increased engine speed allows less time for heat loss to occur and, despite greater turbulence levels, the end-gas temperature will tend towards the adiabatic temperature. Thus, in the case of methanol, where the knock reactions are so fast that there is no benefit derived from the rapid combustion associated with increased engine speed, it may be inferred that squish offers no real potential for knock suppression in high-speed engines.

# CHAPTER 4

## CONCLUSIONS WITH REGARD TO THESIS OBJECTIVES

It is perhaps appropriate, at this stage, to review the thesis objectives. In view of the high octane rating of methanol, it was proposed that the research should look at the possibility of using methanol as a diesel replacement, with particular attention being given to the limitations imposed by the knocking combustion of methanol and gasoline with respect to engine size and combustion chamber shape.

The analysis of the fundamental knock characteristics of gasoline and methanol, using the Ricardo engine, revealed a significant difference between the two fuels. Evidence was found that suggested that the auto-ignition reactions of methanol were very rapid in comparison to gasoline. A consequence of this finding was that the point of auto-ignition reduced to being a function of pressure and temperature only and was virtuallyindependent of the flame transit time and the rate of combustion.This led to the conclusion that the methanol engine was not limited by engine size and that knocking with methanol would not necessarily occur at low engine speed.

As yet unpublished research that has been in progrs at the University of Cape Town, involving the chemical kitic modelling of methanol combustion, has arrived at similar conusions with regard to the very rapid rate of reaction that occs when methanol auto-ignites. Unfortunately, this chemicamodelling was restricted to the use of the available rate consta data that was only valid for atmospheric pressure, and therere the correlation is not strictly conclusive. Also, the fluence of pressure that was observed in the engine test daas not reflected in the chemical model, although this y e also due to the use of low-pressure rate-constant data.

This pressure influence was significant because the trend was opposite to that of gasoline. The trend for gasoline indicated that the maximum temperature that may be tolerated at the knock-limit decreased with an increase in pressure, whilst for methanol the maximum temperature increased with pressure. This would imply that for methanol, knock would be more likely to occur at high engine speed, or at high altitude, assuming constant inlet temperatures. Evidence in support of this conclusion was described by Powell with reference to his motor racing experience, although high-speed knock usually results in such severe engine damage that the cause is generally difficult to ascertain [49].

The study of heat transfer in the end-gas zone of the Daimler Benz 407 engine revealed that whilst squish is indeed a very effective method of suppressing knock with gasoline, the characteristics of methanol auto-ignition render it virtually insensitive to increased turbulence and increased combustion rate. Moreover, the experimental results indicated that the clearance between cylinder head and piston crown are critical for effective cooling of the end-gas zone and that if effective end-gas cooling were achieved, the engine speed would be have to be restricted to prevent the core temperature of the end-gas from reaching the adiabatic temperature.

Whilst end-gas cooling was not found to be a viable option, it was observed that the evaporative cooling of the fuel itself was very effective as a means of lowering the overall temperature. The high latent heat of methanol, coupled with the relatively low stoichiometric air/fuel ratio resulted in the Daimler Benz cylinder temperatures remaining sub-zero for almost half the compression stroke. The effect of evaporating the fuel by heating the inlet mixture could be expected to have a seriously negative impact on the overall knock resistance, more so than would be the case for gasoline. This theoretical observation is borne out in the difference between the Research and the Motor Octane number for methanol which differs by 18 numbers between the two tests. The significant difference between the tests is that the Research

Octane test stipulates an air temperature of 51.6°C and the Motor Octane test requires a mixture temperature of 51.6°C. By comparison, the gasoline used for this research work differs by only 6 numbers between the two Octane tests and by definition, iso-octane does not differ at all.

Although modern carburetted spark-ignition engines utilise some form of inlet manifold heating to minimise the amount of wall-wetting by the fuel, at wide-open throttle, the bulk of the liquid fuel is entrained with the air stream. Thus, in the case of methanol, there is little scope for preventing knock by combustion chamber design. The maximum temperature is thus determined by the compression ratio, the evaporative cooling and the ignition timing. For optimum efficiency, the air/fuel ratio and the ignition timing are constrained and under such circumstances, the maximum compression ratio for a methanol engine appears to be about 12.5:1. For racing purposes, higher compression ratios have been used with deliberate over-fuelling and the attendant evaporative cooling being employed to suppress knocking and to simultaneously increase the charge density.

Interestingly, the report of the development of the Daimler Benz M407 engine, which incorporates a methanol evaporator, does not mention any problems that were encountered with knocking at a relatively high compression ratio of 12.5:1 that was used with this engine [50]. However, in discussions with members of the development team it was conceded that the fuel evaporator was not sized for the full-load fuel flow, and that under full-load operation, fuel in liquid form was being entrained with the air stream and this was a possible explanation for the knock-free operation.

The fact that end-gas cooling is not a viable proposition for methanol operation opens up the possibility for designing the combustion chamber to minimise heat loss. In a computer simulation, Watts [42] showed that in engines designed to maximise end-gas cooling, heat loss may amount to as much as 15% of the total fuel energy input, with most of this loss occurring

during the expansion stroke. However, the simulation indicated that whilst the adiabatic concept could improve efficiency modestly, it would also cause a drop in volumetric efficiency owing to the heating of the intake charge from the hot, insulated cylinder walls. For the methanol engine, this early intake heating would also have an undesirable consequence on the final end-gas temperature.

## 4.1 RECOMMENDATIONS FOR FOLLOW-ON RESEARCH

The study of the abnormal combustion of methanol is largely an unexplored field and there is enormous scope for further research. Some of the most promising avenues are identified below.

- The effect of engine speed was touched on in this thesis but was not studied in depth. The fact that knock may occur preferentially at high engine speeds with methanol would be an important consideration for engine designers if it were to be implemented as an alternative fuel.

- The relatively simple knock model used in this thesis was capable of revealing characteristic differences in the knock mechanism of gasoline and methanol. This could serve as the starting point for a complete chemical-kinetic model to identify the rate-controlling reaction chains, and ultimately to identify possible chemical anti-knock agents for methanol.

- The method of characterising fuels directly in terms of pressure, temperature and time has distinct advantages over the present indirect methods such as the Research Octane test and the Motor Octane test. It was noted that the fact that three constants were required to characterise each fuel could explain much of the confusion that surrounds the applicability of the Research and Motor Octane numbers to modern engines and fuels.

- The gas temperature determination was identified as the greatest source of uncertainty in the knock characterisation analysis. Not only for this type of analysis, but also for engine research in general, there is an urgent need for a reliable, accurate and robust temperature measurement device.

- Although methanol was the focus of this research study, it is probable that the results and findings are, in some measure, applicable to ethanol. Since ethanol is already utilised as a basic fuel in Brazil, this research is obviously pertinent.

- The effect of blending fuels such as methanol and gasoline represents the most difficult analysis situation of all. Although tempting, there is no reason to suppose that the knock reactions of the blend fuel will simply exhibit a gradual transition from the one fuel to the other. Since it is already current practice to blend oxygenated fuels with pure hydrocarbon fuels this would seem to be an area for parametric studies with a view to a more fundamental understanding of the blending process and the effect on abnormal combustion.

## REFERENCES


1 WHITE M D, COOK C G, "Some Economic Implications Of Introducing Methanol As A Motor Fuel", Paper presented at a seminar on Alternative Fuels, 27 July 1987,CSIR, Pretoria.

2 NATES R J, "An Investigation Into Pollution Levels Associated With The Use Of Alcohol Fuel For I.C. Engines", Energy Research Institute Report 46/21/14, May 1982.

3 NAESER D F, "Engine Wear Study", Energy Research Institute Report 107, Feb 1986.

4 LENG I J,"Fuel Systems For Alcohols - Corrosion And Allied Problems", Proc 4th Int Symp Alcohol Fuels Technology, Guraruja, Brazil, Oct 1980, Paper B-13.

5 PLASSMANN E, HASSEL D, "On The Trail Of New Fuels - Alternative Fuels For Motor Vehicles", from "Neuen Kraftstoffen Auf Der Spur - Alternative Kraftstoffe Fur Kraftfahrzeuge", Fed. Ministry for Research and Technology, Bonn, 1974, Translated May 1975, Lawrence Livermore Laboratory, California, USA.

6 MISCHKE A, KOERNER D, BERGMANN H, "The Mercedes Benz Alcohol Gas Engine M407 h GO", Proc 5th Int Symp Alcohol Fuel Technology, Auckland, New Zealand, May 1982, Paper C2-17.

7 NIETZ A, CHMELA F, "The M.A.N. Methanol Engine Powering City Buses", Proc 5th Int Symp Alcohol Fuel Technology, Auckland, New Zealand, May 1982, Paper C2-23.

8 BENNETHUM J E, SRINIVASAN N, "Detroit Diesel Allison's Two Stroke Cycle Compression Ignited Alcohol Engines", Proc 6th Int Symp Alcohol Fuel Technology, Ottawa, Canada, May 1984, Paper A-7.

9 BENNETT K F, YATES A D B, "The Conversion Of Daimler Benz Diesel Engines To Operation On 100% Methanol", Proc 5th Int Symp Alcohol Fuel Technology, Auckland, New Zealand, May 1982, Paper C2-5.

10 RIFKIN E, WALCUTT C, "A Basis For Understanding Anti-Knock Action", Trans SAE, Vol65, 1957.

11 MILLER C D, "Roles Of Detonation Waves And Auto-Ignition In Spark-Ignition Engines", Trans SAE, vol1, no1, 1947, p98.

12 LEWIS B, VON-ELBE G, "Combustion Flames And Explosions Of Gases", Cambridge Univ Press, 1st ed, 1938.

13 JOST W, "Knock Reaction", Proc 9th Int Symp Combustion, 1963, p1013.

14 CURRY S, "A Three-Dimensional Study Of Flame Propagation In A Spark-Ignition Engine", Trans SAE, vol 71, 1963, p628.

15 LICHTY L C, "Combustion Engine Processes", McGraw-hill, 1st ed, 1967.

16 ROBINSON I M, "The Potential Of Dissociated Methanol As A Fuel For Spark-Ignition Engines", MSc Thesis, Univ of Cape Town, 1983.

17 MALY R, ZIEGLER G, "Theoretical And Experimental Investigation Of The Knocking Process", Int Symp Knocking of Combustion Engines, Wolfsburg, W Germany, Nov 1981.

18 TAYLOR C F, "The Internal-Combustion Engine In Theory And Practice", MIT Press, 3rd printing, 1979.

19 MALE T, "Photographs At 500 000 Frames Per Second Of Combustion And Detonation In A Reciprocating Engine", 3rd Int Symp Combustion, 1949, p721.

20 CURRY S, "A Three-Dimensional Study Of Flame Propagation In A Spark-Ignition Engine", Trans SAE, vol 71, 1963, p628.

21 TAYLOR C F, TAYLOR E S, LIVENGOOD J C, RUSSEL W A, LEARY W A, "Ignition Of Fuels By Rapid Compression", SAE Quart Trans, vol4, no2, April 1950, p232.

22 DOWNS D, WHEELER R W, "Recent Developments In Knock Research", Proc Inst of Mech Engrs, 1952, p88.

23 MINKOFF G J, TIPPER C F H, "Chemistry Of Combustion Reactions", Butterworth Publishers, 1962.

24 FISH A, READ A, AFFLECK W S, HASKELL W W, "The Controlling Role Of Cool Flames In Two-Stage Ignition", Jour of the Combustion Inst, vol13, 1969.

25 DOWNS D, WALSCH A D, WHEELER R W, "A Study Of The Reactions That Lead To Knock In The Spark-Ignition Engine", Proc Inst of Mech Engrs, vol243, 1951, p62.

26 PITZ W J, WESTBROOK C K, "Modeling Chemical Kinetic Aspects Of Engine Knock", Lawrence Livermore National Lab, Publication UCRL-90577, 1984.

27 MILLER J A, FISK G A, "Combustion Chemistry", Special report, Chem and Eng, Aug 1987, p22.

28 GLUKSTEIN M E, WALCUTT C, "End-Gas Temperature-Pressure Histories And Their Relation To Knock", Trans SAE, vol69, 1961, p529.

29 AGNEW W G, "End-Gas Temperature Measurement By A Two-Wavelength Infrared Radiation Method", Trans SAE, vol69, 1961, p495.

30 AMMAN C A, "Classical Combustion Diagnostics For Engine Research", SAE Paper 850395, 1985

31 BORMAN G, NISHIWAKI K, "Internal Combustion Engine Heat-Transfer", Progress in Energy and Combustion Science, Vol13, No1, 1987.

32 ENOMOTO Y, FURUHAMA S, "Measurement Of The Instantaneous Surface Temperature And Heat Loss Of Gasoline Engine Combustion Chamber", SAE paper 845008, 1984.

33 BY A, KEMPINSKI B, RIFE J M, "Knock In Spark Ignition Engines", SAE Paper 810147, Feb 1981.

34 COLLINS D, "Gasoline Combustion Chambers", SAE paper 830866, 1983.

35 DYE A, "A New Approach To Combustion Analysis", Automotive Engineer, Feb-Mar 1985, p32.

36 CARIS D F, MITCHELL B J, MCDUFFIE A D, WYCZALEC F A, "Mechanical Octanes For Higher Efficiency", Trans SAE, vol64, 1956, p76.

37 GATOWSKI J, HEYWOOD J, "Faster Burning In Spark Ignition Engines", Energy Lab report, MIT, July-Sept 1985.

38 DIGGS D R, "Effect Of Combustion Time On Knock In A Spark-Ignition Engine", Trans SAE, vol61, 1953, p402.

39 MALY R, ZIEGLER G, "Thermal Combustion Modeling - Theoretical And Experimental Investigation Of The Knocking Process", SAE paper 820759, 1982.

40 LUCAS G G, BRUNT M F, "The Effect Of Combustion Chamber Shape On Rate Of Combustion In A Spark Ignition Engine", SAE paper 820165, 1982.

41 BENSON R S, WHITEHOUSE N D, "Internal Combustion Engines", Pergamon Press, vol1 & 2, 1979.

42 WATTS P A, HEYWOOD J B, "Simulation Studies Of The Effects Of Turbocharging And Reduced Heat Transfer On Spark-Ignition Engine Operation", SAE paper 800289, 1980.

43 BLUMBERG P N, LAVOIE G A, TABACZYNSKI R J,"Phenomenological Models For Reciprocating Internal Combustion Engines", Prog Energy Combustion Sci, vol5, 1979, p12.

44 HOLMAN J P, "Heat Transfer", McGraw-Hill, 4th ed, 1976.

45 SCHLICHTING H, "Boundary Layer Theory", McGraw-Hill, 7th ed, 1979.

46 BAKER A, "Petroleum Based Fuels: Cyclic Dispersion And Knock Aspects", Conference report, Automotive Engineer, vol12, no1, 1987, p49.

47 LEE W, SCHAEFER H J, "Analysis Of Local Pressures, Surface Temperatures And Engine Damage Under Knock Conditions", SAE Paper 830508, Feb 1983.

48 ALKIDAS A C, COLE R M, "Transient Heat Flux Measurements In A Divided-Chamber Diesel Engine", Trans ASME, Jour of Heat Transfer, vol107, 1985, p439.

49 POWELL D, "Racing Experiences With Methanol And Ethanol Based Motor Fuel Blends", SAE Paper 770792, 1977.

50 BERGMANN H, "First Experience With Methanol-Vapor-Powered City Buses Used In Regular Service In Auckland And Berlin", Proc 5th Int Symp Alcohol Fuel Tech, Vol3, May 1982.

51 DOUAUD A, "Modeling The Knocking Phenomenon In Engines", Int Symp Knocking of Combustion Engines, Wolfsburg, W Germany, Nov 1981.

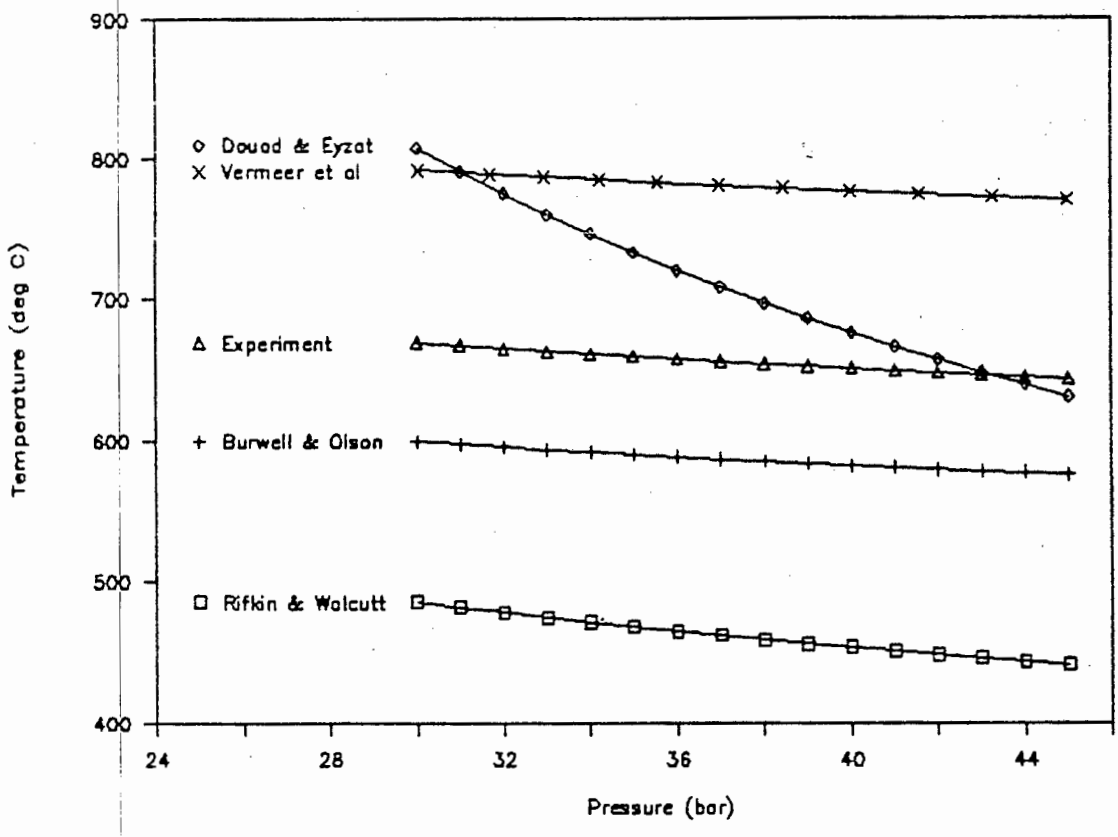


Figure 1. The gas temperature corresponding to an ignition delay of 2msec, based on the theoretical expressions.

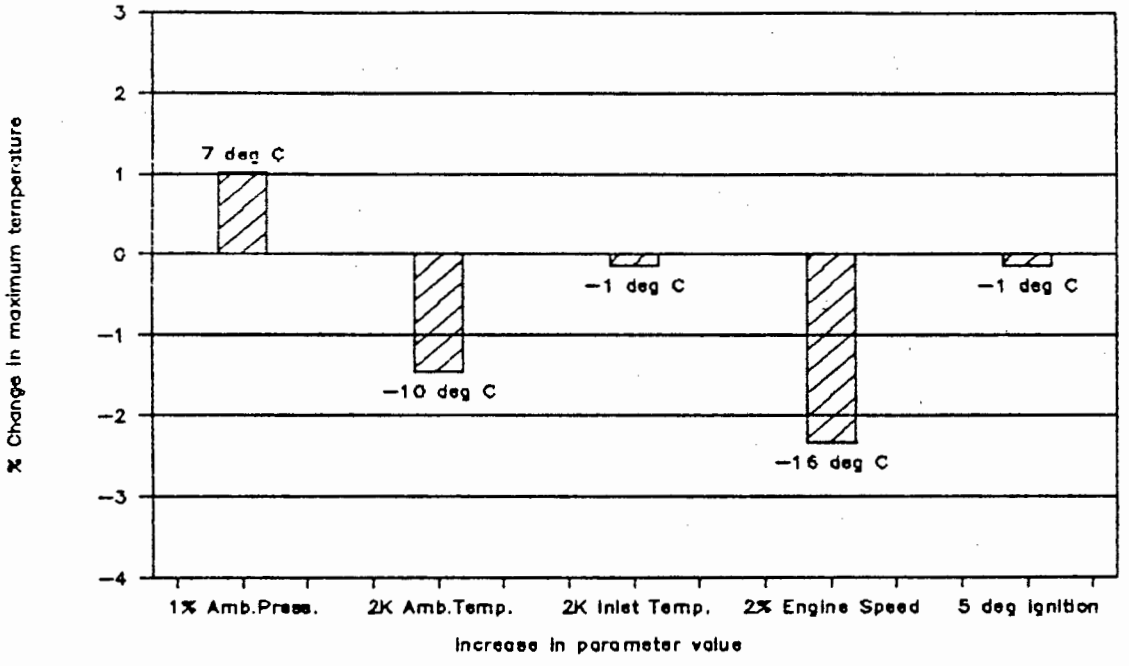


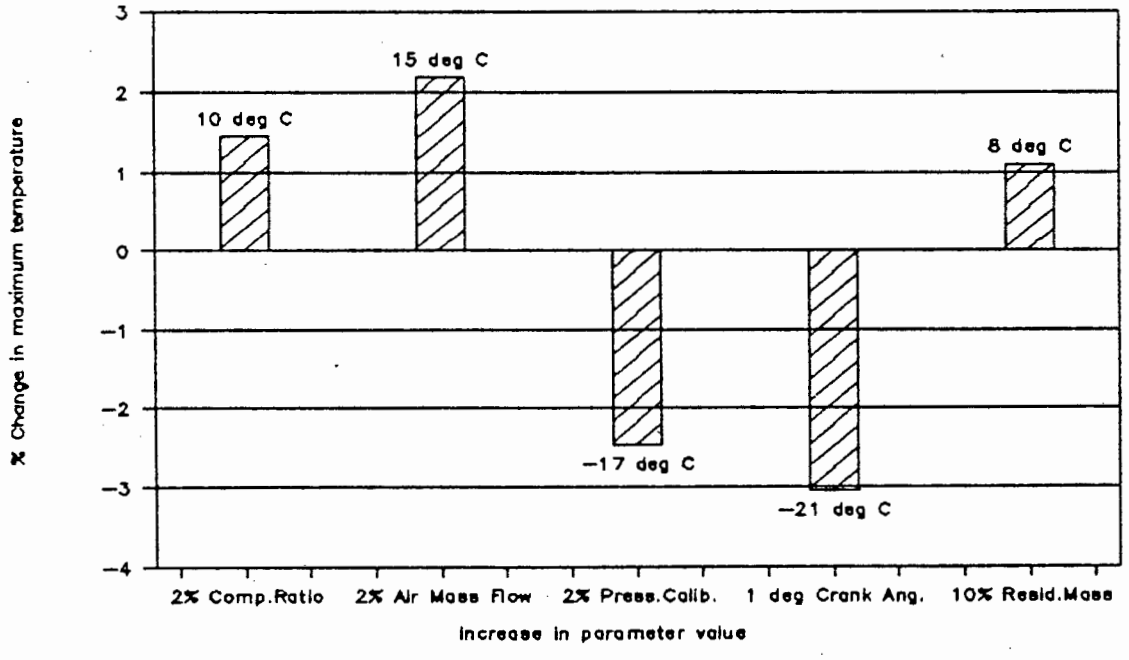


Figure 2. Sensitivity of the gas temperature calculation to inaccuracy of the input parameters.

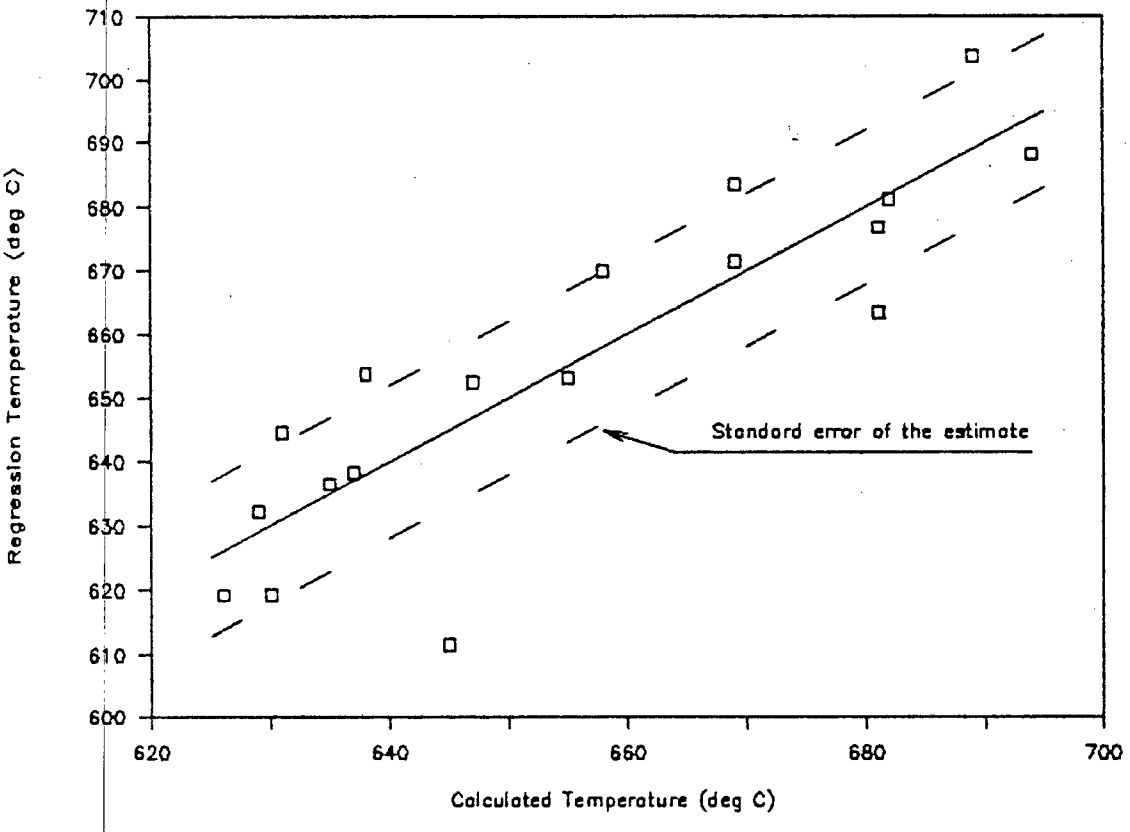


Figure 3. Gasoline data - The gas temperature, as determined from the theoretical regression constants, compared to the original calculated values.

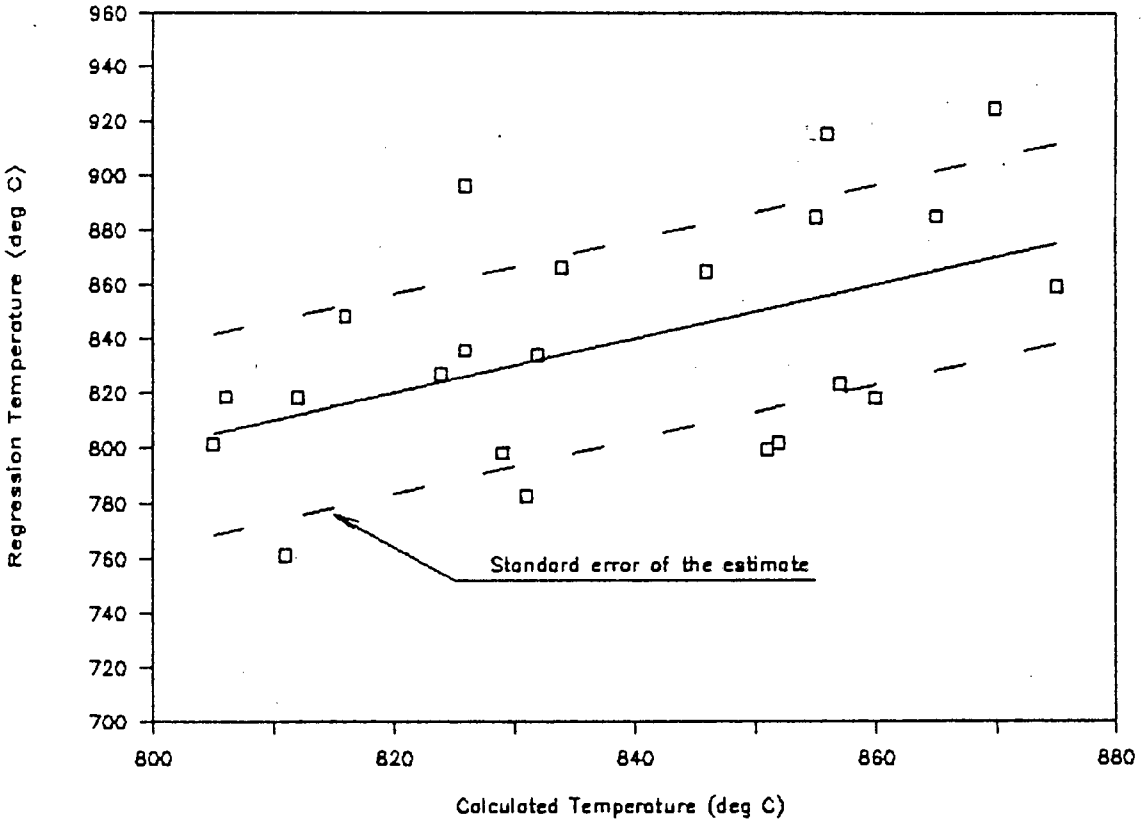


Figure 4. Methanol data - The gas temperature, as determined from the theoretical regression constants, compared to the original calculated values.

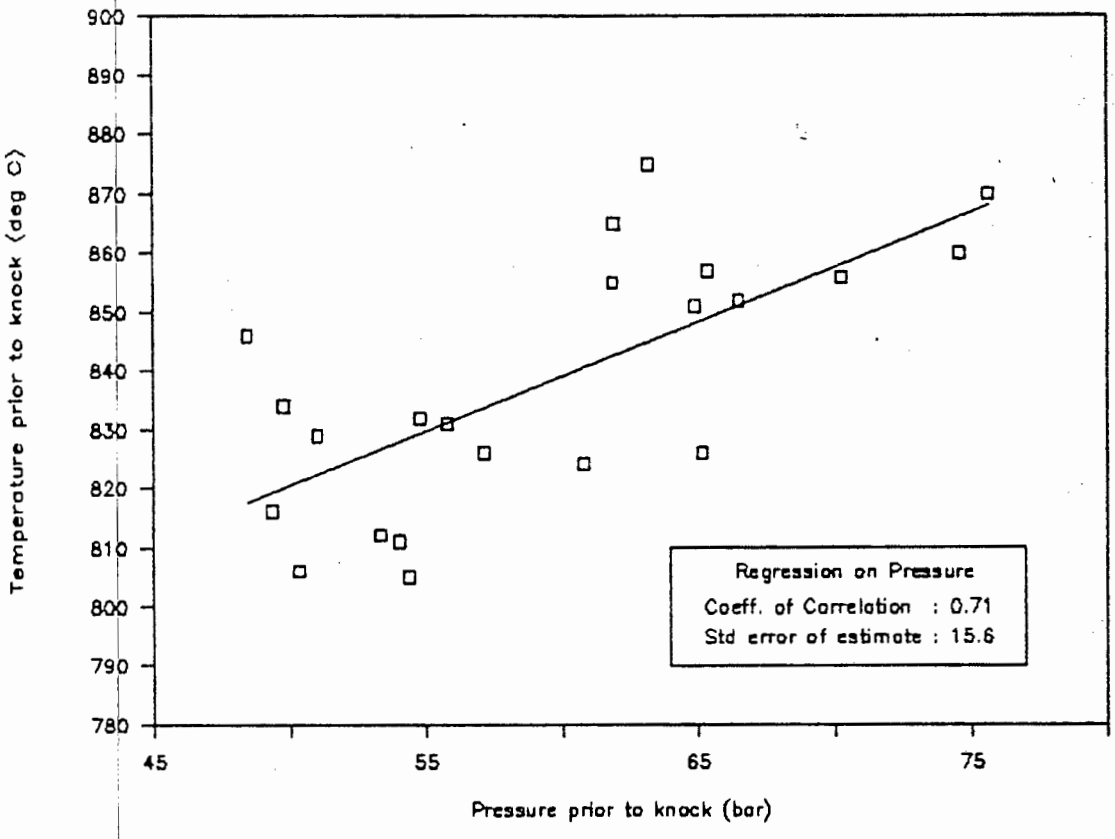


Figure 5. Methanol data - The correlation between the gas temperature prior to knock and the corresponding pressure.

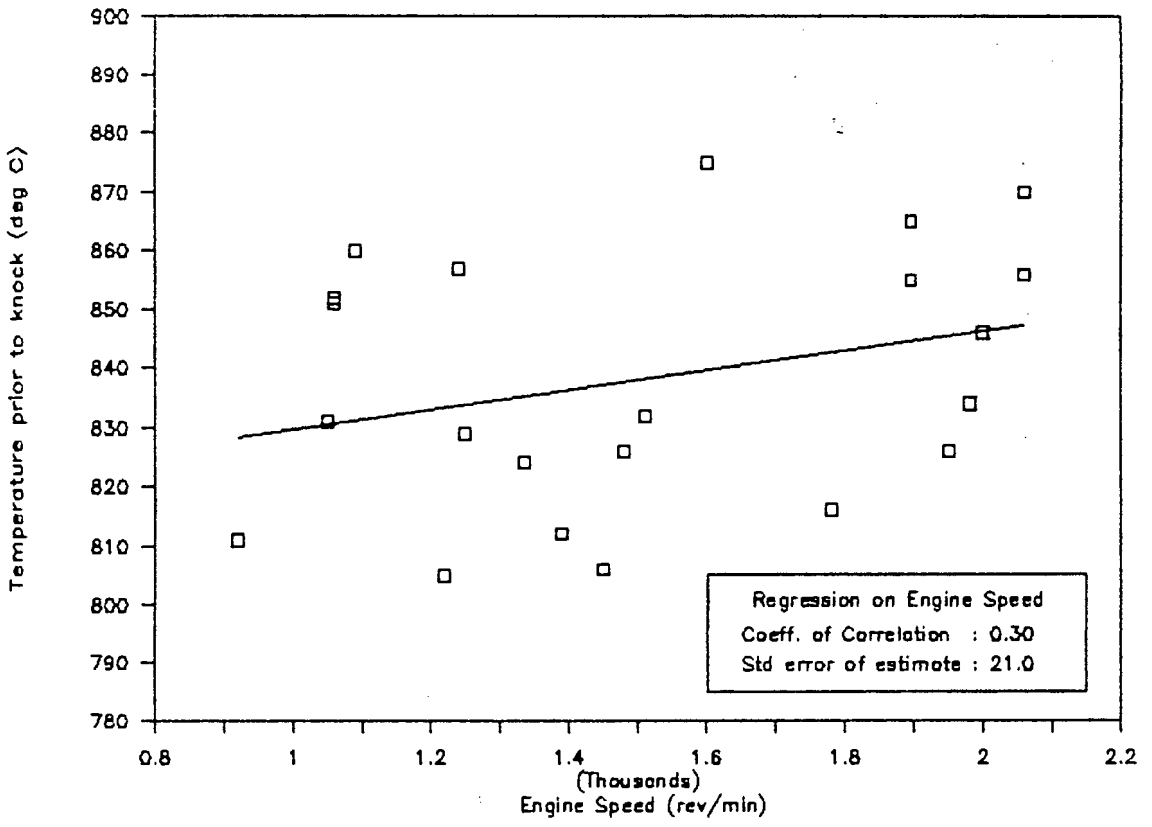


Figure 6. Methanol data - The correlation between the gas temperature prior to knock and the corresponding engine speed.

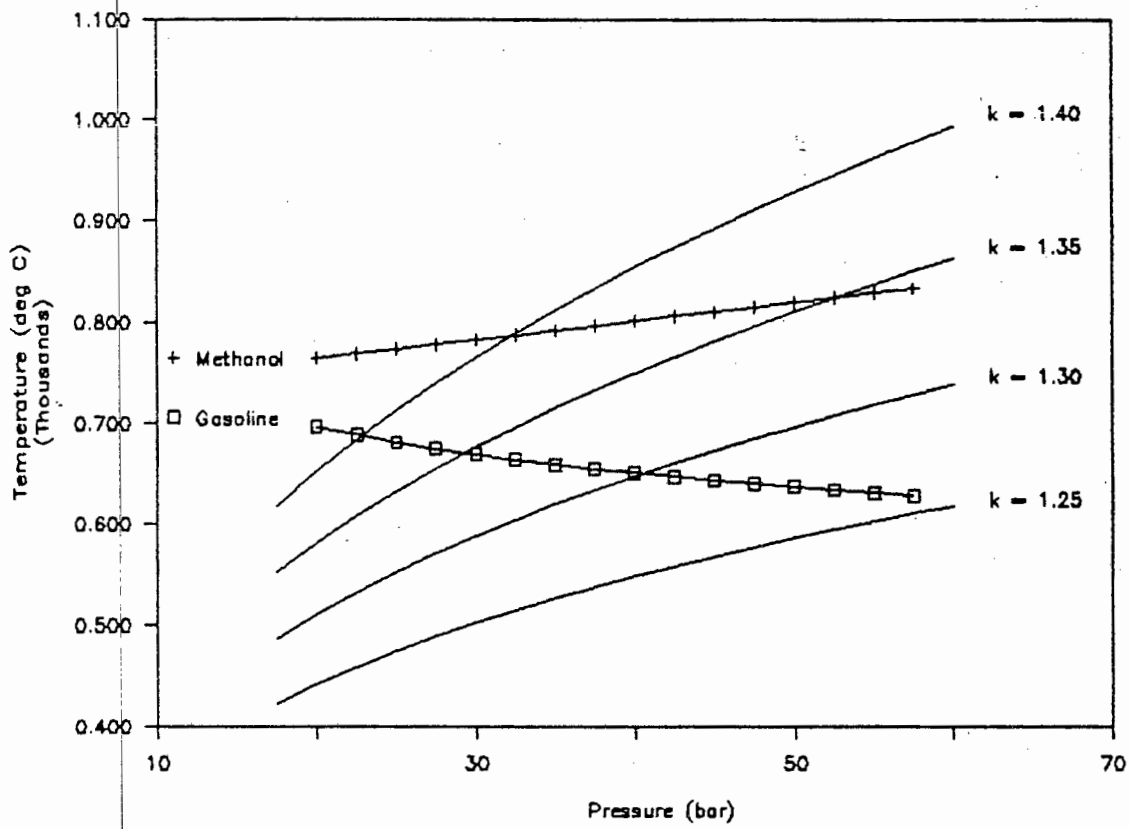


Figure 7. The gas temperature corresponding to an ignition delay of 2msec for gasoline, compared with the critical gas temperature for methanol. Also showing the polytropic compression lines with origin at 1bar and 120°C.

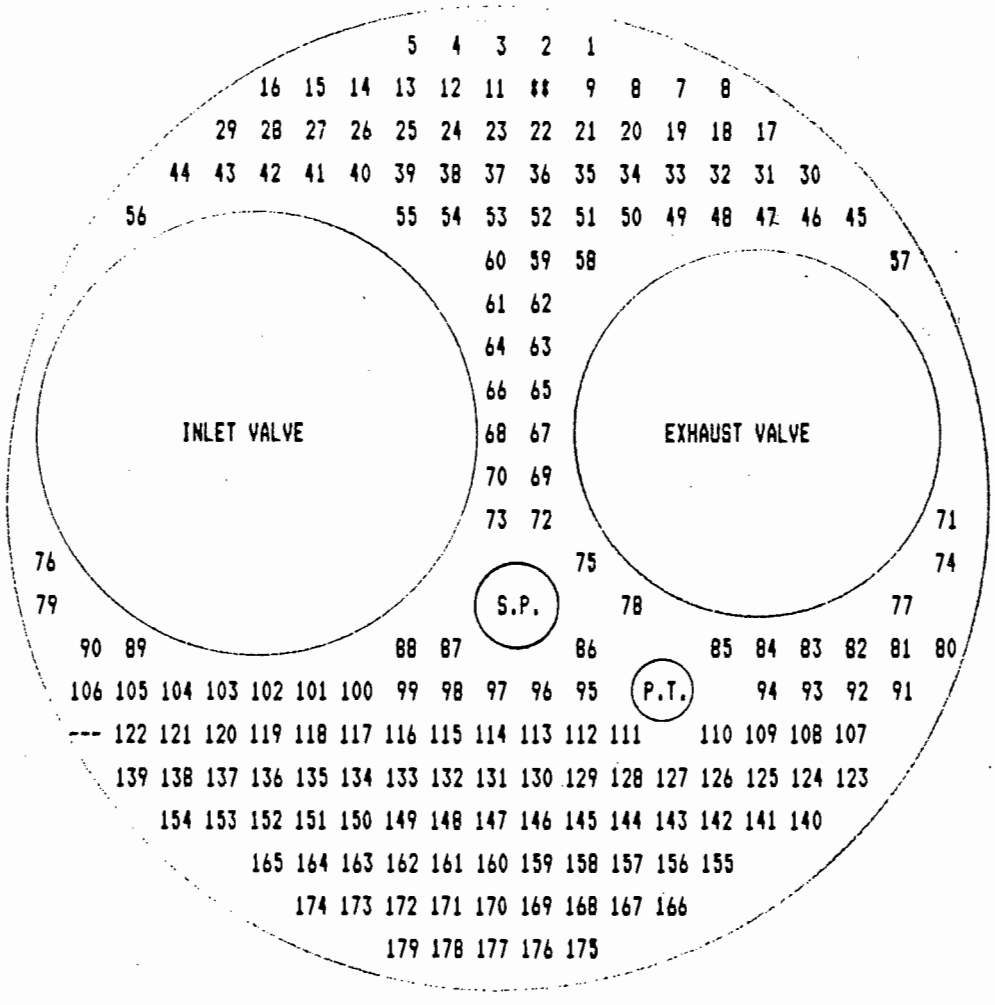


Figure 8. A plan view of the special cylinder head showing the arrangement and numbering of the surface thermocouples. (S.P.= Spark Plug, P.T.= Pressure Transducer)

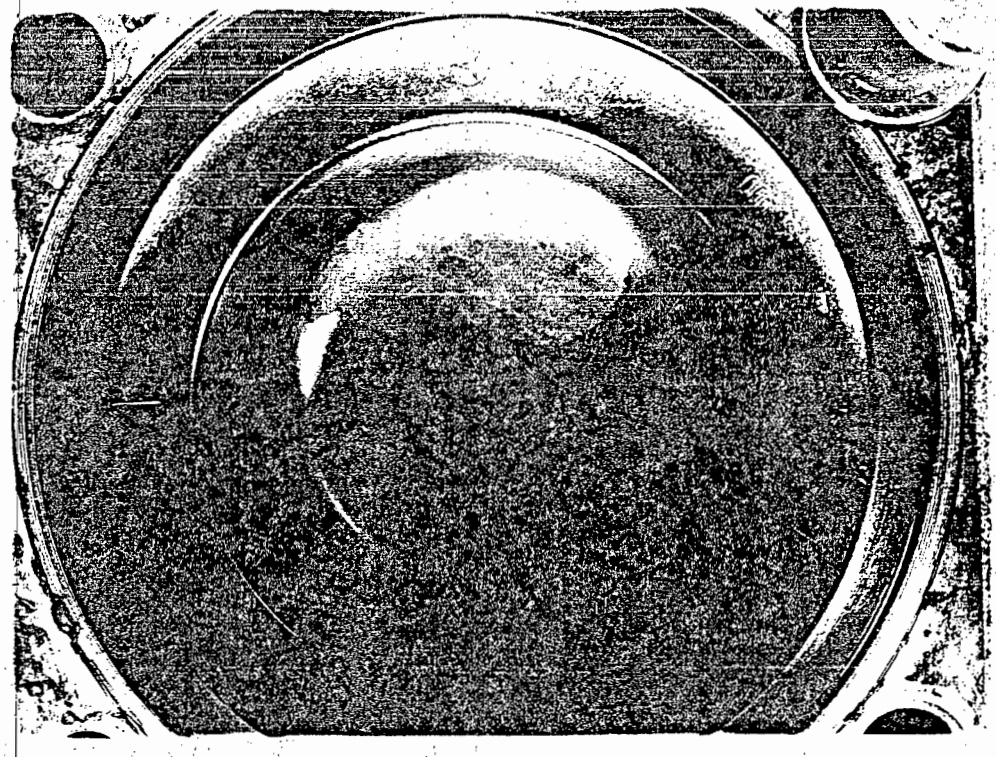

Figure 9. Piston damage resulting from petrol knock. (Note: The light section at the top of the piston bowl was not caused by reflection but was an area that appeared to be burnt clean)

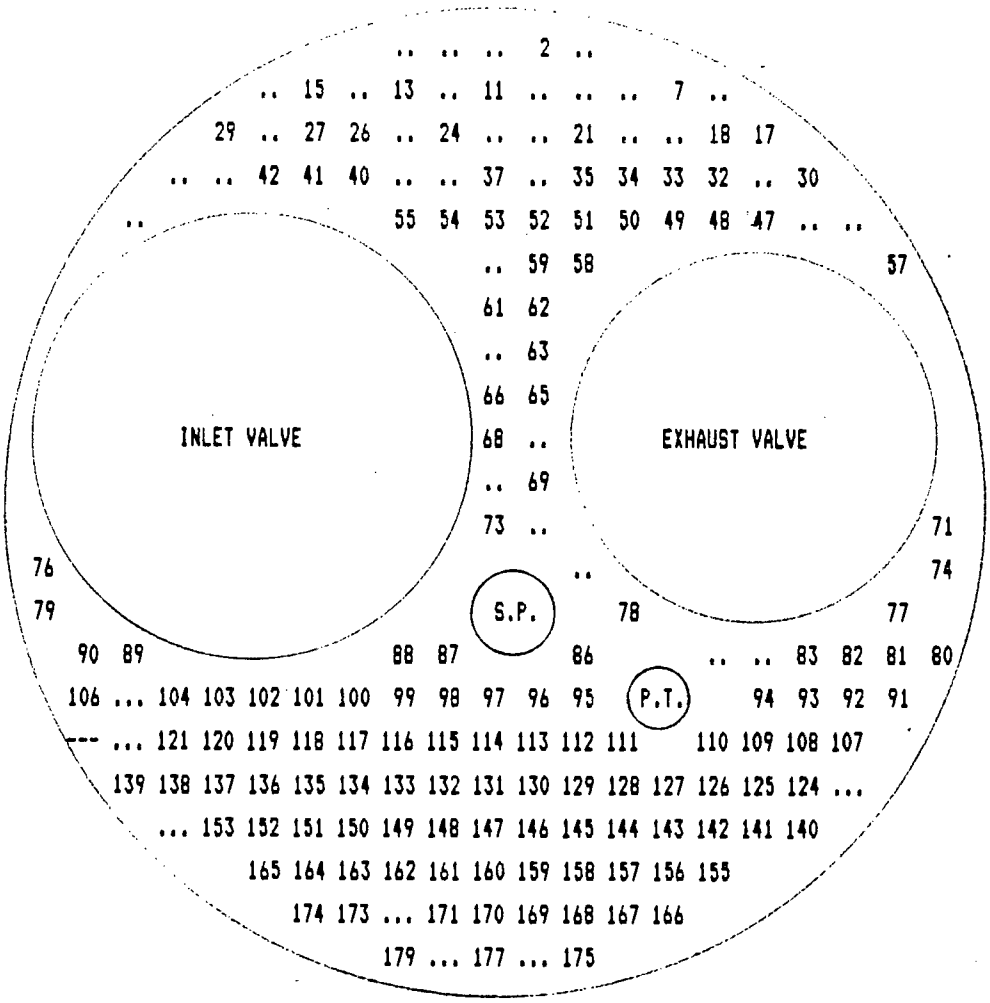


Figure 10. The thermocouple locations where methanol knock damage occurred following pre-ignition during warm-up. (S.P.= Spark Plug, P.T.= Pressure Transducer)

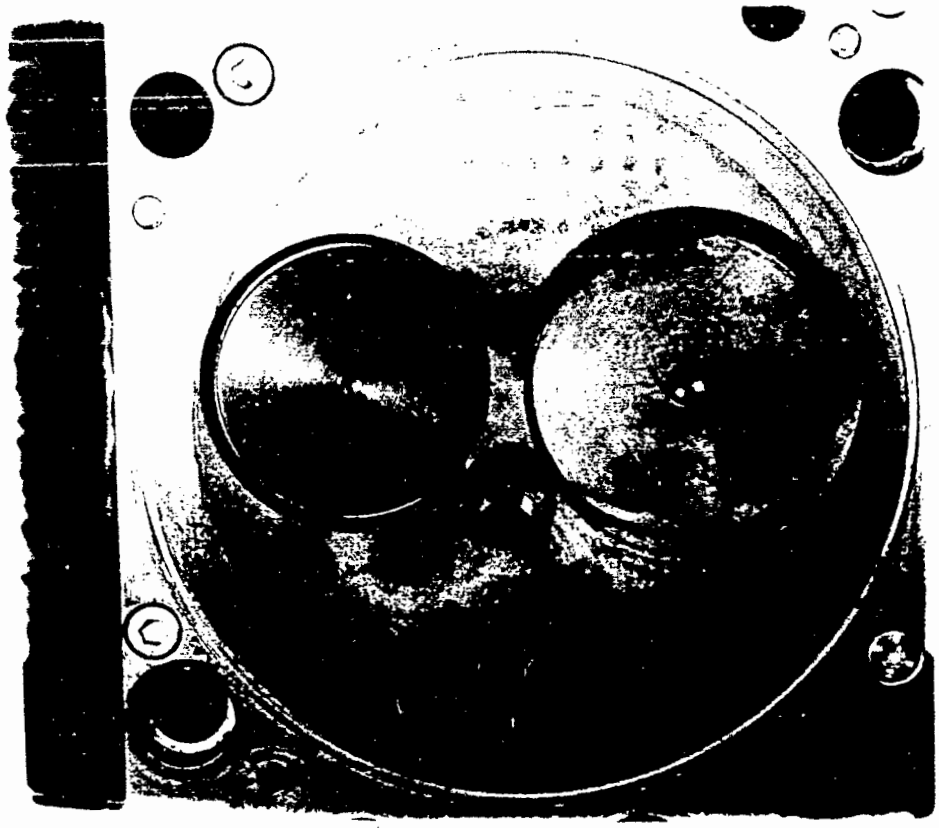

Figure 11. Thermocouple cylinder head following severe methanol knocking which removed some of the gold plating.

Figure 12. A close view of the cracks in the cylinder head.

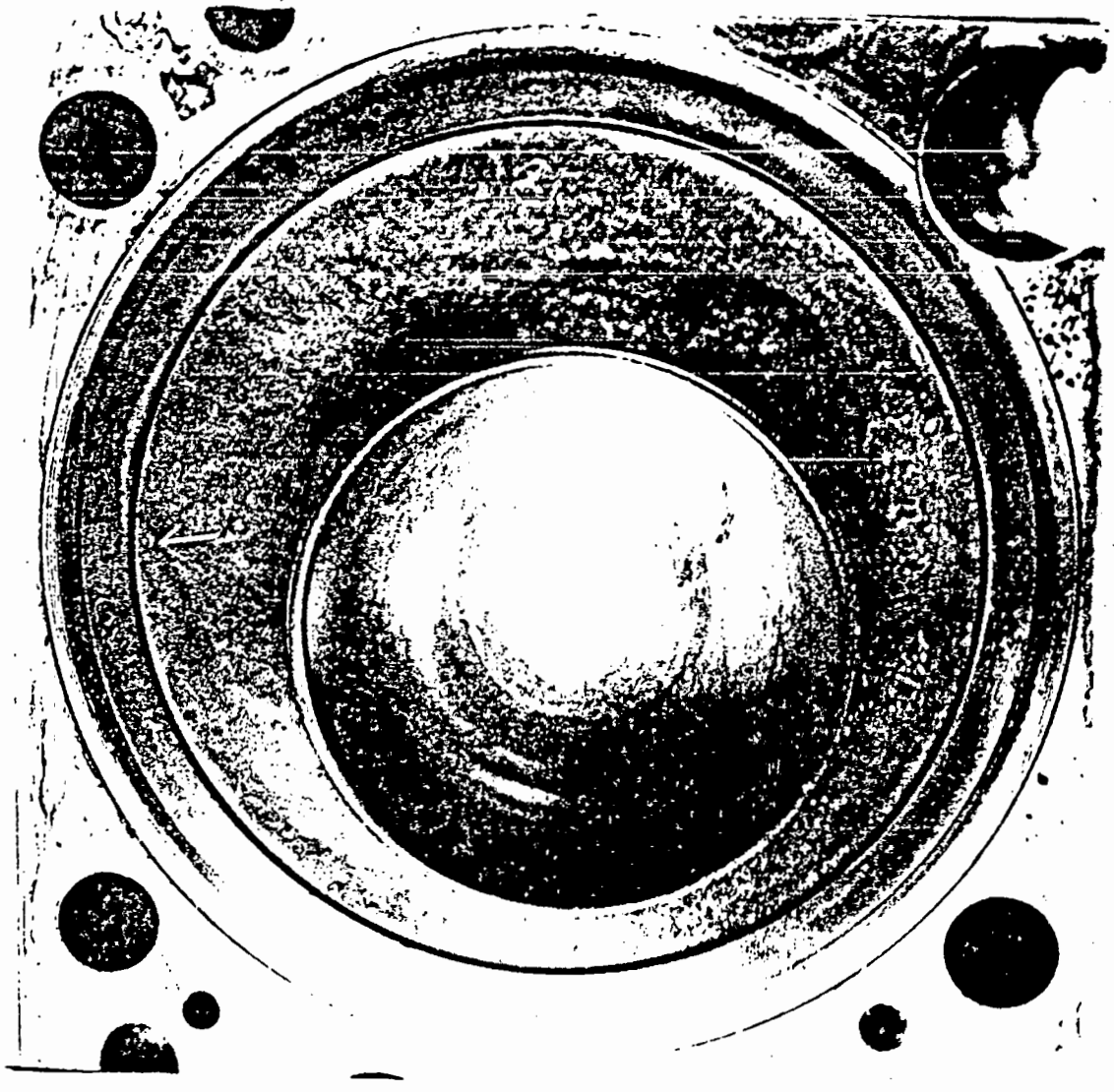

Figure 13. Piston condition after severe methanol knocking.
(Note: The marks on the piston were burnt oil stains)

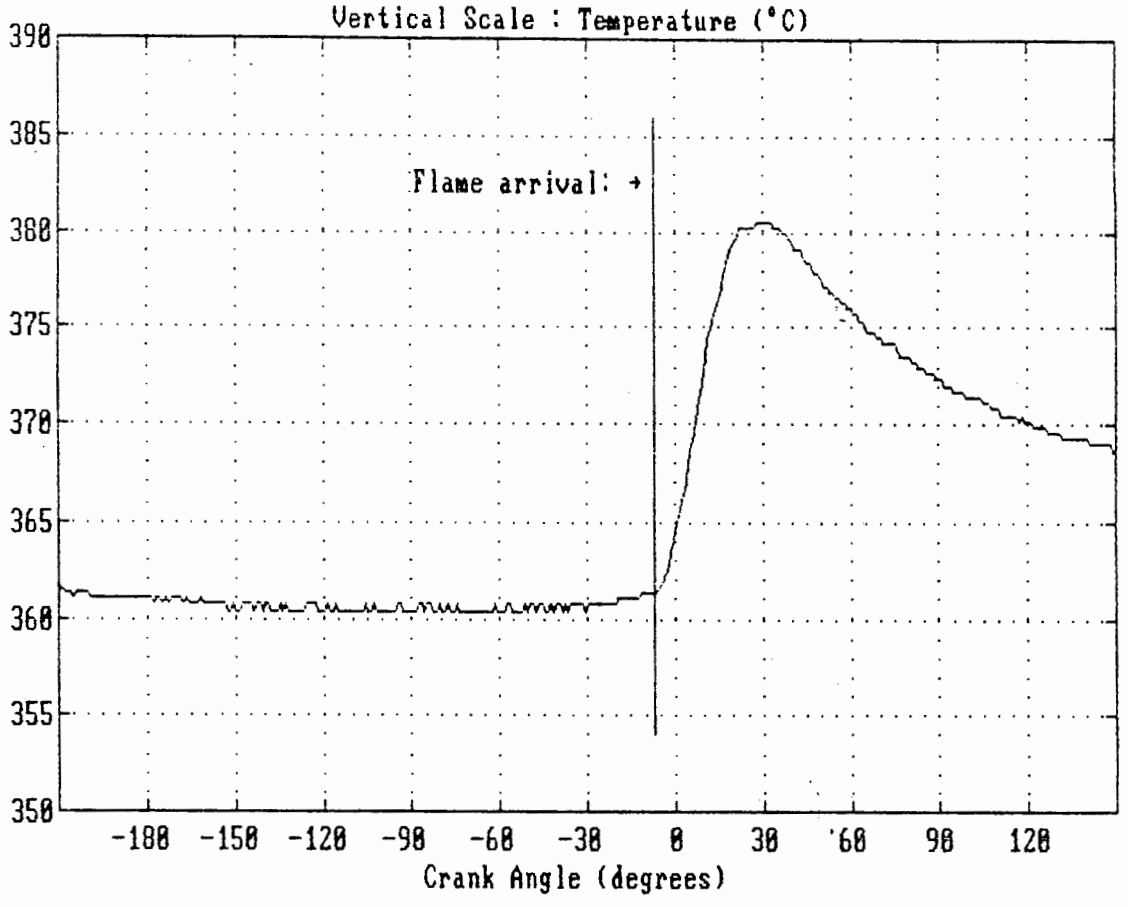


Figure 14. Thermocouple number 113 signal for normal gasoline combustion

| | |
|---|---|
| Engine | : OM 407 |
| Compression ratio | : 9.5 |
| Engine speed (rev/min) | : 1311 |
| Ignition (°BTDC) | : 16 |
| Fuel type | : Gasoline (98 RON) |
| A/F Equiv. ratio | : 1.03 |

Schematic diagram showing the thermocouple location

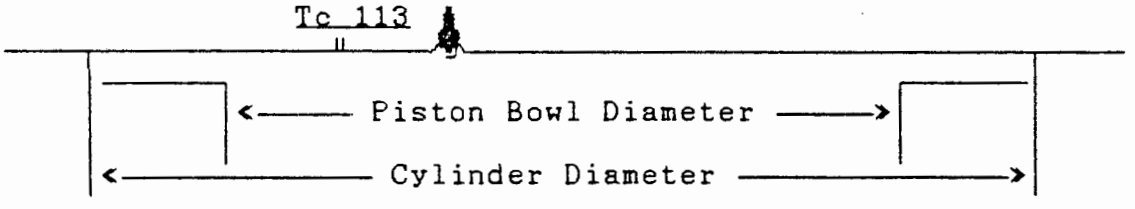

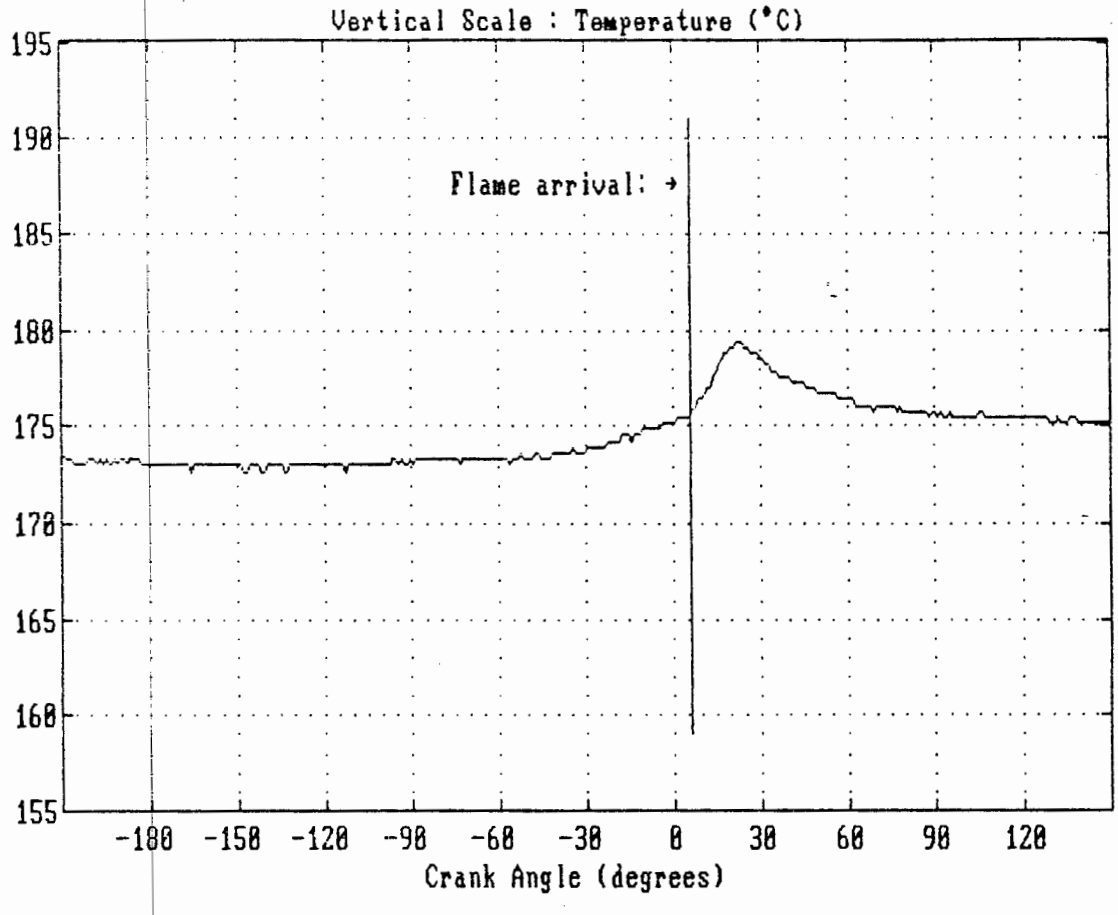


Figure 15. Thermocouple number 17 signal for normal gasoline combustion

| | |
|---|---|
| Engine | : OM 407 |
| Compression ratio | : 9.5 |
| Engine speed (rev/min) | : 1311 |
| Ignition (°BTDC) | : 16 |
| Fuel type | : Gasoline (98 RON) |
| A/F Equiv. ratio | : 1.03 |

Schematic diagram showing the thermocouple location

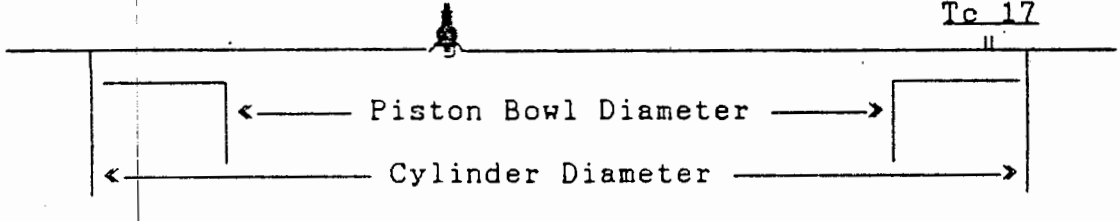

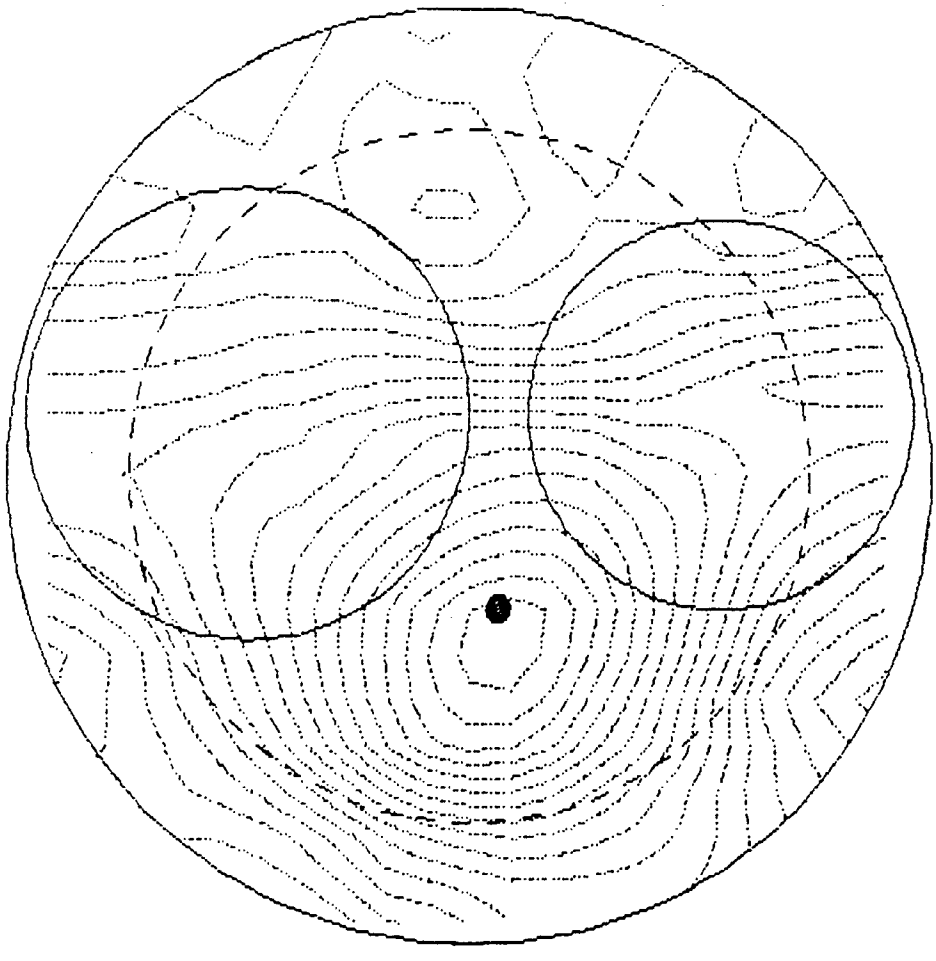

Figure 16. Flame contours for gasoline combustion at incipient knock conditions.

Inner contour at -6°c.a.
Increments at +1°c.a.
Outer contour at 10°c.a.

| | |
|---|---|
| Engine | : OM 407 |
| Compression ratio | : 9.5 |
| Engine speed (rev/min) | : 1311 |
| Ignition (°BTDC) | : 16 |
| Fuel type | : Gasoline (98 RON) |
| A/F Equiv. ratio | : 1.03 |

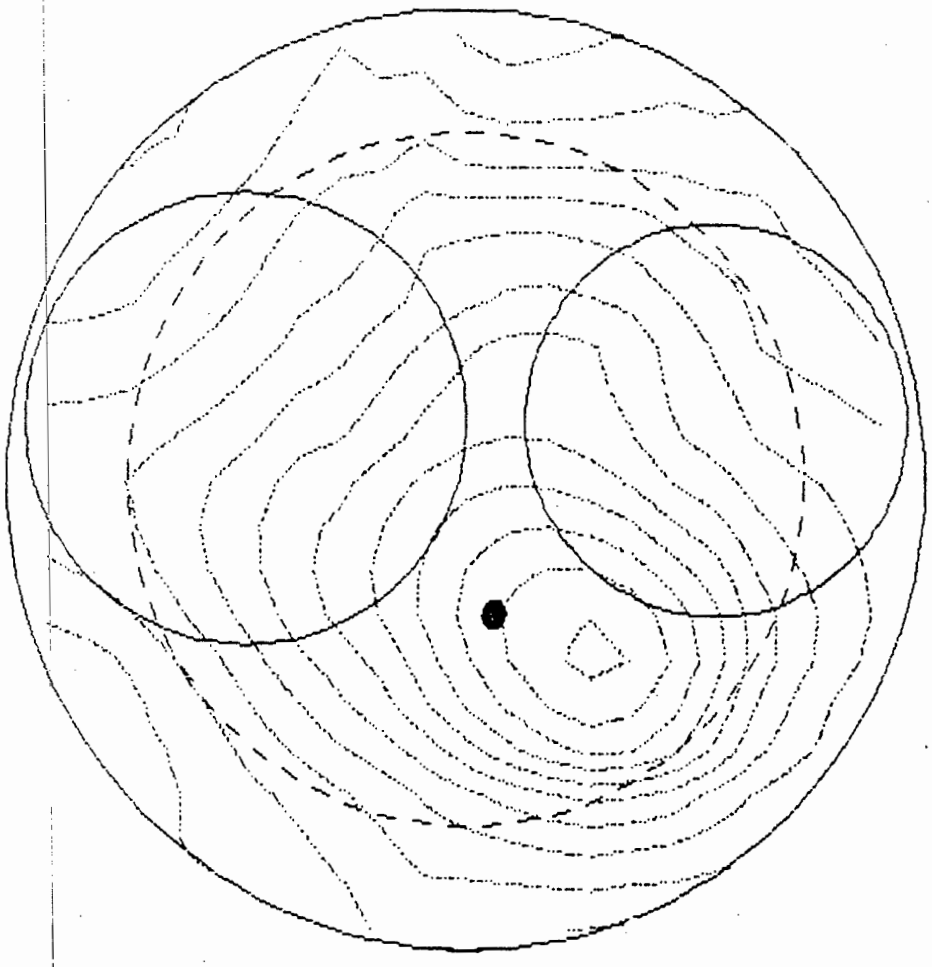

Figure 17. Cylinder head iso-therms for gasoline combustion at incipient knock conditions.

Inner contour at 450°C
Increments at -25°C
Outer contour at 175°C

| | |
|---|---|
| Engine | : OM 407 |
| Compression ratio | : 9.5 |
| Engine speed (rev/min) | : 1311 |
| Ignition (°BTDC) | : 16 |
| Fuel type | : Gasoline (98 RON) |
| A/F Equiv. ratio | : 1.03 |

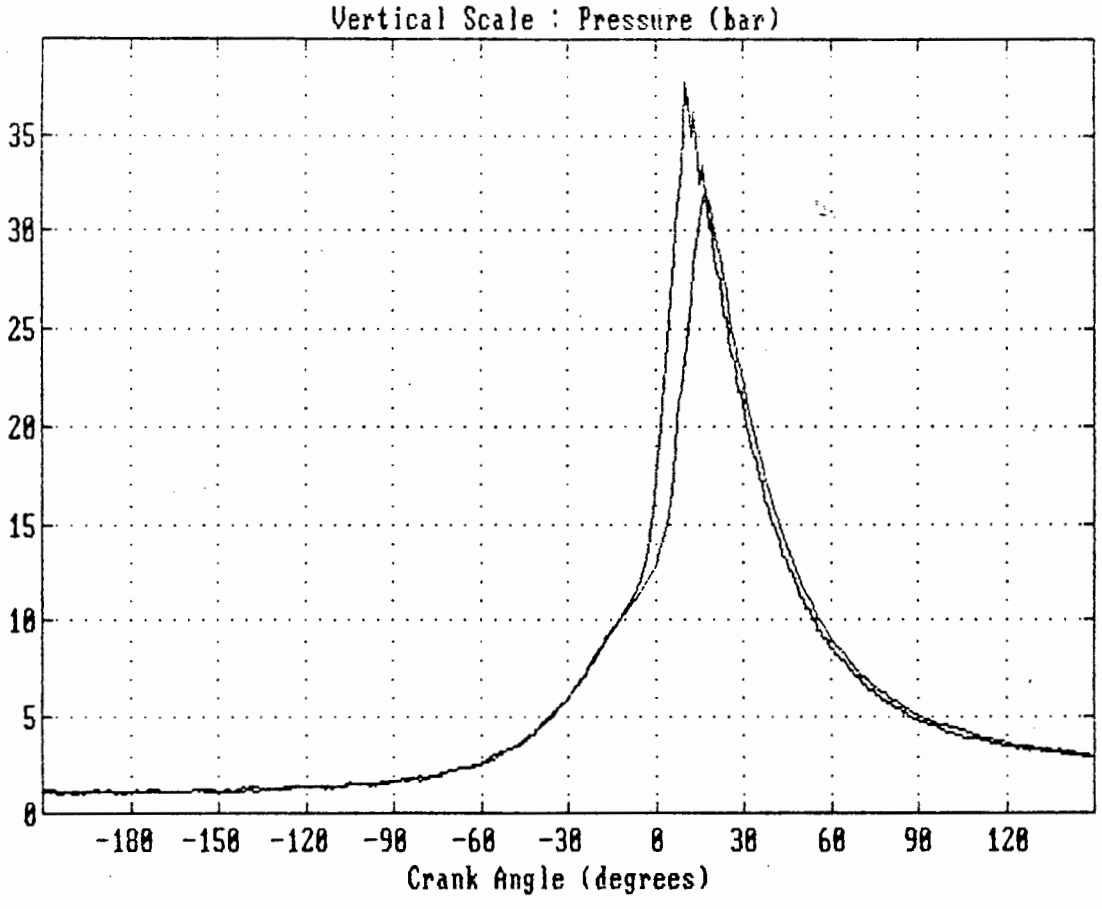


Figure 18. Pressure diagram overlay for normal and knocking combustion for gasoline.

| | |
|---|---|
| Engine | : OM 407 |
| Compression ratio | : 9.5 |
| Engine speed (rev/min) | : 1495 |
| Ignition (°BTDC) | : 16 |
| Fuel type | : Gasoline (98 RON) |
| A/F Equiv. ratio | : 1.03 |

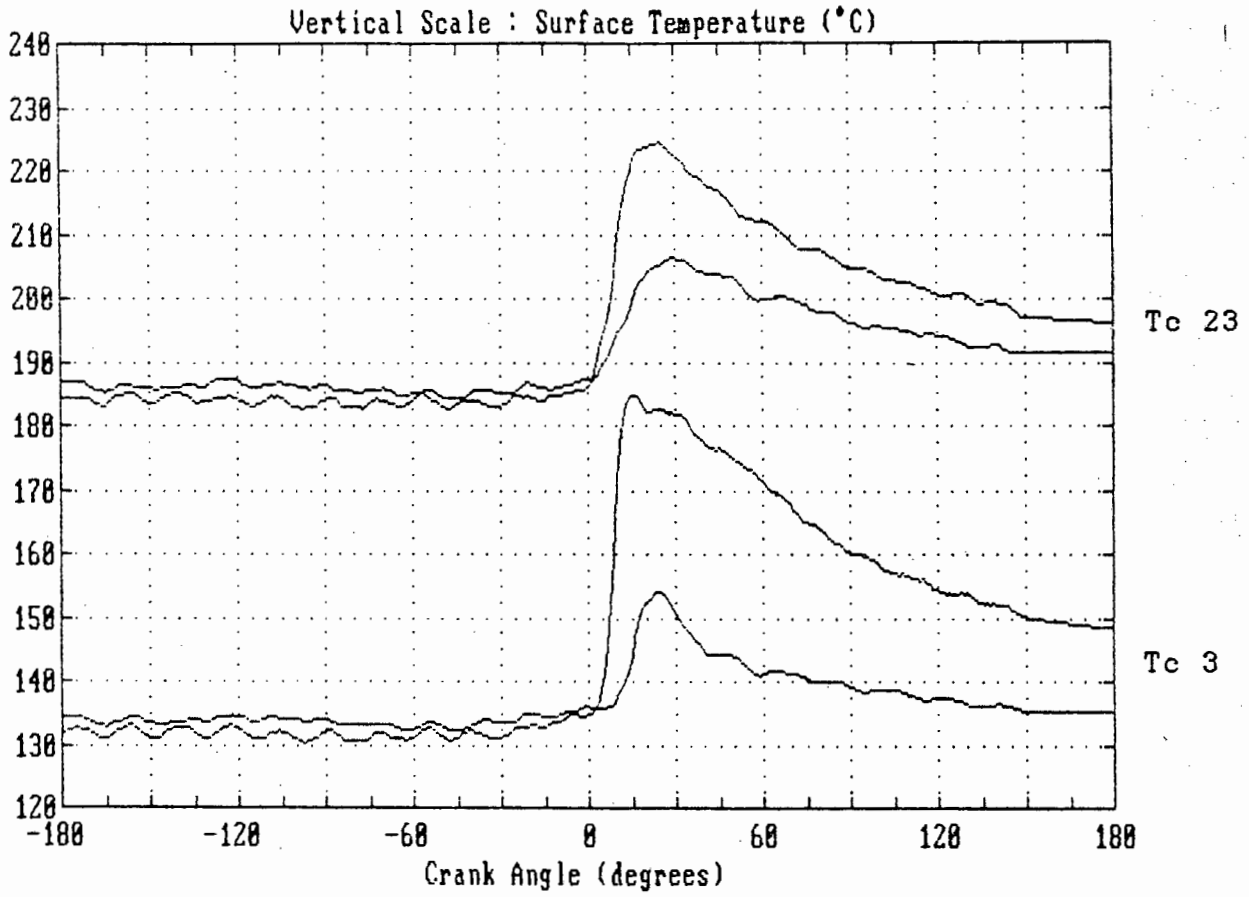


Figure 19. Thermocouple signals at locations Tc 3 and Tc 23 compared for normal and knocking combustion of gasoline.

| | |
|---|---|
| Engine | : OM 407 |
| Compression ratio | : 9.5 |
| Engine speed (rev/min) | : 1350 (nominal) |
| Ignition (°BTDC) | : 16, 20 |
| Fuel type | : Gasoline (98 RON) |
| A/F Equiv. ratio | : 1.0 (nominal) |

Schematic diagram showing the thermocouple location

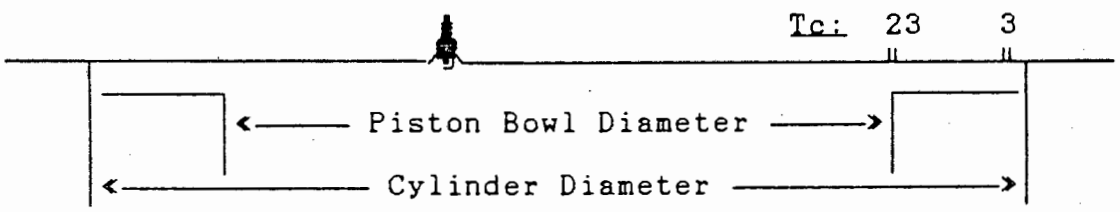

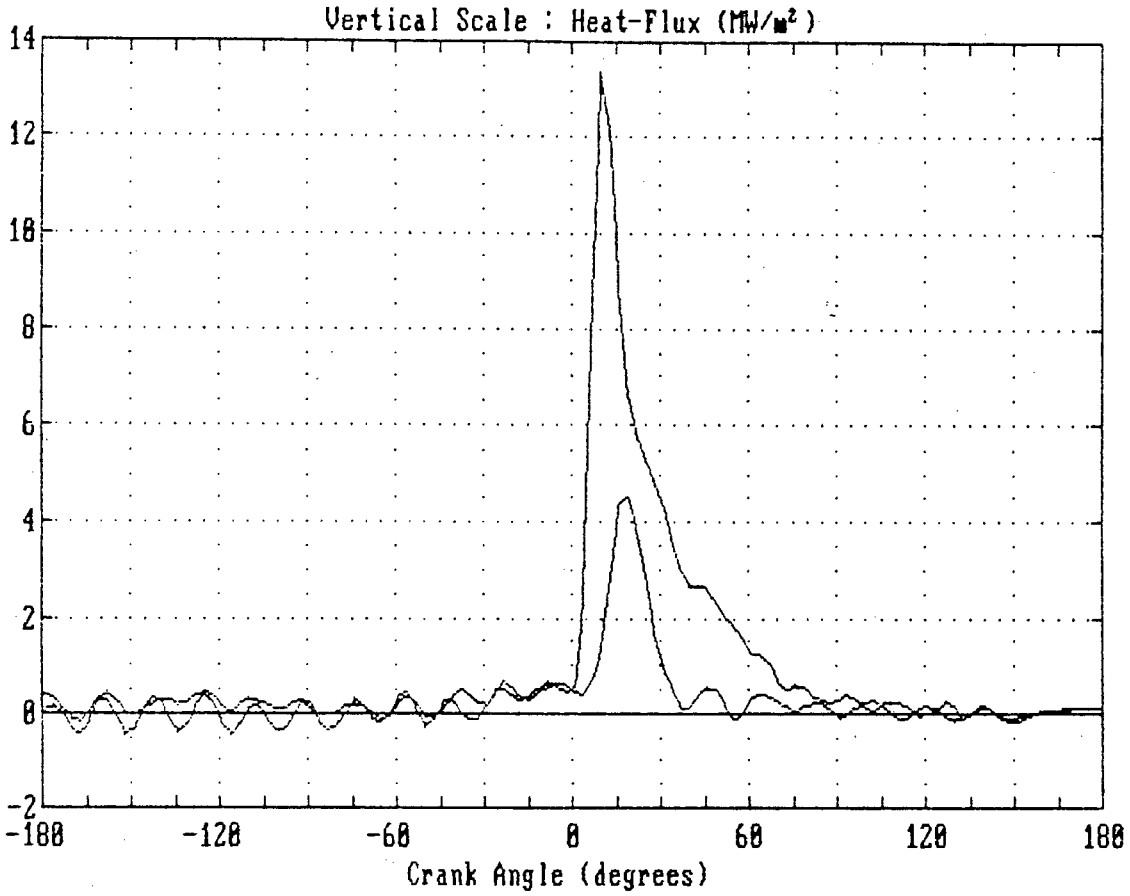


Figure 20. Heat flux computed from Tc 3 data for normal and knocking combustion of gasoline.

| | |
|---|---|
| Engine | : OM 407 |
| Compression ratio | : 9.5 |
| Engine speed (rev/min) | : 1495 |
| Ignition (°BTDC) | : 16 |
| Fuel type | : Gasoline (98 RON) |
| A/F Equiv. ratio | : 1.03 |

Schematic diagram showing the thermocouple location

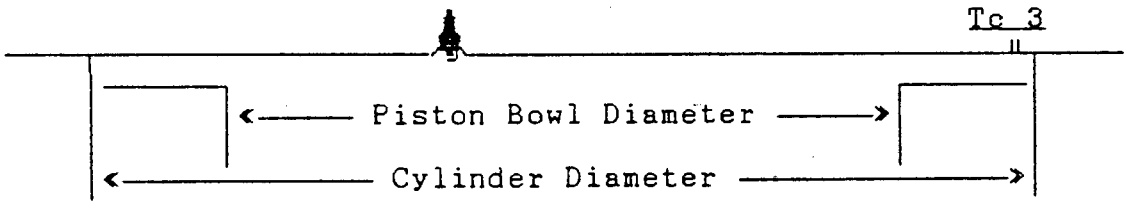

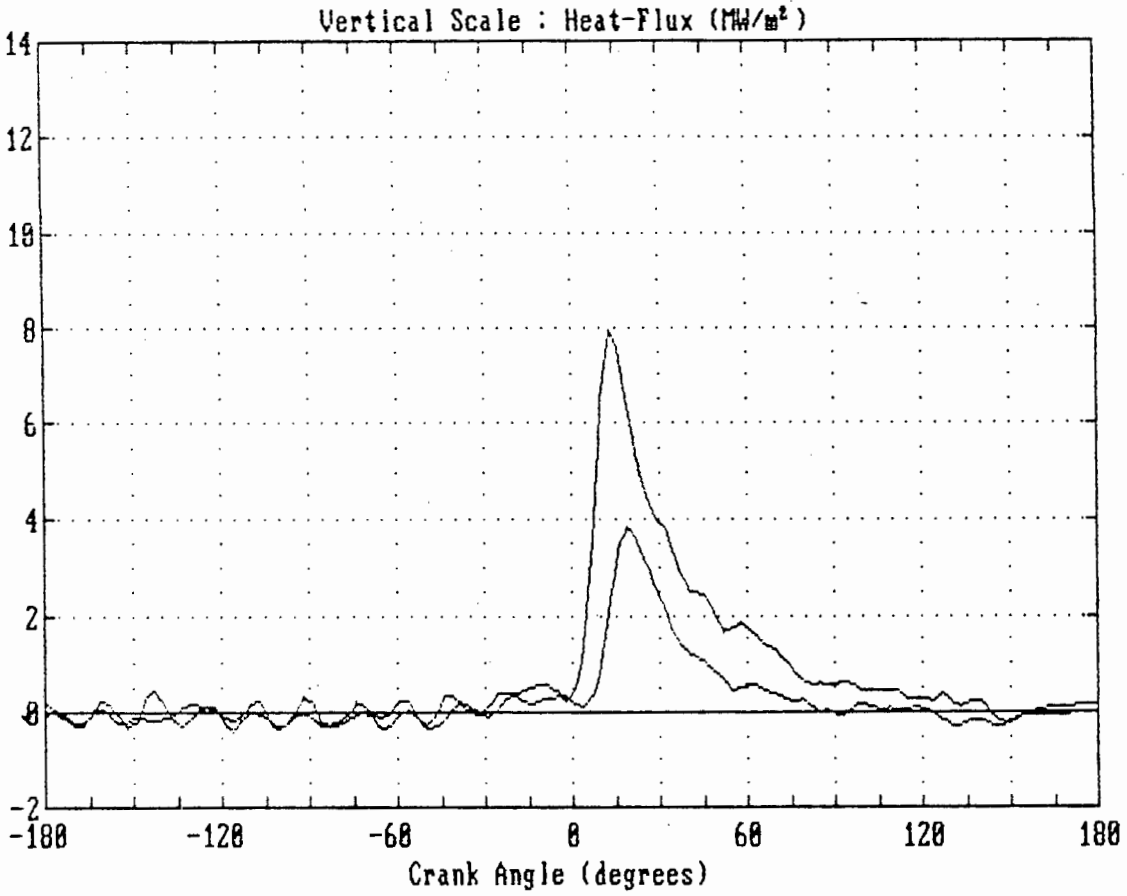


Figure 21. Heat flux computed from Tc 23 data for normal and knocking combustion of gasoline.

| | | |
|---|---|---|
| Engine | : | OM 407 |
| Compression ratio | : | 9.5 |
| Engine speed (rev/min) | : | 1495 |
| Ignition (°BTDC) | : | 16 |
| Fuel type | : | Gasoline (98 RON) |
| A/F Equiv. ratio | : | 1.03 |

Schematic diagram showing the thermocouple location

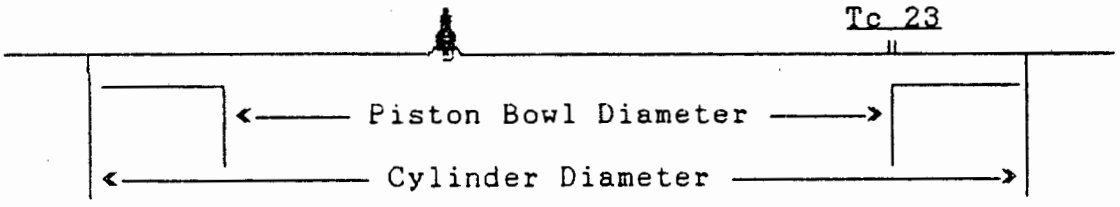

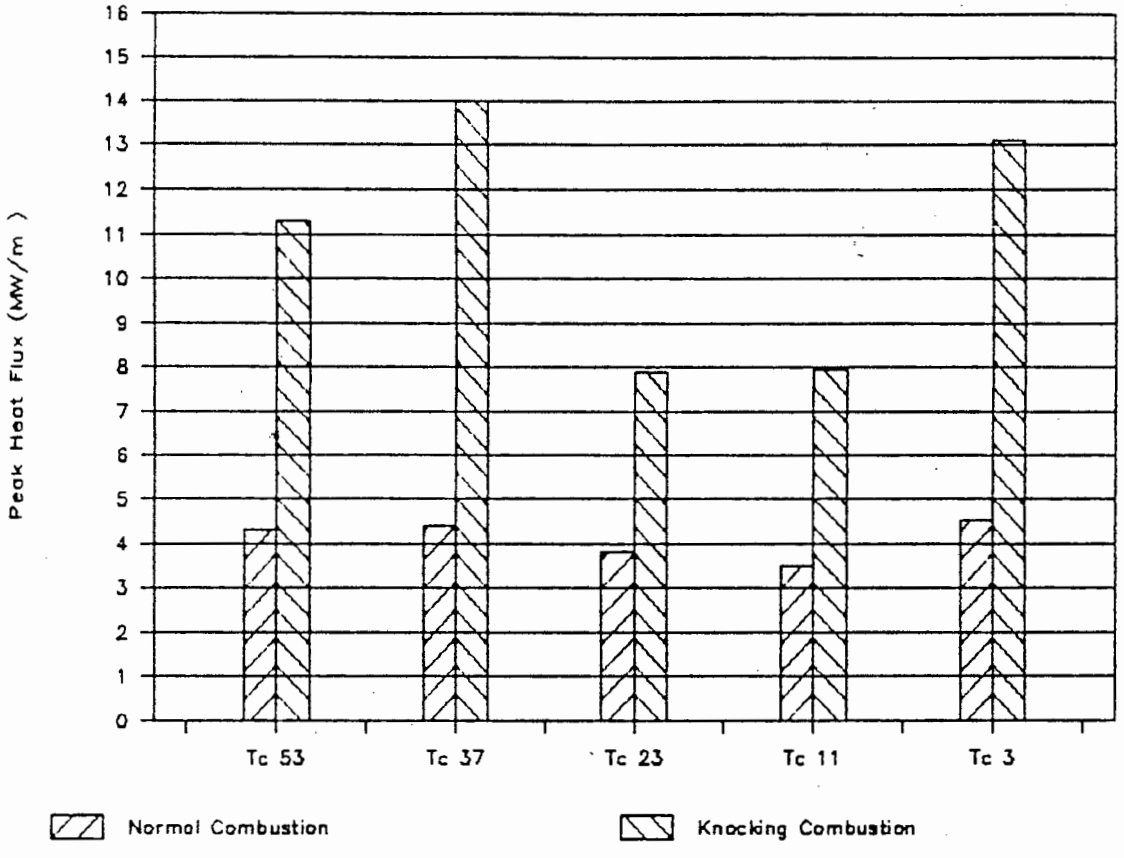


Figure 22. Diagram showing the peak heat flux for normal and knocking combustion of gasoline.

| | |
|---|---|
| Engine | : OM 407 |
| Compression ratio | : 9.5 |
| Engine speed (rev/min) | : 1350 (nominal) |
| Ignition (°BTDC) | : 16, 20 |
| Fuel type | : Gasoline (98 RON) |
| A/F Equiv. ratio | : 1.0 (nominal) |

Schematic diagram showing the thermocouple location

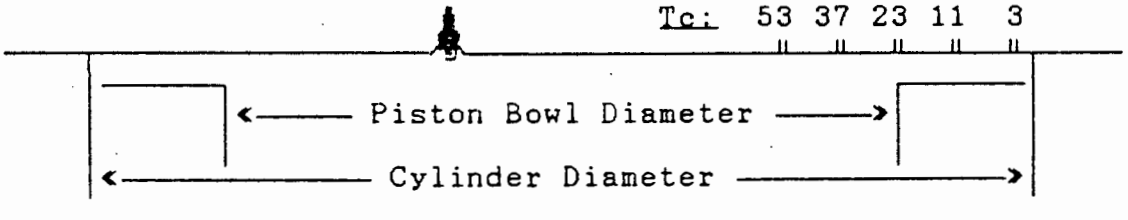

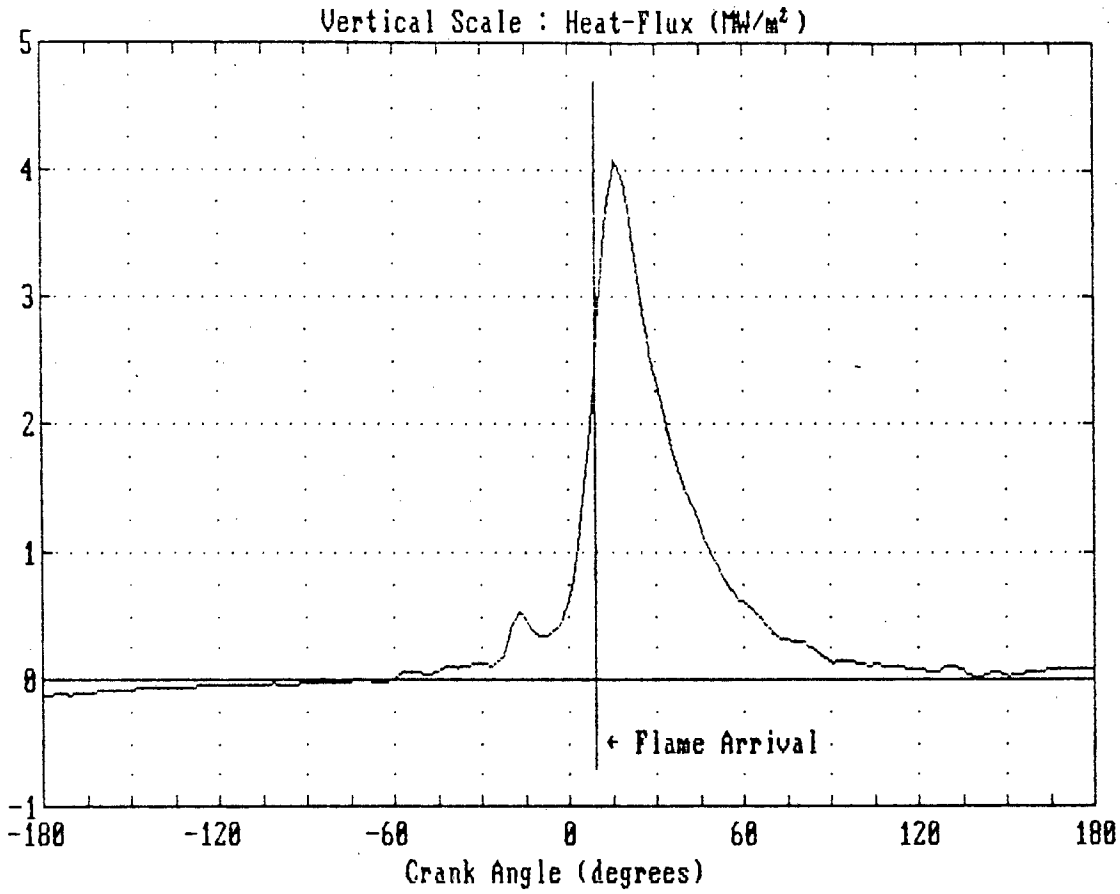


Figure 23. Heat flux computed from the average of 50 engine cycles at thermocouple location Tc 11. Engine operation at incipient knock conditions.

| | |
|---|---|
| Engine | : OM 407 |
| Compression ratio | : 9.5 |
| Engine speed (rev/min) | : 1311 |
| Ignition (°BTDC) | : 16 |
| Fuel type | : Gasoline (98 RON) |
| A/F Equiv. ratio | : 1.03 |

Schematic diagram showing the thermocouple location

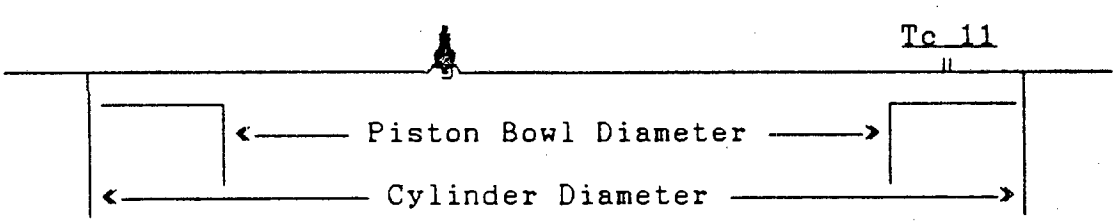

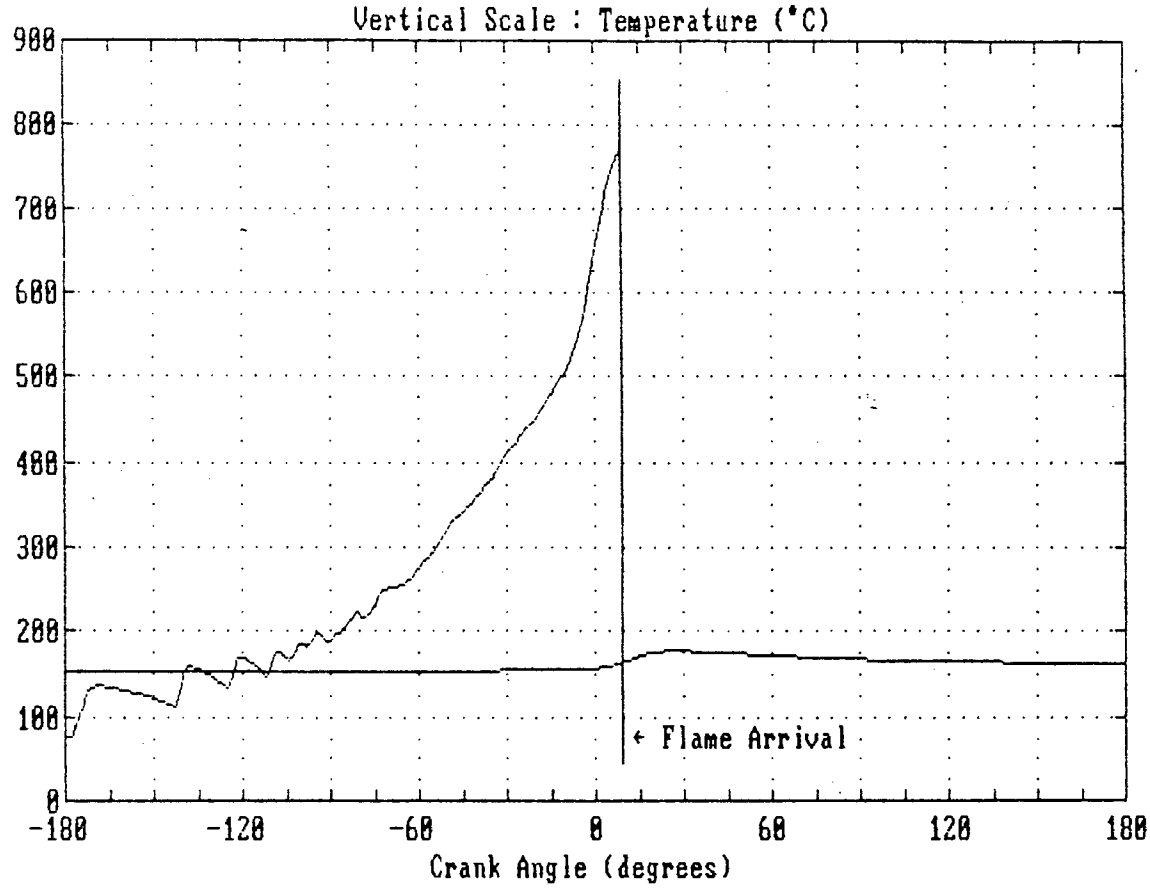


Figure 24. Gas temperature diagram at thermocouple location 11, calculated with the aid of the characteristic fuel constants for knocking gasoline combustion. Also showing the wall-surface temperature at the same location.

| | |
|---|---|
| Engine | : OM 407 |
| Compression ratio | : 9.5 |
| Engine speed (rev/min) | : 1311 |
| Ignition (°BTDC) | : 16 |
| Fuel type | : Gasoline (98 RON) |
| A/F Equiv. ratio | : 1.03 |

Schematic diagram showing the thermocouple location

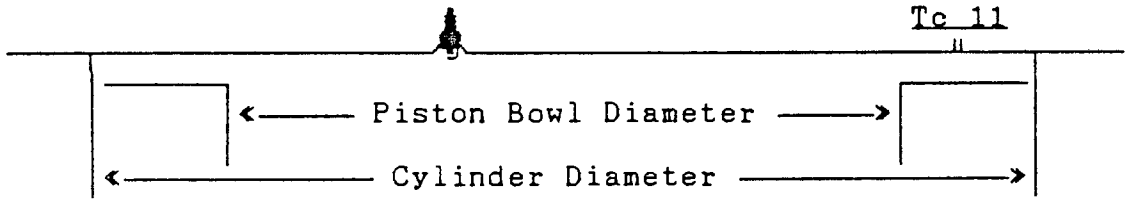

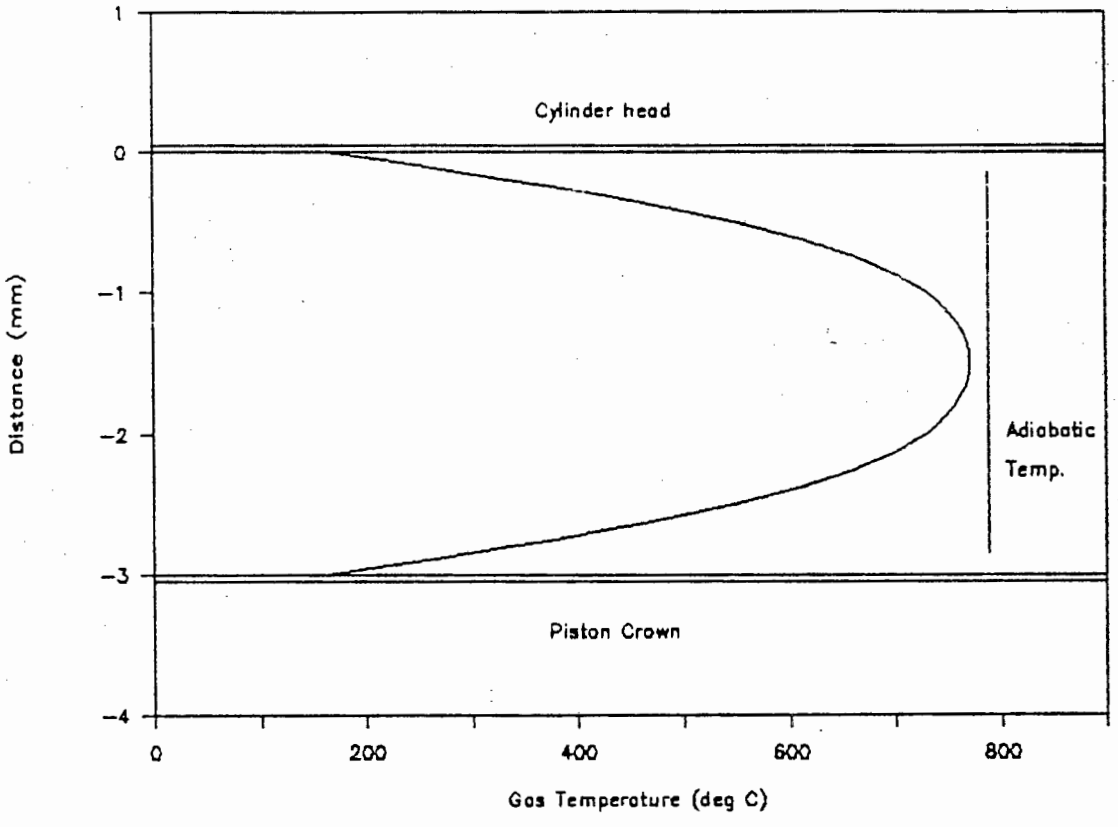


Figure 25. End-gas temperature profile at the instant of flame arrival at the location of thermocouple number 11 for gasoline combustion. Also showing the adiabatic temperature for the same instant.

| | |
|---|---|
| Engine | : OM 407 |
| Compression ratio | : 9.5 |
| Engine speed (rev/min) | : 1311 |
| Ignition (°BTDC) | : 16 |
| Fuel type | : Gasoline (98 RON) |
| A/F Equiv. ratio | : 1.03 |

Schematic diagram showing the thermocouple location

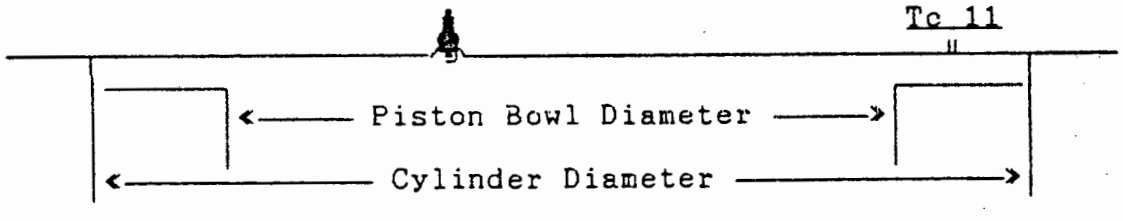

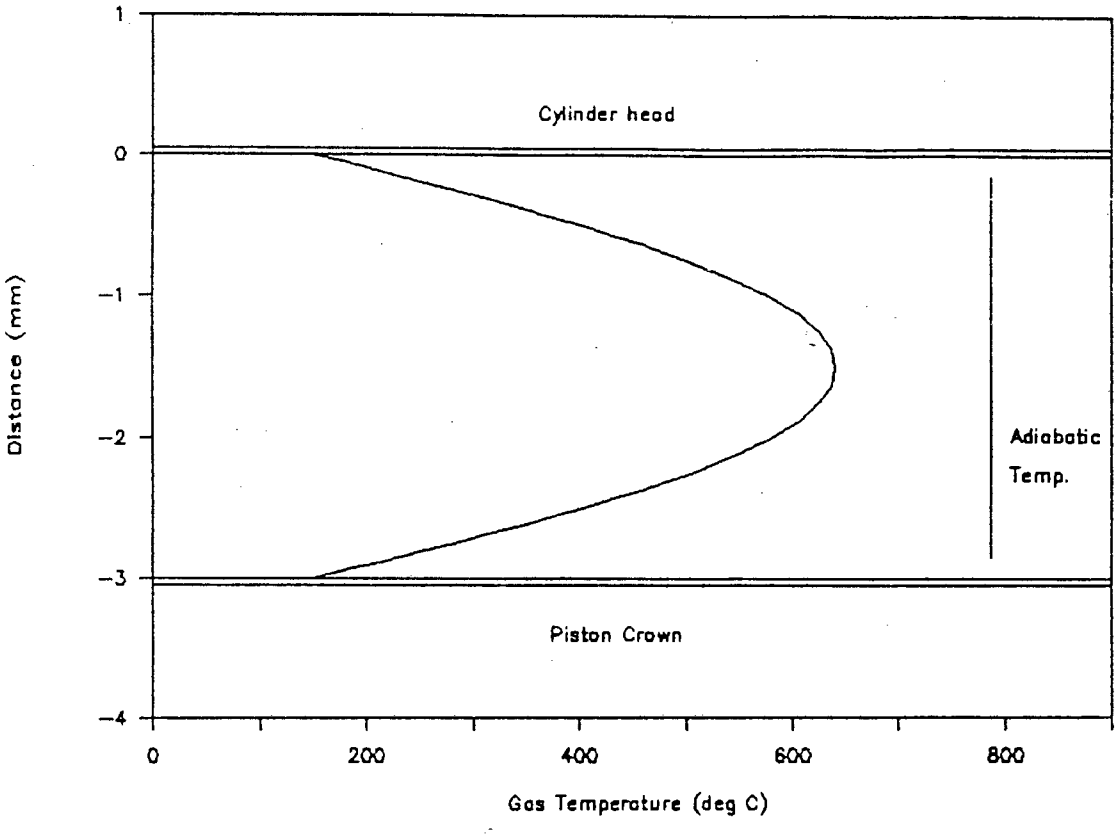


Figure 26. End-gas temperature profile at the instant of flame arrival at the location of thermocouple number 3 for gasoline combustion. Also showing the adiabatic temperature for the same instant.

| | |
|---|---|
| Engine | : OM 407 |
| Compression ratio | : 9.5 |
| Engine speed (rev/min) | : 1311 |
| Ignition (°BTDC) | : 16 |
| Fuel type | : Gasoline (98 RON) |
| A/F Equiv. ratio | : 1.03 |

Schematic diagram showing the thermocouple location

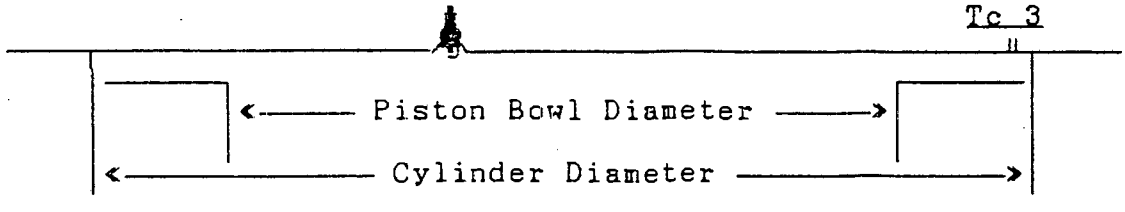

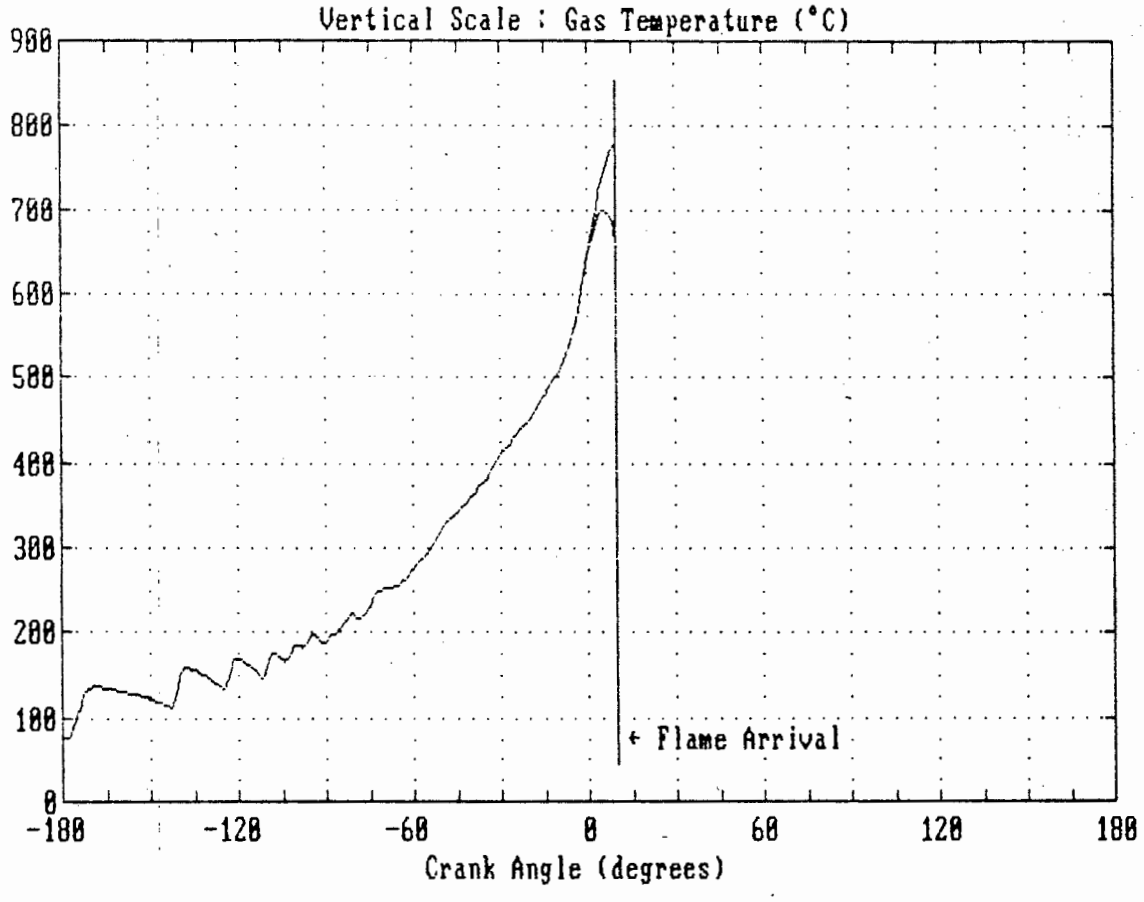


Figure 27. Gas temperature diagram at thermocouple location 3, calculated with the aid of the characteristic fuel constants for knocking gasoline combustion. Also showing the superimposed adiabatic temperature diagram.

| | |
|---|---|
| Engine | : OM 407 |
| Compression ratio | : 9.5 |
| Engine speed (rev/min) | : 1311 |
| Ignition (°BTDC) | : 16 |
| Fuel type | : Gasoline (98 RON) |
| A/F Equiv. ratio | : 1.03 |

Schematic diagram showing the thermocouple location

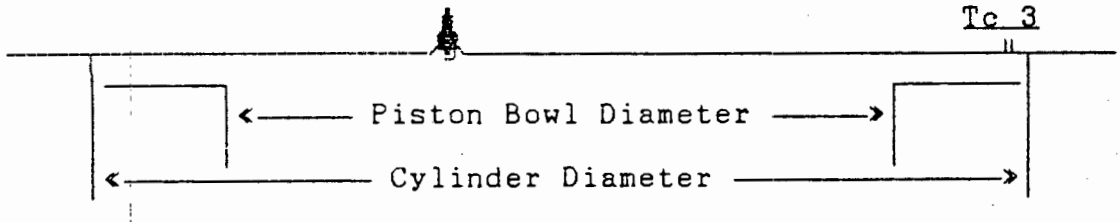

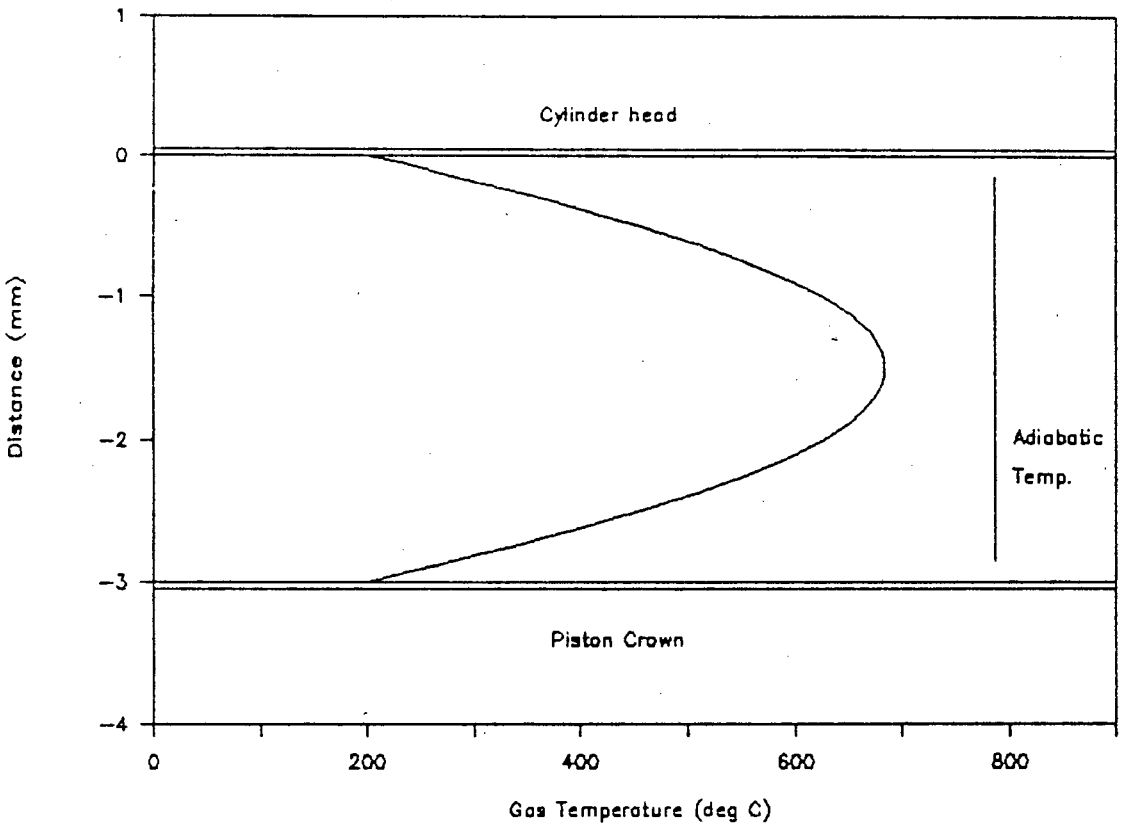


Figure 28. End-gas temperature profile at the instant of flame arrival at the location of thermocouple number 23 for gasoline combustion. Also showing the adiabatic temperature for the same instant.

| | |
|---|---|
| Engine | : OM 407 |
| Compression ratio | : 9.5 |
| Engine speed (rev/min) | : 1311 |
| Ignition (°BTDC) | : 16 |
| Fuel type | : Gasoline (98 RON) |
| A/F Equiv. ratio | : 1.03 |

Schematic diagram showing the thermocouple location

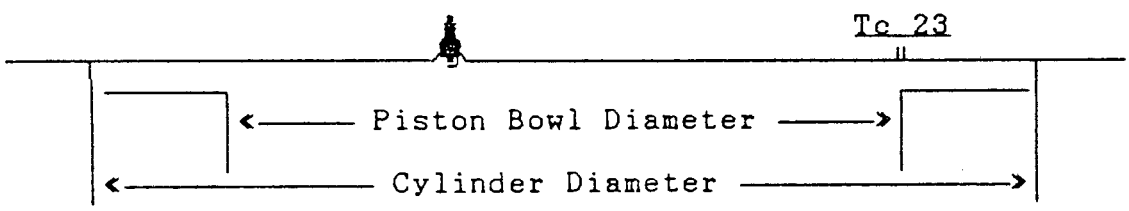

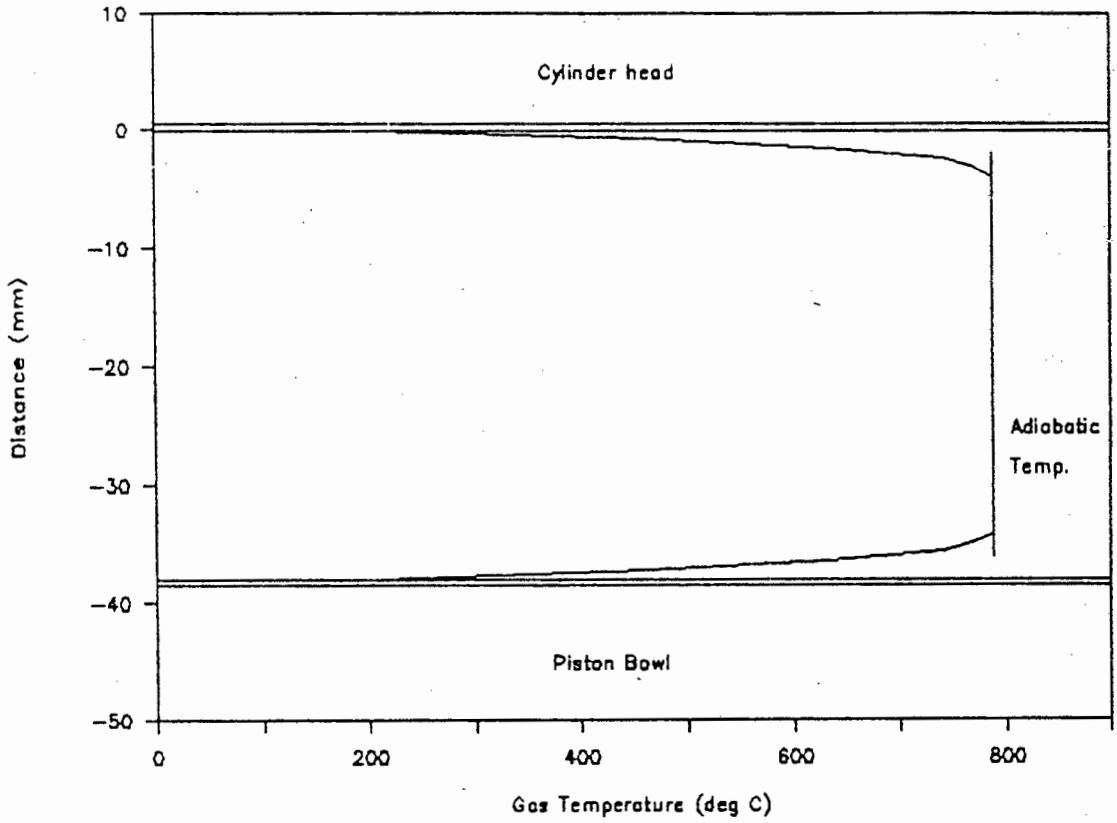


Figure 29. End-gas temperature profile at the instant of flame arrival at the location of thermocouple number 37 for gasoline combustion. Also showing the adiabatic temperature for the same instant.

| | |
|---|---|
| Engine | : OM 407 |
| Compression ratio | : 9.5 |
| Engine speed (rev/min) | : 1311 |
| Ignition (°BTDC) | : 16 |
| Fuel type | : Gasoline (98 RON) |
| A/F Equiv. ratio | : 1.03 |

Schematic diagram showing the thermocouple location

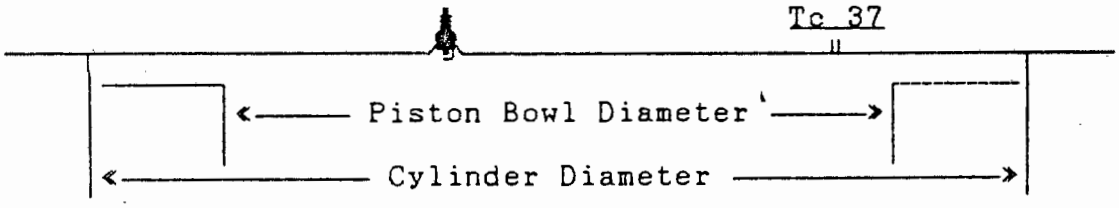

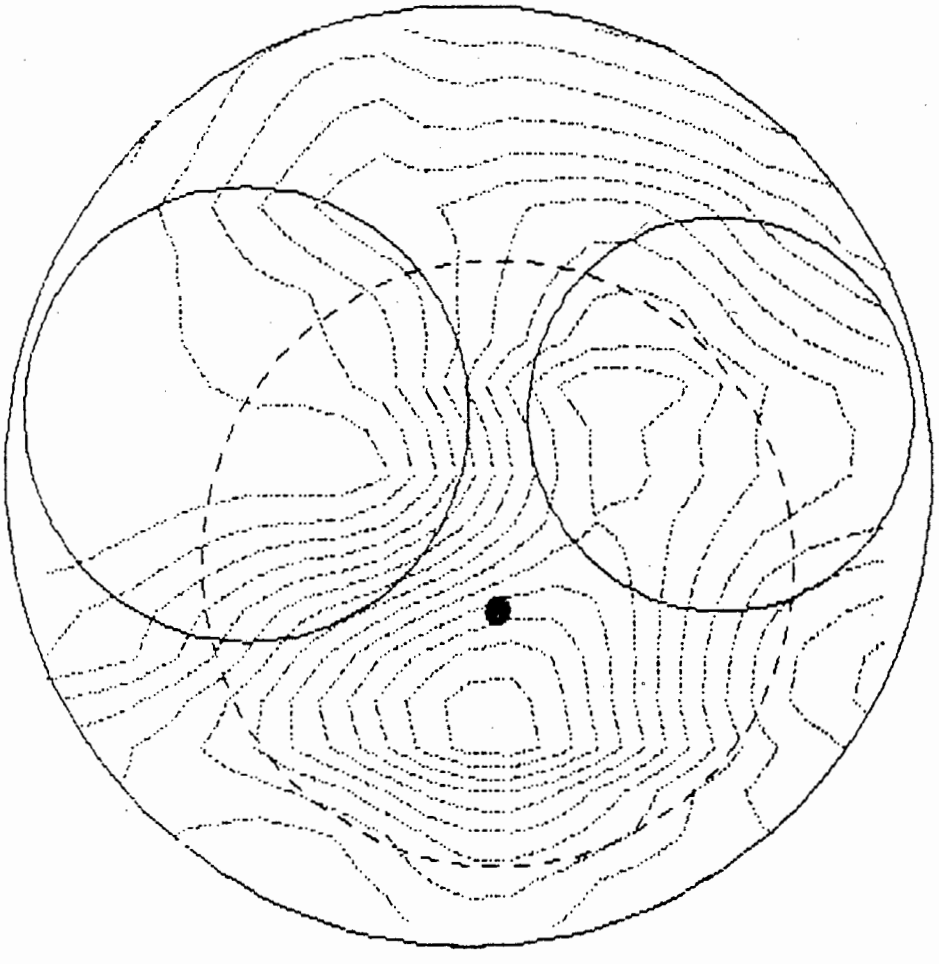

Figure 30. Flame contours for methanol combustion at incipient knock conditions.

Inner contour at -8° c.a.
Increments at +1 ° c.a.
Outer contour at 5° c.a.

| | |
|---|---|
| Engine | : OM 407 |
| Compression ratio | : 12.5 |
| Engine speed (rev/min) | : 1364 |
| Ignition (°BTDC) | : 18 |
| Fuel type | : Methanol |
| A/F Equiv. ratio | : 0.97 |

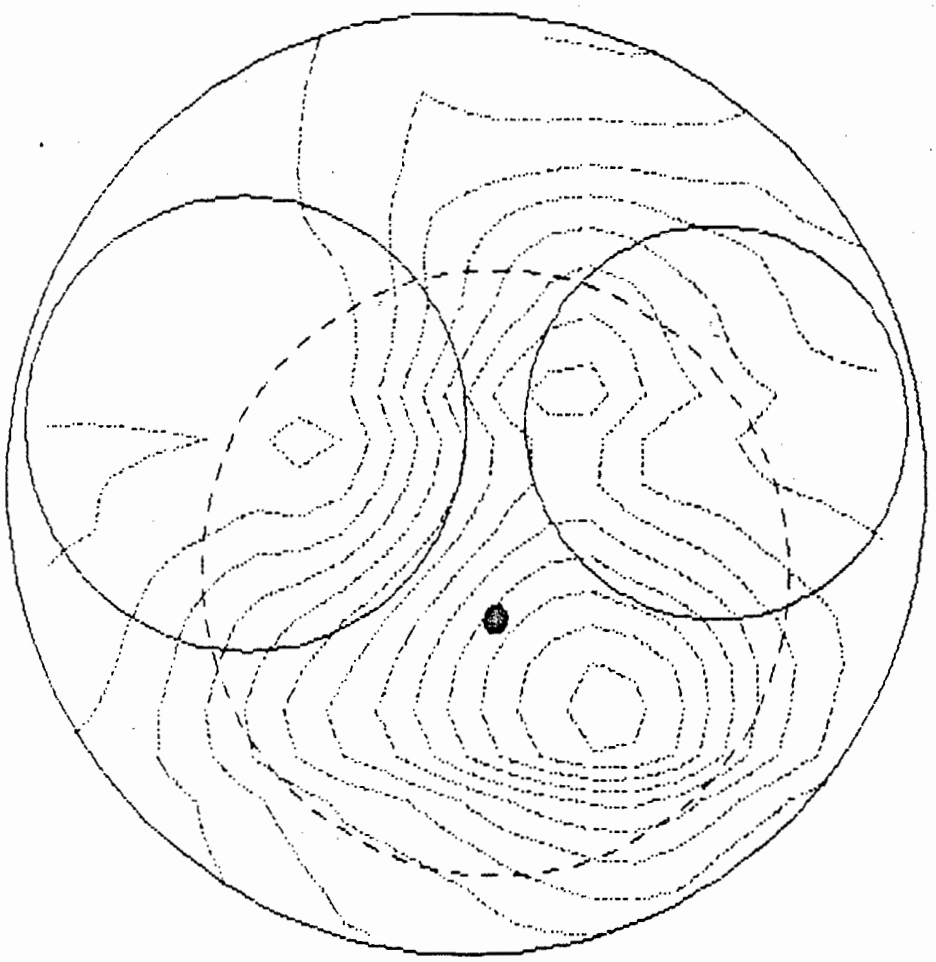

Figure 31. Cylinder head iso-therms for methanol combustion at incipient knock conditions.

Inner contour at 475°C
Increments at -25°C
Outer contour at 175°C

| | |
|---|---|
| Engine | : OM 407 |
| Compression ratio | : 12.5 |
| Engine speed (rev/min) | : 1364 |
| Ignition (°BTDC) | : 18 |
| Fuel type | : Methanol |
| A/F Equiv. ratio | : 0.97 |

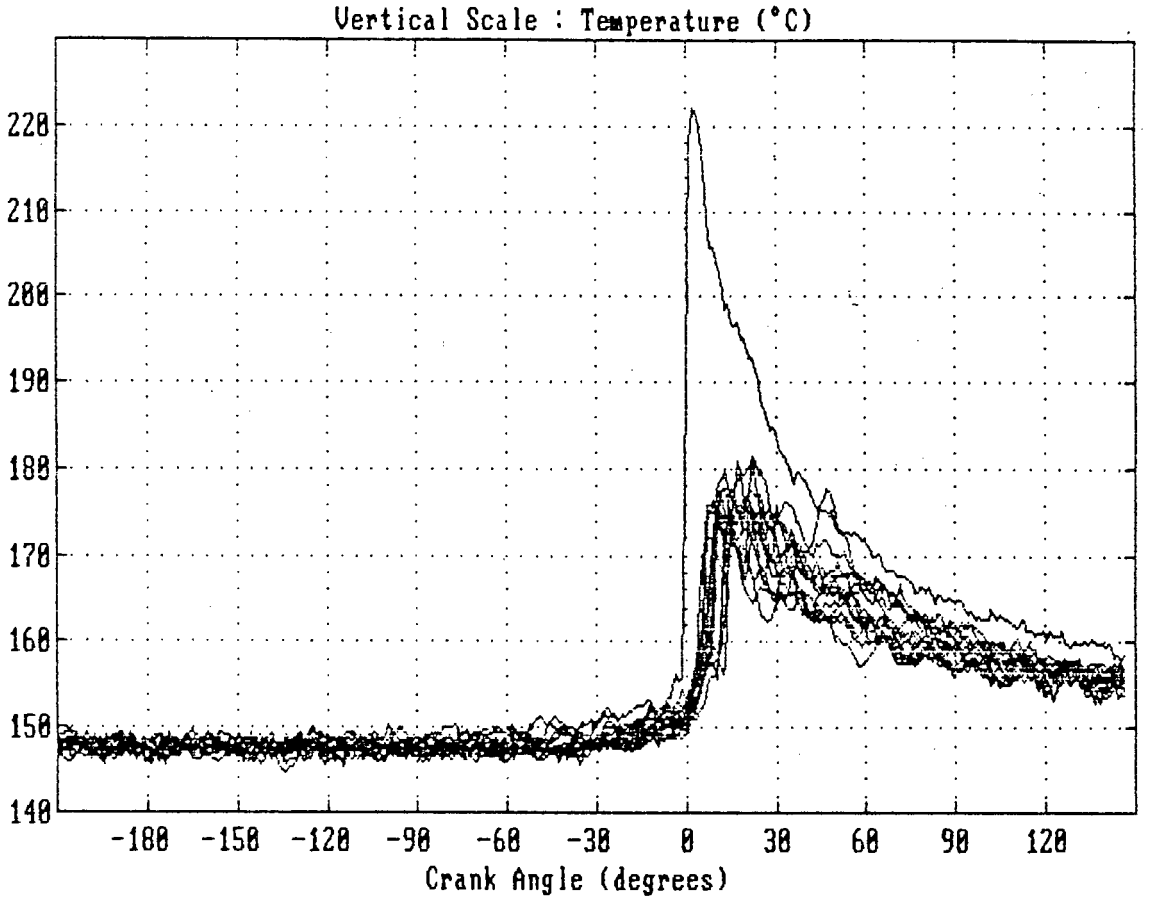


Figure 32. Thermocouple number 27 signal for 20 successive cycles showing an isolated case of methanol knocking.

| | |
|---|---|
| Engine | : OM 407 |
| Compression ratio | : 12.5 |
| Engine speed (rev/min) | : 1398 |
| Ignition (°BTDC) | : 18 |
| Fuel type | : Methanol |
| A/F Equiv. ratio | : 0.98 |

Schematic diagram showing the thermocouple location

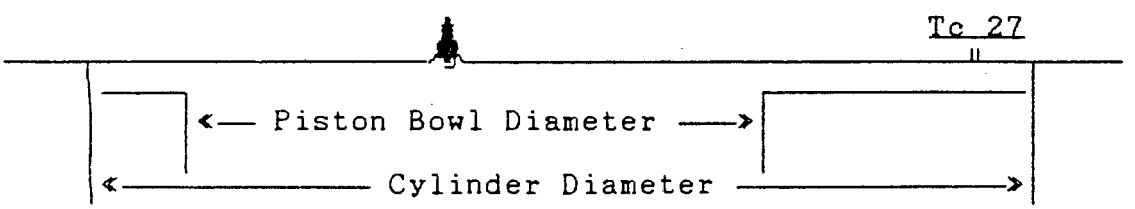

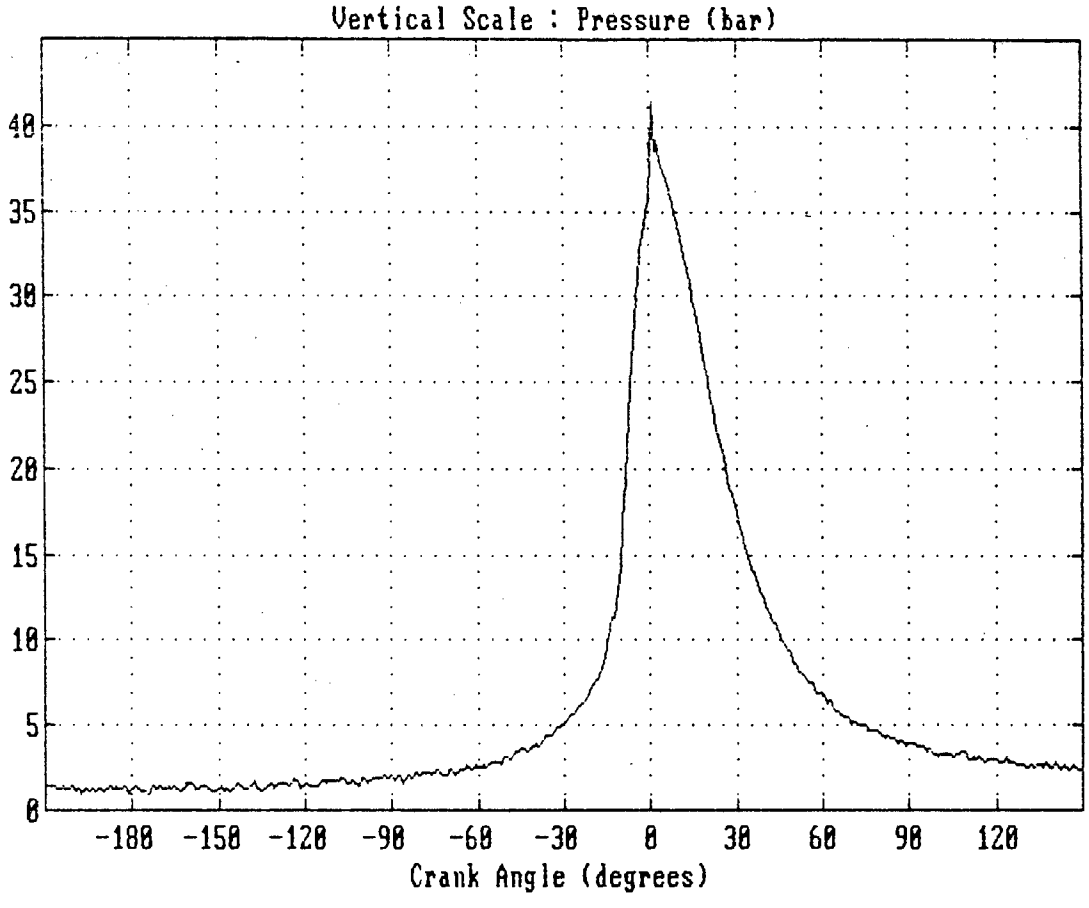


Figure 33. Pressure diagram corresponding to the knocking cycle in figure 32.

| | |
|---|---|
| Engine | : OM 407 |
| Compression ratio | : 12.5 |
| Engine speed (rev/min) | : 1399 |
| Ignition (°BTDC) | : 18 |
| Fuel type | : Methanol |
| A/F Equiv. ratio | : 0.98 |

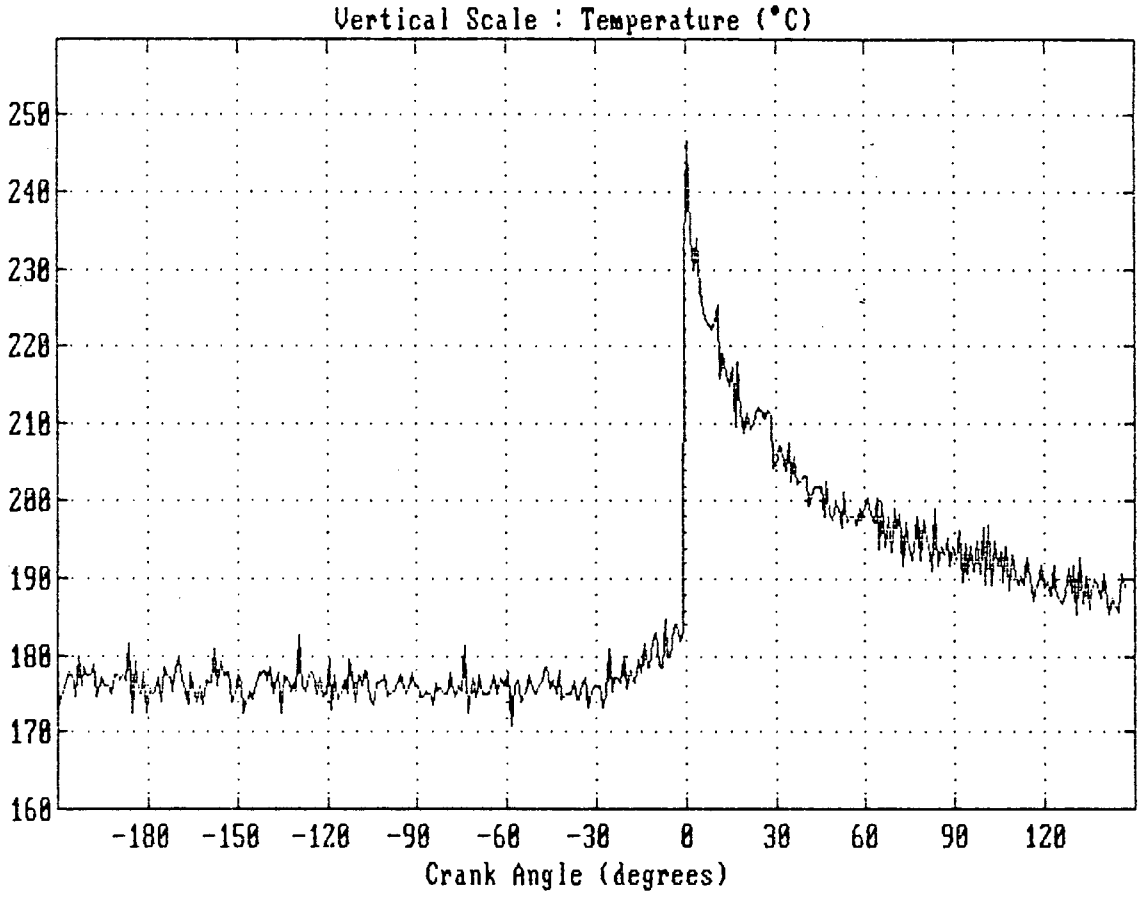


Figure 34. Thermocouple number 153 signal corresponding to the knocking cycle in figure 32.

| | |
|---|---|
| Engine | : OM 407 |
| Compression ratio | : 12.5 |
| Engine speed (rev/min) | : 1399 |
| Ignition (°BTDC) | : 18 |
| Fuel type | : Methanol |
| A/F Equiv. ratio | : 0.98 |

Schematic diagram showing the thermocouple location

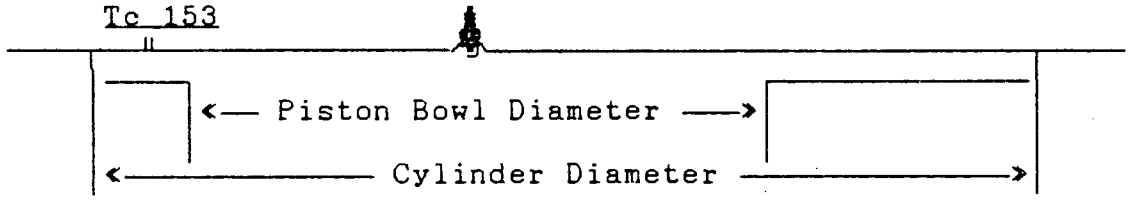

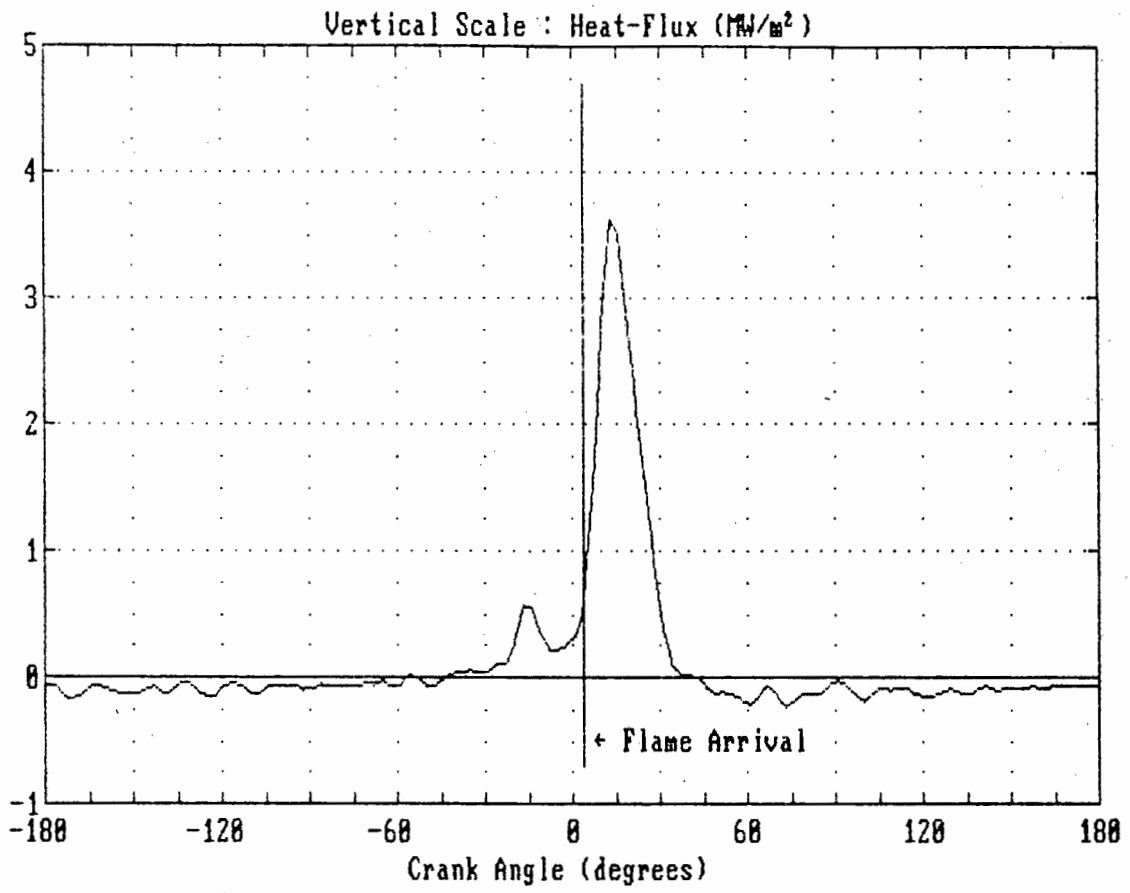


Figure 35. Heat flux computed from the average of 50 engine cycles at thermocouple location Tc 17. Engine operation at incipient knock conditions using methanol.

| | |
|---|---|
| Engine | : OM 407 |
| Compression ratio | : 12.5 |
| Engine speed (rev/min) | : 1399 |
| Ignition (°BTDC) | : 18 |
| Fuel type | : Methanol |
| A/F Equiv. ratio | : 0.98 |

Schematic diagram showing the thermocouple location

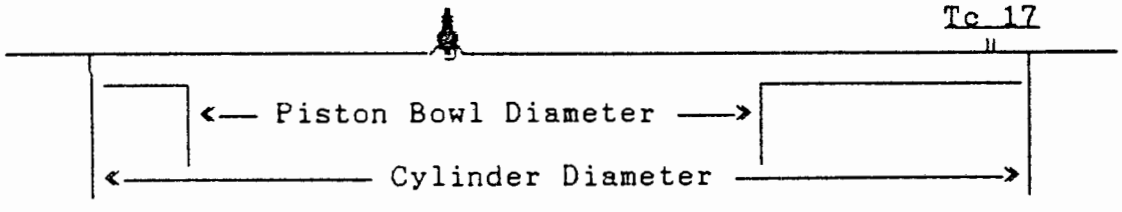

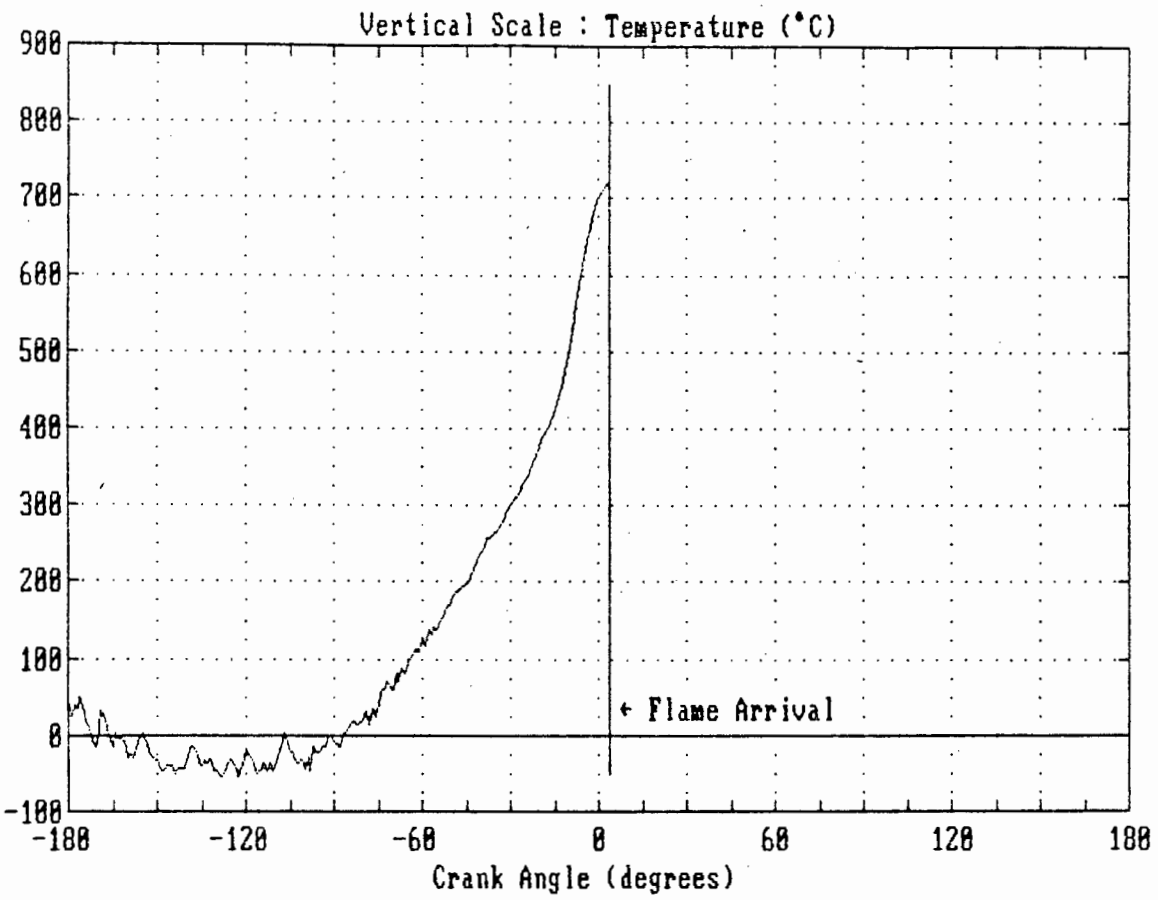


Figure 36. Gas temperature diagram at thermocouple location 17, calculated with the aid of the characteristic fuel constants for knocking methanol combustion.

| | |
|---|---|
| Engine | : OM 407 |
| Compression ratio | : 12.5 |
| Engine speed (rev/min) | : 1399 |
| Ignition (°BTDC) | : 18 |
| Fuel type | : Methanol |
| A/F Equiv. ratio | : 0.98 |

Schematic diagram showing the thermocouple location

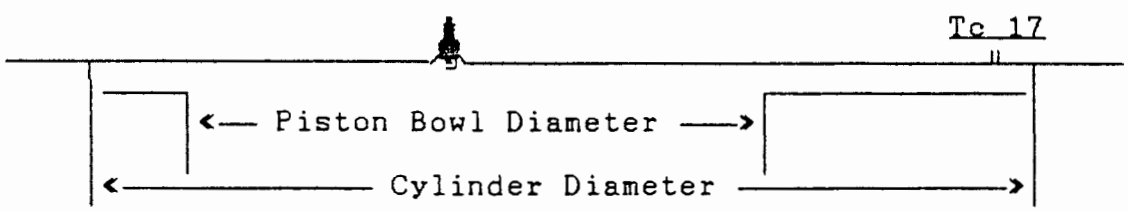

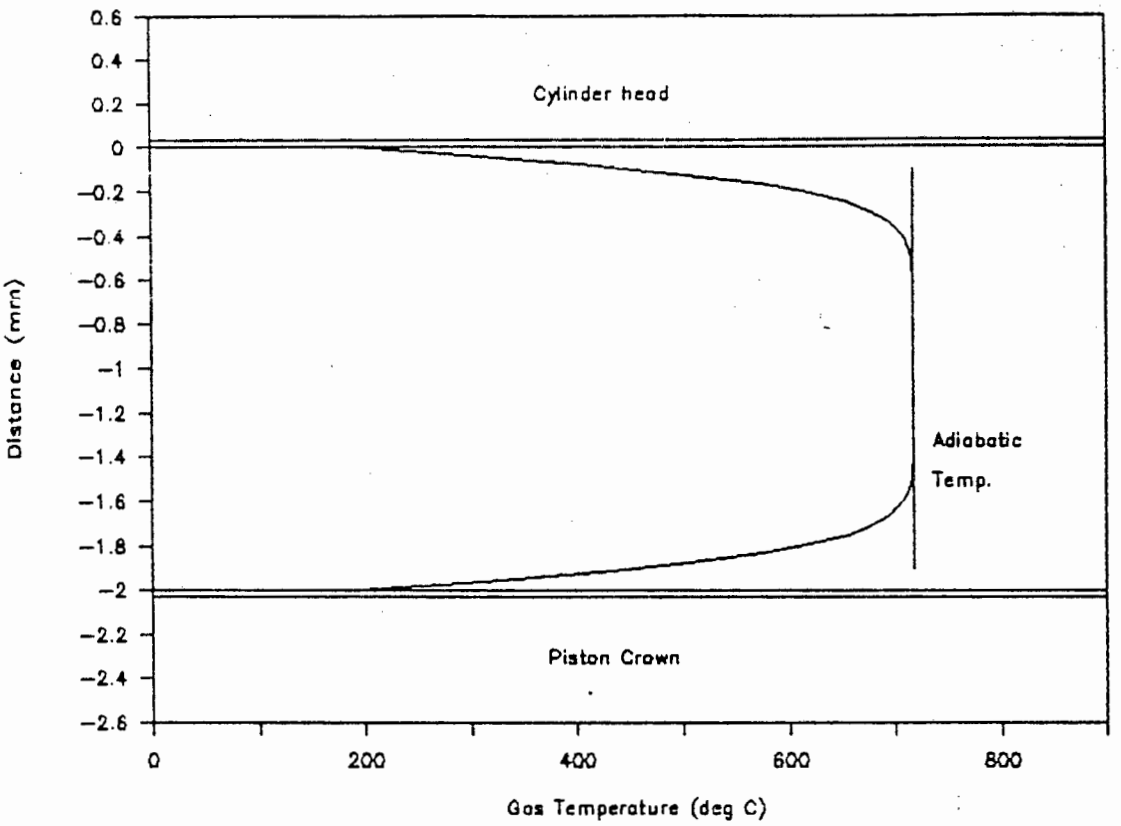


Figure 37. End-gas temperature profile at the instant of flame arrival at the location of thermocouple number 17 for methanol combustion. Also showing the adiabatic temperature for the same instant.

| | |
|---|---|
| Engine | : OM 407 |
| Compression ratio | : 12.5 |
| Engine speed (rev/min) | : 1399 |
| Ignition (°BTDC) | : 18 |
| Fuel type | : Methanol |
| A/F Equiv. ratio | : 0.98 |

Schematic diagram showing the thermocouple location

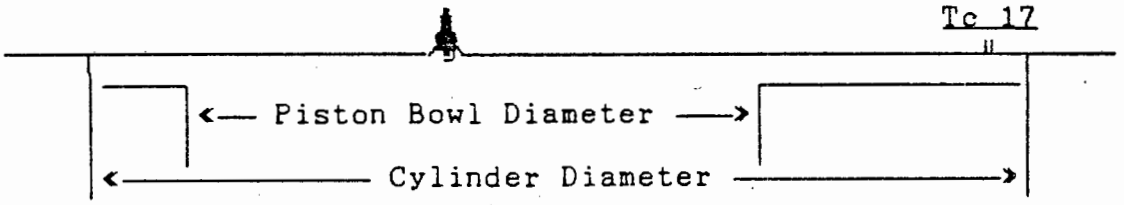

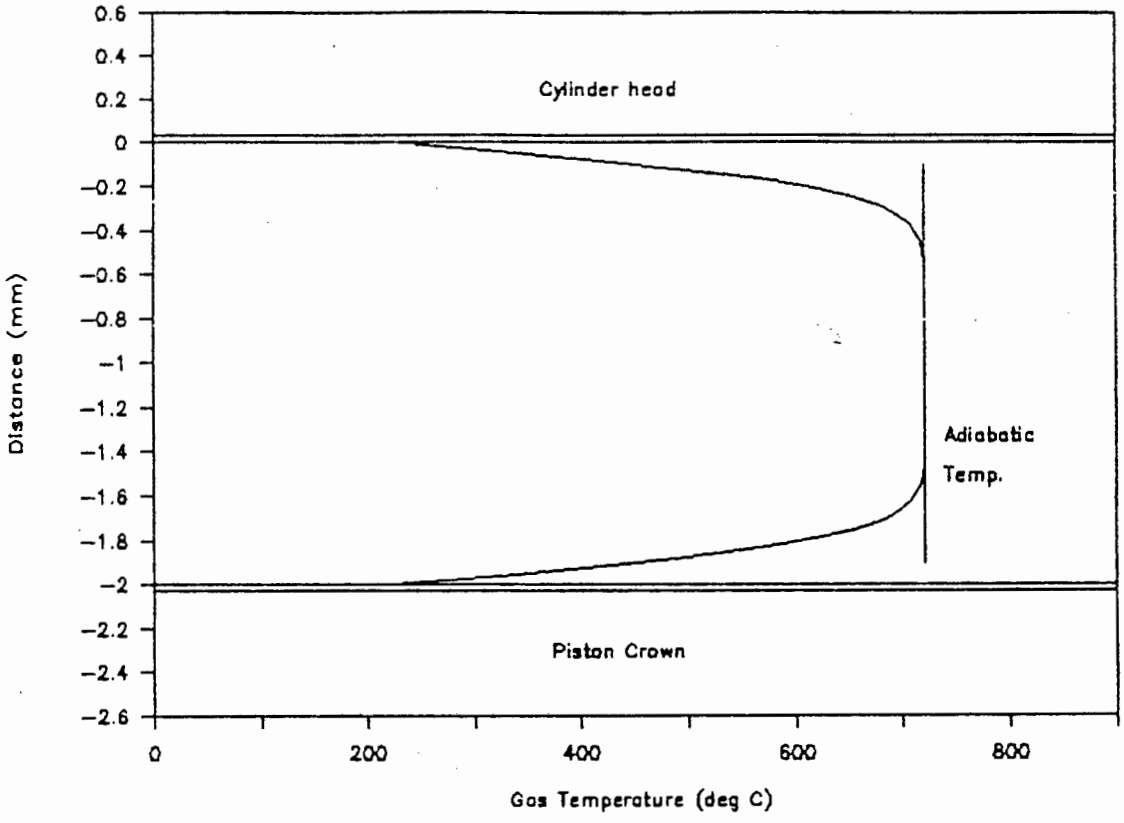


Figure 38. End-gas temperature profile at the instant of flame arrival at the location of thermocouple number 19 for methanol combustion. Also showing the adiabatic temperature for the same instant.

| | |
|---|---|
| Engine | : OM 407 |
| Compression ratio | : 12.5 |
| Engine speed (rev/min) | : 1399 |
| Ignition (°BTDC) | : 18 |
| Fuel type | : Methanol |
| A/F Equiv. ratio | : 0.98 |

Schematic diagram showing the thermocouple location

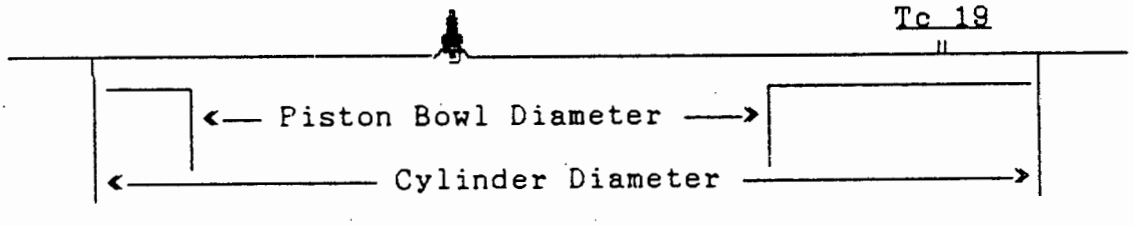

# APPENDICES

## APPENDIX A - KNOCK MODEL DERIVATION

In a pioneering paper by Rifkin and Walcutt [10], an attempt was made to characterise fuels in terms of an ignition delay time using a rapid-compression machine. Their approach assumed that the production of the chemical species or chain-carriers necessary for auto-ignition to take place, could be expressed by a generalised gross reaction which was expected to be valid for the limited pressure and temperature range encountered in spark-ignition engine operation. The proposed reaction was assumed to have the form:

$$\frac{d\alpha}{dt} = f\{ \alpha, T, P, \phi, \text{fuel} \} \qquad (A.1)$$

Where: $\alpha$ = concentration of the pertinent reaction component
$T$ = the gas temperature
$P$ = the pressure, and
$\phi$ = the equivalence ratio of the fuel/air mixture.

Equation (A.1) implies that, for a given fuel/air mixture, there exists a fixed functional relationship between the rate of the aggregate reaction, the instantaneous physical state and time. The form of this relationship was assumed to have a simple Arrhenius dependency on temperature:

$$\frac{d\alpha}{dt} = \alpha A' P^{n} e^{-\frac{B}{T}} \qquad (A.2)$$

Where: $A'$ = constant
$n$ = pressure coefficient
$B$ = temperature coefficient

It was assumed further that the ultimate consequence of the gross reaction of equation (A.2), was a sudden transition to a process

with a much faster reaction rate that rapidly completes the reaction. The critical time, $t_c$, for the occurrence of auto-ignition thus corresponded to the attainment of a critical concentration of the chain carriers, $\alpha_c$. If the pressure and temperature were constant, this critical time could be computed by a straightforward integration of the equation (A.2) from some time origin, "$t_o$".

$$\tau = t_c - t_o = A\, P^{-n}\, e^{\frac{B}{T}} \qquad (A.3)$$

Where: $A = \dfrac{\mathrm{Ln}(\alpha_c)}{A'\ \mathrm{Ln}(\alpha_o)}$

The time interval, "$\tau$", was referred to as the auto-ignition delay. Rifkin and Walcutt determined the characteristic constants of several pure fuels, using the rapid-compression machine to generate sharp steps of constant pressure and temperature. When they attempted to correlate their ignition delay data with the peak pressure and temperature that occurred in an actual engine, they encountered significant discrepancies. However, they concluded that:

> "It is difficult to evaluate the seriousness of this discrepancy because of the uncertainty in the calculation of the temperatures, both in the rapid compression machine and in the engine. In fact, systematic errors in these calculations, which would bring the two sets of data almost completely into line, can easily be imagined."

Besides this convenient explanation for the discrepancy in their data, their analysis technique also erred in that they used the peak engine pressure and temperature as a basis for comparison. When applied to time-variable pressure and temperature, such as exists within an engine, equation (A.2) may be solved in integral form provided that the critical concentration of chain carriers obtained at the critical time at which knock occurs is independent of the pressure and temperature levels. Thus the critical time, $t_c$, is determined by the equation:

$$1 = \int_{t_o}^{t_c} \frac{dt}{A\, P^{-n}(t)\, e^{\frac{B}{T(t)}}} \qquad (A.4)$$

Expressed in this form, the singleness of the phenomenon between auto-ignition in the rapid compression machine and knock in an engine was shown by Taylor [18]. The instant that knock occurred in the engine was predicted by the auto-ignition model based on rapid-compression machine data, with sufficiently accuracy to validate the assumptions.

This approach, where the delay parameters of the fuel were determined with a rapid compression machine and then used to predict knock occurrence, has limited practical application to the wide variety of commercial fuels and engines. A rapid compression machine is not suited to operation with a wide boiling-range fuel in the pressure and temperature range encountered in engines. Also, the rate at which data is produced is very slow and moreover, the general extrapolation of data to an actual engine always has the risk of introducing error of interpretation.

An alternative technique was proposed by Douaud [51] wherein an attempt was made to use the engine itself, running under knocking conditions, as a source of data from which the auto-ignition delay coefficients of the fuel could be deduced. The engine was operated under a wide variety of knocking conditions and the pressure and temperature history of the end-gas was recorded and used to solve the non-linear set of equations:

$$1 = \int_{t_o}^{t_{ci}} \frac{dt}{A\, P_i(t)^{-n}\, e^{\frac{B}{T_i(t)}}} \qquad (A.5)$$

$$i = 1,2,\ldots,n$$

From a mathematical view point, since there are three unknown constants, at least three different conditions must be fulfilled to determine a solution which characterise the fuel. In practice, it was desired that the number of independent conditions be greater in order to improve the uniqueness of the solution using statistical analysis. A mathematical optimisation procedure was therefore used to minimise the standard deviation, "SQ", between

the value of the integral and the theoretical value of 1 for all the tests.

$$SQ = \sum_{i=1}^{n} \left[ 1 - \int_{t_o}^{t_{ci}} \frac{dt}{A\, P_i(t)^{-n}\, e^{\frac{B}{T_i(t)}}} \right]^2 \qquad (A.6)$$

The standard deviation also served to indicate the accuracy of the fuel coefficients.

The method of solution of equation (A.6) consisted of treating "n" and "B" as independant variables, and solving for the value of "A" that would give the lowest value of "SQ". An example of a range of "n" and "B" values and the corresponding standard deviation of the mean of "A" are shown in the table below for gasoline. The solution, "n" ≈ -1.6 and "B" ≈ 9000, was found by inspection as indicated. The range of "n" and "B" could be narrowed to find a solution to the desired precision, and hence the value of "A" and "SQ".

Non-linear regression to solve equation (A.6)

| Standard Deviation Of The Mean Of "A" (Percent) | | | | | | | |
|---|---|---|---|---|---|---|---|
| n \ B | 6000 | 7000 | 8000 | 9000 | 10000 | 11000 | 12000 |
| -0.00 | 11.90 | 10.29 | 9.05 | 8.31 | 9.19 | 11.05 | 13.68 |
| -0.30 | 10.40 | 9.27 | 7.94 | 7.13 | 7.99 | 9.93 | 12.62 |
| -0.60 | 9.11 | 7.98 | 6.78 | 6.25 | 7.11 | 9.87 | 12.96 |
| -0.90 | 7.82 | 7.41 | 7.17 | 6.76 | 7.94 | 10.10 | 13.23 |
| -1.20 | 8.57 | 8.03 | 7.55 | 7.45 | 8.89 | 11.22 | 14.43 |
| -1.50 | 9.29 | 8.66 | 7.78 | 8.69 | 10.63 | 13.05 | 16.86 |

## APPENDIX B - EXPERIMENTAL DETAILS OF THE RICARDO TESTS

The single cylinder engine used for these studies was the Ricardo E6 research engine. Principal details of the engine are:

| | |
|---|---|
| Bore | 75 mm |
| Stroke | 111 mm |
| Connecting Rod | 242 mm |
| Compression Ratio | Variable |

The engine was operated naturally aspirated with the water temperature held constant at 69°C and the oil temperature constant at 60°C. An Alcock viscous air flow meter was used to measure the inlet air flow. The fuel was carburetted with a facility for pre-heating the air before the carburettor. The tests were conducted at borderline knock with wide open throttle and under a variety of speeds, compression ratios, ignition timing and inlet temperatures. A stoichiometric air/fuel ratio was maintained throughout the tests.

The combustion chamber of this engine was cylindrical in shape, the piston crown and cylinder head being flat. The spark-plug was situated 12mm from the center axis of the cylinder. The pressure transducer aperture was also 12mm from the center of the cylinder, diametrically opposite the spark-plug.

The two fuels tested were commercial grade 98 RON pump gasoline and standard commercial grade methanol. The gasoline comprised approximately 60% paraffins, 20% napthenes, 10% aromatics and 10% olefins. The lead content was 0.6g/l.

## B.1 ANALYTICAL EQUIPMENT

An AVL water-cooled pressure transducer, type 12QP, was used for pressure measurement. The transducer signal was processed using a Kistler model 568 charge amplifier. The pressure transducers' calibration was checked periodically using a dead-weight tester.

A computer-based data acquisition system was used for logging the cylinder pressure signal. The acquisition system had the capability to digitise analogue signals at a rate of up to $10^6$ conversions per second although, if more than one analogue input was required, the signals had to be multiplexed and the maximum analogue-to-digital conversion rate per channel was correspondingly reduced. The system was based on a hardware card by RC Electronics, the ISC-16 system, which was designed to slot into an IBM XT personal computer.

For the engine tests, three channels were used and the rate of digitisation was regulated by an external clock facility which was part of the ISC-16 system. The clock trigger signal was obtained from an AVL type 360c/600/s optical crank-angle marker unit. This shaft encoder unit also provided an accurate crank-angle reference trigger signal which was recorded on one of the channels. The reference trigger position was calibrated by means of the pressure signal. Under motoring conditions and allowing for the effects of heat transfer, the peak motoring pressure was assumed to occur at 0.7° BTDC (31).

The engine tests were conducted with the engine operating at borderline knock and the engine knock itself was used to initiate the data capture. The pressure signal was passed through a 0.33 octave band-pass filter which was tuned to the knocking frequency of about 7kHz. The filtered signal was captured on the third analogue-to-digital channel and the high frequency vibration that signified a knocking cycle was used to trigger the data capture. A special feature of the ISC-16 system software was its ability to initiate data capture on a delayed trigger. Thus, the data spanning a full engine revolution before and after the trigger

event was captured. An advantage of this method of data capture was that the engine cycle immediately preceding the data capture had to be a non-knocking cycle (or it would have initiated the data capture) and the pressure transducer signal was therefore free from the after-effects of thermal shock that could follow a knocking cycle.

The crank angle marker unit was also used to calibrate the engine speed indicator using a digital frequency counter. Accuracies of better than 0.2% were possible by this method.

## B.2 ANALYSIS SOFTWARE

The data capture was controlled by the ISC-16 system software which included facilities for viewing and printing the raw data. The system had the capability of holding up to 64 kilo-bytes of buffer storage which was saved to floppy disk for subsequent analysis. Two main software routines were written to analyse this data.

The first program processed the raw pressure signal and determined the temperature of the unburned portion of the cylinder contents up to the point of knock. The processed pressure and temperature data from 90° BTDC up to the point of knock was saved for subsequent analysis. The flow-diagram below shows the main program steps.

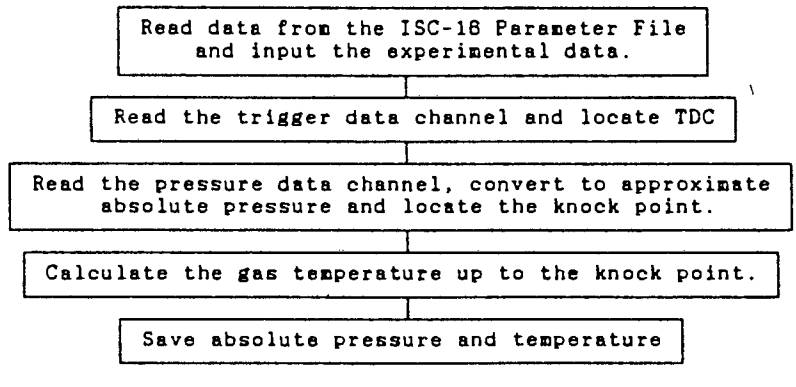


Ricardo engine data analysis flow diagram

The following experimental data was also required in order to perform the analysis:

- the pressure transducer calibration (Bar/V)
- the atmospheric pressure (mm Hg)
- the atmospheric temperature (°C)
- the inlet temperature after the inlet heater (°C)
- the air manometer reading (mm)
- the engine speed (Rev/min)
- the compression ratio
- the ignition timing (°BTDC)
- the heat input (W)
- the fuel type (Gasoline=1, Methanol=2)

Since the start of the data capture was post-triggered by the filtered high-frequency component of the pressure trace that signalled a knocking cycle, the TDC mark was determined from a separate channel. This checked visually from the graphical plot shown below.

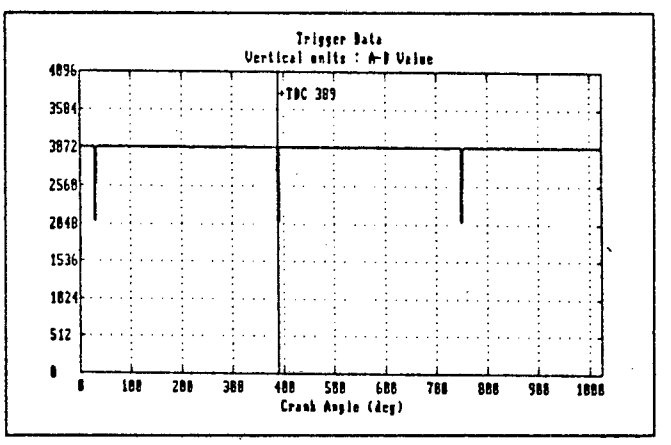


Marker signal showing the combustion TDC offset

The absolute pressure was estimated for the purposes of plotting the pressure trace to identify the knock point. The program searched the data for the highest pressure reading which was proposed as the knock point. However, owing to the rate of data capture, the digitised peak pressure sometimes corresponded to the second or third pressure fluctuation and it was necessary to identify the start of knocking visually by moving the "knock" hair-line, shown in the example overleaf.

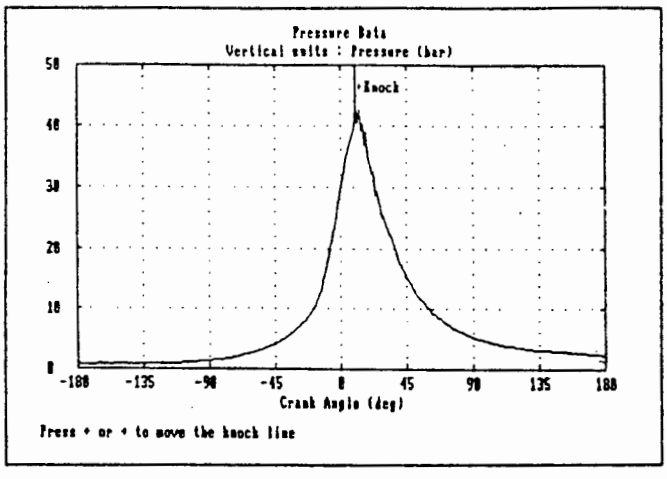


Pressure data identifying the knock point

An energy balance was performed on the inlet mixture at the point of inlet valve closure (IVC) to solve for the absolute pressure and the temperature. Details of this calculation are discussed in section 2.3. With this as the starting point, the temperature was calculated up to the point of ignition assuming ideal gas relationships. After ignition had occurred, the volume of the unburned gas was unknown and the calculation of the temperature was continued in small time increments. For each time increment, the calculation involved two steps. First, a theoretical pressure and temperature was determined for the whole mixture as if no further combustion had taken place, the only considerations being the piston work and the heat loss. Secondly, the mixture was imagined to undergo an adiabatic compression process to raise the pressure up to the measured value, from which the final temperature was determined. The calculation was performed in steps of one crankshaft degree, corresponding with the measured pressure data. The calculation was halted at the point that knock occurred.

The figure shown overleaf illustrates a typical temperature profile calculated by this method.

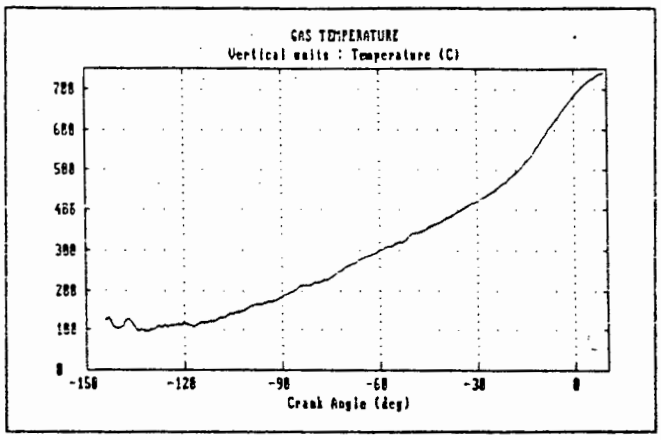


Calculated gas temperature from IVC to the knock point

Finally, the absolute pressure and calculated temperature were saved to disk for subsequent analysis by the second program.

The second program's function was to characterise the fuel in terms of its knock behaviour, utilising the pressure and temperature data which originated from a wide variety of engine operating conditions. The program consisted of simply identifying the data files pertaining to a particular fuel, after which the fuel-characteristic constants were calculated according to the method described in Appendix A.

The development of the integral function for each set of pressure and temperature data could be viewed graphically as shown below.

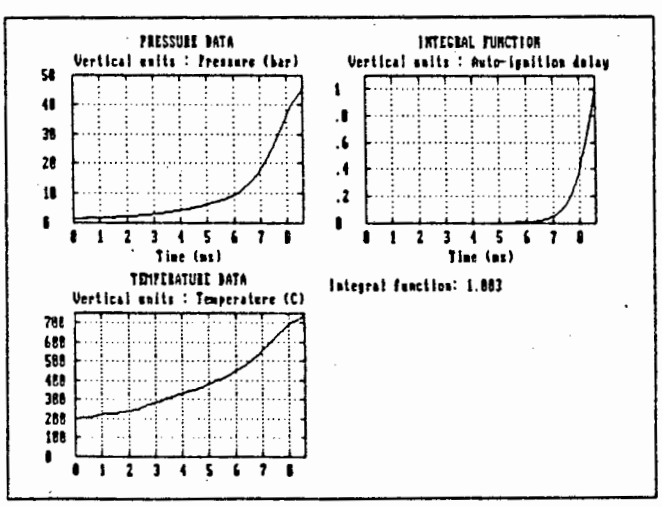


Integral function development for one engine test condition

Besides the theoretical knock model analysis, a multiple linear regression option was also included which expressed the maximum temperature prior to the onset of knock as a function of pressure and engine speed. This latter option was added since it contained no implicit assumptions about the underlying kinetics of the knock mechanism and was used to study the behaviour of methanol more closely. The linear regression data was saved as a data file and imported into a spread-sheet program for plotting graphs such as that shown below.

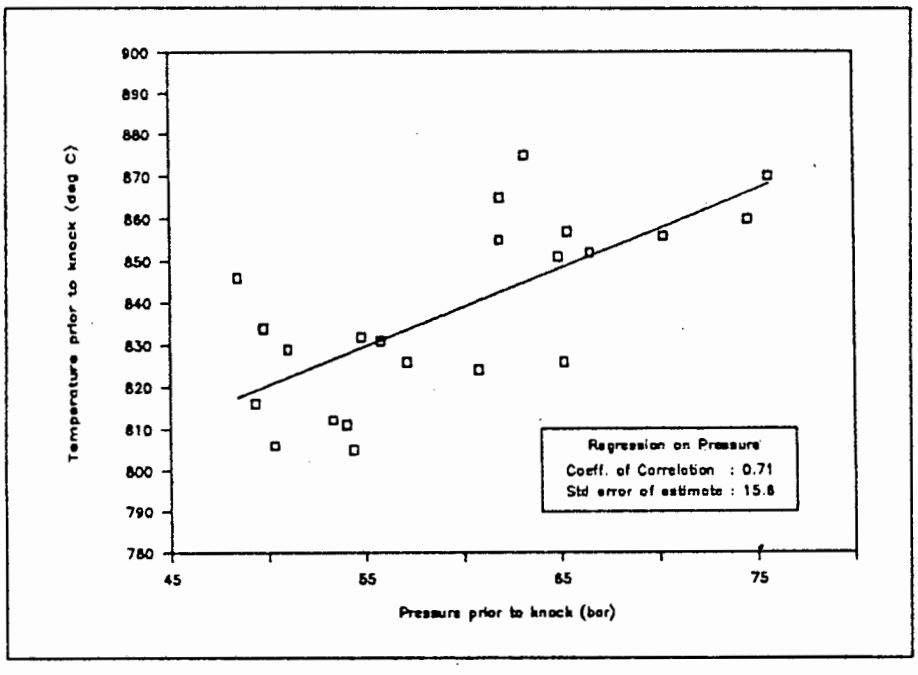


Knock-limited temperature correlation with pressure

# APPENDIX C - SOLUTION OF THE ONE-DIMENSIONAL UNSTEADY STATE HEAT CONDUCTION EQUION

The one-dimensional, unsteady heat conductionquation is given by:

$$\frac{\delta T}{\delta t} = \frac{1}{\rho c} \frac{\delta}{\delta x}\left[k \frac{\delta T}{\delta x}\right] \qquad (C.1)$$

where $\rho$ = the density of the wall material
c = the specific heat of the wall mateal
k = the thermal conductivity of the wa material.

Since the surface temperature variation is perlic, equation (C.1) may be conveniently solved by using a Foier series approximation of the temperature profile to perrm the integration. The heat capacity, "$\rho c$", and the trmal conductivity, "k", are assumed to be constant a equation (C.1) reduces to:

$$\frac{\delta T}{\delta t} = \alpha \frac{\delta^2 T}{\delta x^2} \qquad (C.2)$$

where $\alpha = \frac{k}{\rho c}$ = the thermal diffusivity oftl wall material.

The steady periodic surface temperature, "$T_w$", chan with angular velocity, "ø" rad/s, and can be expanded inthe Fourier series given by:

$$T_w = T_m + \sum_{n=1}^{N} \left[ A_n \operatorname{Cos}(n\omega t) + B_n \operatorname{Sin}(n\omega t) \right. \qquad (C.3)$$

where $T_m$ = the time-averaged component of $T_w$ and $A_n$, $B_n$ are the Fourier coefficients.

Solving equation (C.2) with the boundary condition n as

$$T = T_w(t) \quad \text{at } x = 0,$$

the value of temperature as a function of time and position is given by:

$$T(x,t) = T_m - x\frac{\dot{q}_m}{k} + \sum_{n=1}^{N} e^{\Phi_n}\left[A_n \cos(n\omega t-\Phi_n) + B_n \sin(n\omega t-\Phi_n)\right] \quad (C.4)$$

where $\Phi_n = -x\left[\frac{n\omega}{2\alpha}\right]^{0.5}$

$\dot{q}_m$ = the mean heat flux over the full period.

From equation (C.4), the surface heat flux may be computed as:

$$\left[\frac{dq}{\delta t}\right]_{x=0} = -k\left[\frac{\delta T(t,x)}{\delta x}\right]_{x=0} \quad (C.5)$$

Thus, inserting equation (C.4) into equation (C.5), performing the differentiation and setting x=0, the heat flux at the surface simplifies to:

$$\frac{dq}{dt} = \dot{q}_m + k\sum_{n=1}^{N}\left[\frac{n\omega}{2\alpha}\right]^{0.5}\cdot\left[(A_n+B_n)\cos(n\omega t) + (B_n-A_n)\sin(n\omega t)\right] \quad (C.6)$$

In practice, the value of average heat flux, "$\dot{q}_m$", is not known. However, at some point during the compression stroke, the wall surface temperature must equal the gas temperature and at that point, the heat flux is zero. Since the gas temperature may be calculated with reasonable accuracy during the compression stroke, and the wall temperature was measured, the value of "$\dot{q}_m$" may be determined for that condition as:

$$\dot{q}_m = -k\sum_{n=1}^{N}\left[\frac{n\omega}{2\alpha}\right]^{0.5}\cdot\left[(A_n+B_n)\cos(n\omega t_o) + (B_n-A_n)\sin(n\omega t_o)\right] \quad (C.7)$$

where $T_o$ = the temperature at the point where the gas and the wall temperatures are equal.

# APPENDIX D - EXPERIMENTAL DETAILS OF THE DAIMLER BENZ OM 407 TESTS

The engine used for these studies was a Daimler Benz OM 407 diesel engine, of which one cylinder was fitted with low compression ratio pistons and instrumented with the special thermocouple cylinder head.

The principal details of the test cylinder were:

| | |
|---|---|
| Bore | 125 mm |
| Stroke | 155 mm |
| Connecting rod | 256 mm |
| Compression Ratio | 9.5 (Gasoline tests) |
| | 12.5 (Methanol tests) |

The air supply to number six cylinder (nearest the flywheel) was isolated and fitted with a separate air supply system having a throttle valve, a surge tank of 40 litre capacity and an air flow measuring facility. The air flow measurement was based on the pressure depression at the vena-contractor of a thin-walled plain intake. The air flow measuring system was found to resonate at an engine speed of about 1600 rev/min. At the time that the problem was diagnosed, a number of tests had already been conducted and the basis of air flow measurement was subsequently checked against a calculated air mass flow using the recorded pressure and the swept volume at the intake temperature.

An ignition distributor and contact breaker unit was mounted in the place of the tachometer drive. The ignition timing control was achieved by means of a linkage system to rotate the ignition unit. Initial trials indicated that the ignition point was subject to considerable fluctuation but this was diagnosed to excessive clearance in the tongue and groove coupling of the tachometer drive. The problem was cured by incorporating a spring element into the coupling to eliminate the free play.

Provision was made for continuous fuel injection in the inlet port of number six cylinder, with a second identical fuel injector mounted so as to feed into an empty container. The fuel nozzles were designed to incorporate an air bleed that rendered them insensitive to the manifold pressure. Either fuel injector could be selected by means of solenoid valves. This arrangement permitted adjustment of the fuel pressure to yield a desired fuel flow, before the fuel was actually fed to the engine.

A trigger system to initiate the data capture was built which utilised the exhaust valve movement on cylinder number 1. The system comprised an electrically insulated, spring-loaded plunger that touched the valve rocker whilst the valve was closed. The exact point in the valve actuation at which the plunger broke contact with the rocker could be accurately adjusted. The earthing of the plunger that occurred as the valve shut was found to provide an accurate and repeatable trigger signal.

The trigger was calibrated dynamically using the peak pressure of a motoring pressure trace. With the engine fully warmed up, the peak pressure was assumed to occur 0.7° BTDC (the shift from TDC being caused by heat loss from the compressed gas). The trigger point was re-checked periodically throughout the test program and was found to remain unaltered at 210° BTDC.

The special thermocouple cylinder head that was supplied by Daimler Benz with 179, type K, thin-film thermocouples was tested for integrity. The ø1mm, sheathed thermocouple wires were routed to the combustion-chamber surface and a 4µm layer of gold plating was used to form the electrical junction, as shown in the sketch overleaf. A plan view of the cylinder head indicating the arrangement and numbering of the thermocouples is shown in figure 3.1. On commissioning, it was found that thermocouple number 10 was defective.

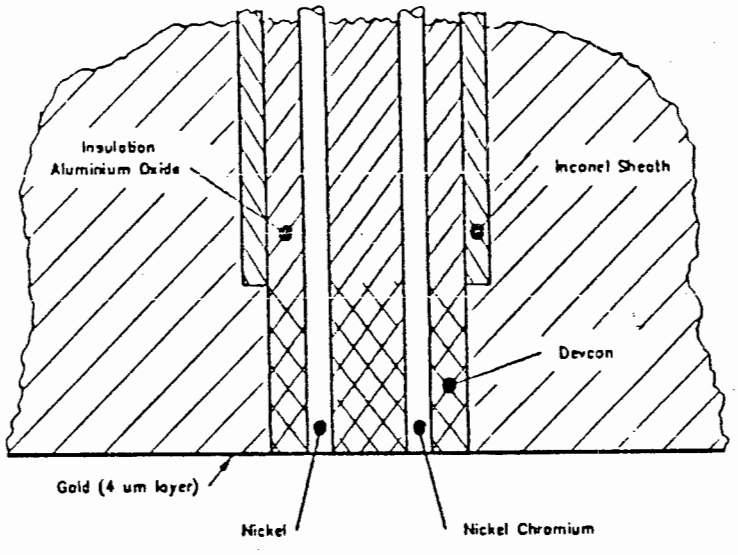


Thin-film thermocouple construction

The tests were conducted with the engine fully warmed, the water temperature being controlled by the thermostat in the usual manner. The tests were conducted at borderline knock with wide-open throttle. Only one engine speed of 1300 rev/min was investigated because the thermocouple cylinder head was damaged during the methanol testing as a result of a brief run-away preignition situation.

The combustion chamber of the engine consisted of a bowl in piston design. The compression ratio was determined by the size of the bowl. The spark-plug was situated near the centre axis of the piston bowl and the pressure transducer was slightly offset as shown in figure 3.1.

As with the Ricardo tests, the fuels used were commercial grade 98 RON gasoline, and standard grade methanol.

## D.1 ANALYTICAL EQUIPMENT

An AVL water-cooled pressure transducer, type 12QP, was used for all the tests. The transducer signal was processed using a Kistler model 568 charge amplifier. The pressure transducer calibration was checked periodically and was found to remain within specification. During the final test with methanol on the OM 407 engine the diaphragm of the transducer cracked and developed a gas leak into the transducer's waterjacket. The cylinder head was damaged during this test and therefore the experiment could not be repeated. A subsequent calibration test indicated that the pressure transducer was still operating and the results of the last test were apparently not compromised.

The thermocouple signals from the special cylinder head were amplified through six thermocouple amplifiers which were specially calibrated for "K" type thermocouples. They were based on the Analogue Devices integrated circuit AD594. A switchable scanner unit was constructed to enable the selection of groups of six thermocouples. The control of the selection of each bank of thermocouples was achieved by means of a five-bit selectable digital signal. The circuit diagram of the scanner unit is shown diagrammatically below

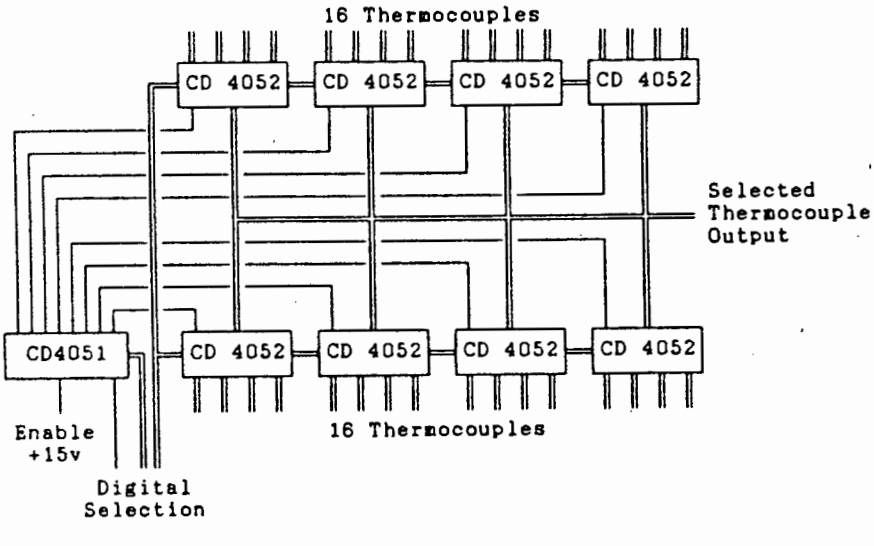


Schematic Diagram Of The Scanner Electronics

A computer-based data acquisition system was used having the capability to multiplex and digitise up to eight analogue signals at a rate of up to 27000 conversions per second. The system was based on a hardware card by Data Translation, the DT2801a, which was designed to slot into an IBM XT personal computer. Since the sample frequency was too slow to permit simultaneous capture of six thermocouple signals, a multi-channel instrumentation tape recorder was used for the raw data capture.

The tape recorder that was used, a Philips EL 1020, had seven instrument channels and one voice track. One channel was required for the trigger signal leaving six channels available for thermocouple or pressure data. At the maximum tape speed, and using frequency modulated DC recording, the recorder had a frequency response specification:

| | |
|---|---|
| 0 to 5 kHz | -0.0 dB |
| 5 to 10 kHz | -0.5 dB |
| 10 to 15 kHz | -3.0 dB |

The recorded signal could be played back at reduced speed to permit simultaneous transfer of the information on all channels to the computer for analogue to digital conversion.

A number of checks were performed to test the analytical equipment for signal integrity, background noise levels, frequency response, etc. The tape recorder was found to be a source of high frequency noise greater than 10 kHz which could not be completely eliminated by cable shielding and equipment grounding. The possibility of capturing the data directly on line was considered but this would have limited the sample rate to one reading every two crankshaft degrees which was not considered sufficient. Furthermore, the security of having all the tests recorded continuously was thought to out-weigh the disadvantage of a degree of signal degradation.

The digitisation was initiated using the external trigger facility and the rate of digitisation was set on an internal clock which was computed to be equivalent to one reading on each

channel every crankshaft degree for one rotation. Since a crankshaft encoder was not used (to save a tape recorder channel), the engine speed had to be measured very accurately. This was achieved by monitoring the trigger channel on the tape recorder during playback using an accurate frequency counter. A low-pass filter was constructed for each channel that could be set according to the rate of digitisation to 40% of the conversion frequency.

## D.2 ANALYSIS SOFTWARE

Because of the large quantity of data involved, a number of programs were written to handle the file organisation and manipulation. The following diagram shows the main program structure:

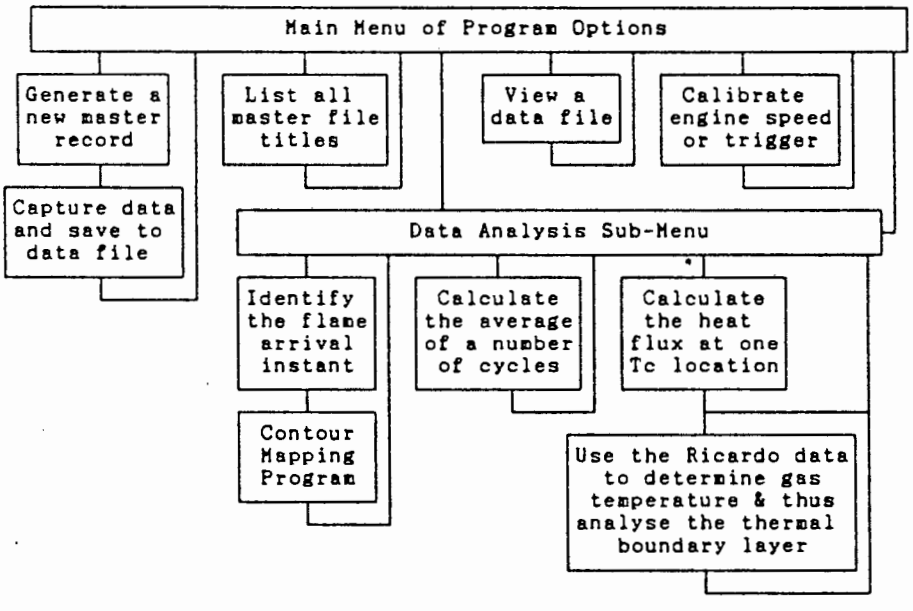


Daimler Benz program organisation

The master file contained records of the experimental setup for each test. After creating a new master record, the data

acquisition program created a corresponding data file. An example of a master record is shown below.

```
                    Experimental Test Conditions

Test NO:  17        Date (mm/dd/yy): 02-17-1986        Engine: OM 407

Title:  Tc group 7 - Non-knocking with gasoline

Ambient Pressure (mm hg): 750        Ambient Temperature (°C): 25

Engine Settings -  Compression Ratio : 8.5
                   Speed (rev/min)   : 1311
                   Ignition (°BTDC)  : 18
                   Fuel type         : P(98)

Parameters - Air Flow (g/s) : 20.8   Coolant Temperature (°C): 72
             Fuel Flow (g/s): 1.44   Exhaust Temperature (°C): 685

Tape Recorder -    Trigger Angle (°BTDC)    : 210
                   Data Read Interval (°CA): 1
                   Number of Cycles         : 50

Channel NO      :   1   :   2   :   3   :   4   :   5   :   6   :
Transducer      :Tc-178 :Tc-168 :Tc-158 :Tc-148 :Tc-130 :Tc-113 :
Unit Full Scale :  500  :  500  :  500  :  500  :  500  :  500  :
```

Example of a Master Record

Utility programs for scanning through the master file titles and for viewing the test data were written. The viewing program included a facility to superimpose data from several engine cycles, different thermocouple channels and also different tests. An example of one such combination, showing several different thermocouple traces is given below.

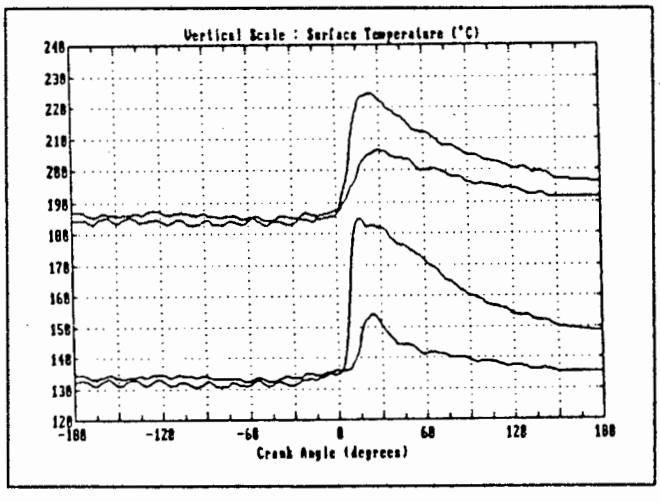


Example of the view-data program

The flame-arrival identification program was based on the processed data from the cycle-averaging program. The instant of flame arrival was determined visually with the use of moveable hair-lines. An example, illustrating of the program graphics is shown below.

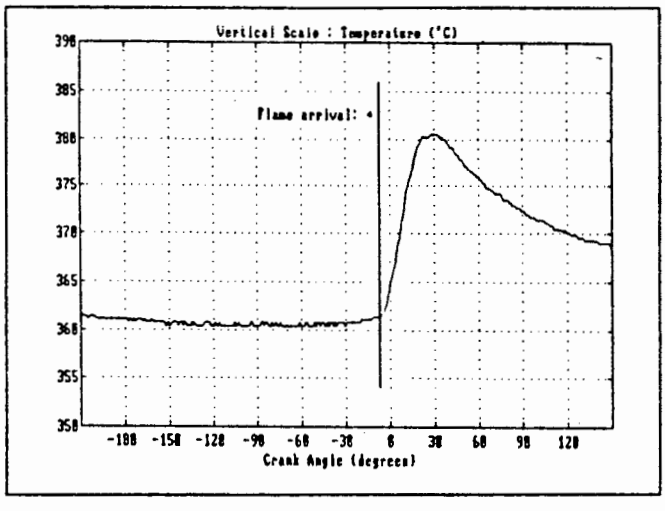


Identification of the flame-arrival instant

The contour mapping could be selected from the flame-arrival data or from the average surface temperature. Linear interpolation of any missing data (under the valves for example) was carried out first, followed by nearest-data point extrapolation where data was missing at the outer periphery. An X-Y smoothing routine was required to produce a contour plot such as that illustrated overleaf.

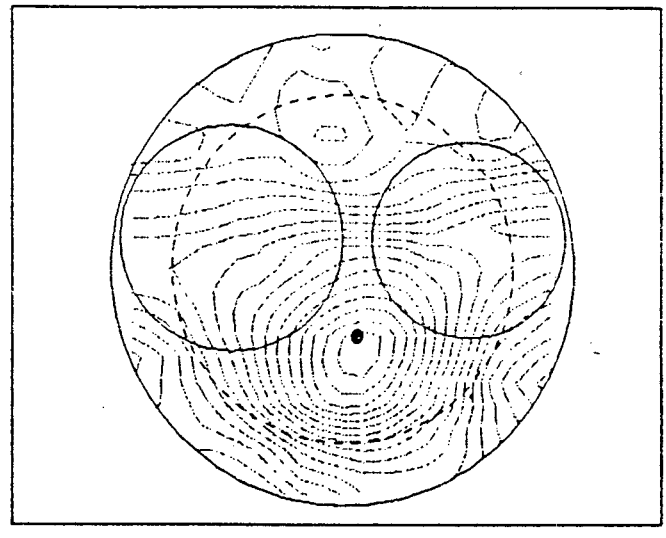

Illustration of the contour-mapping program output

The heat-flux calculation method is described in Appendix C. An example of the result of this calculation is shown below.

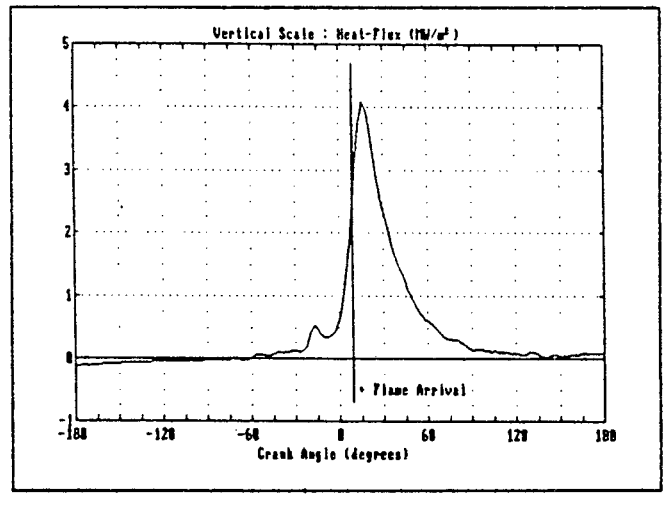


Heat flux calculation example

Finally, a program was written to calculate the thermal boundary layer temperature, utilising the knock model constants that characterised each fuel which were determined from the Ricardo test analysis. Details of the calculation method is given in

section 3.2.2. The gas temperature was found by trial-and-error, manipulating the temperature at the point of inlet-valve closure until the knock point predicted by the model agreed with the actual knock point. The final boundary layer temperature profile was saved as a data file which was subsequently imported into a spread-sheet program for graphical representation, as illustrated below.

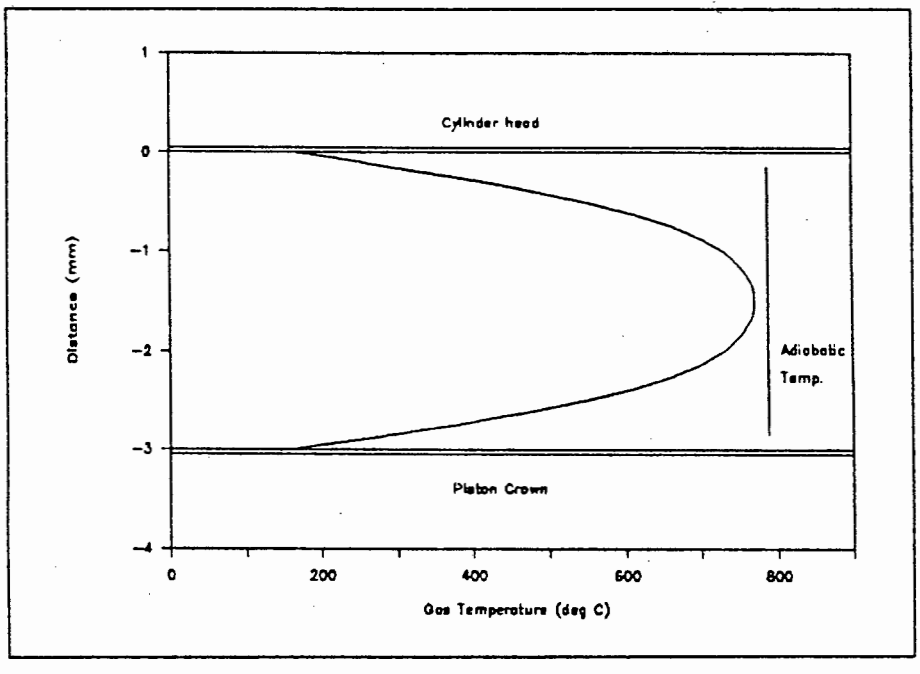


Example of the calculated thermal boundary-layer profile